Naturalness in Beyond the Standard Model Physics

Isabel García García

Balliol College

University of Oxford

A thesis submitted for the degree of

Doctor of Philosophy

Trinity Term 2017

Abstract

Being consistent with every experimental measurement made to date, the current paradigm of particle physics, the Standard Model, remains a successful parametrization of nature. Together, the Standard Model plus the theory of General Relativity seem to provide a consistent picture of physics at all scales, yet there is plenty of room to believe the story is incomplete.

Puzzles that remain unanswered within the context of the Standard Model include (*i*) an explanation of the origin of Dark Matter, which accounts for no less than $\sim 25\%$ of the Universe's energy budget, (*ii*) a meaningful answer to the question of electroweak naturalness, (*iii*) a rationale for the absence of anti-matter in our observable patch of the Universe, (*iv*) a dynamical picture of the vast hierarchies we observe in fermion masses, and (*v*) a resolution to the strong CP problem. With the exception of the Dark Matter mystery, all other objections to the Standard Model listed here take the guise of a 'hierarchy' problem: why is some quantity (either a scale or coupling) so small? This work addresses two of the objections to the Standard Model: the necessity of an explanation to the origin of Dark Matter, and the question of *naturalness* as a guiding principle in nature, understood as the necessity for a dynamical mechanism behind unexplained hierarchies.

Chapters 1 and 2 introduce the topics of naturalness and Dark Matter respectively. The former makes an emphasis on the electroweak hierarchy problem, and a particular class of theories that provide a solution to this puzzle: models based on the Twin Higgs mechanism. Chapters 3 and 4 are based on work published in [1] and [2], where novel theories of Dark Matter, and their phenomenology, are explored in the context of Twin Higgs models. Chapter 5 explores structural aspects of a particular mechanism – the so-called 'clockwork' – for generating hierarchies in parameters in a way that can be considered natural, and it is based on [3]. Finally, chapter 6 summarizes our conclusions and future outlook.

Other work published during my time as a graduate student include [4–7], but those publications are not the focus of this thesis.

Acronyms

Acronym	*Meaning*	*Page*
ADM	Asymmetric Dark Matter	32
BH	Black Hole	33
BBN	Big Bang Nucleosynthesis	28
BSM	Beyond the Standard Model	1
CMB	Cosmic Microwave Background	27
DM	Dark Matter	26
DR	Dark Radiation	40
HDO	Higher Dimensional Operator	40
LH	Left-handed	1
MSSM	Minimal Supersymmetric Standard Model	11
NGB	Nambu-Goldston boson	4
pBH	primordial Black Hole	33
pNGB	pseudo Nambu-Goldston boson	4
RG	Renormalization group	1
RH	Right-handed	1
SD	Spin-dependent	36
SI	Spin-independent	36
SM	Standard Model	1
SUSY	Supersymmetry	9
WGC	Weak Gravity Conjecture	87
WIMP	Weakly interacting massive particle	31

Acknowledgements

I am very grateful to Nathaniel Craig, Kiel Howe, Robert Lasenby, John March-Russell, and Dave Sutherland, with whom I have collaborated on different projects during my time as a graduate student.

I am particularly grateful to Asimina Arvanitaki and Savas Dimopoulos, as well as their group of students and postdocs, for hospitality when visiting both PI and the Stanford Institute for Theoretical Physics.

I would like to sincerely thank John Wheater, who has provided instrumental guidance during my DPhil degree. His academic advice and support have been key.

I feel indebted to Kiel Howe and Stephen West, who have contributed significantly to all the physics I have learned. As friends, their support has been trully priceless.

My mother, Amor, and my brother, Álvaro, have always been my most faithful supporters under all kinds of circumstances, and their inconditional love and encouragement are the pillars of this thesis. It is not possible to convey in words how grateful I feel to them.

Finally, I wish to express my deepest gratitude to John March-Russell, who persuaded me to come to Oxford in the first place. As a physicist, John has been my best collaborator and a deeply inspiring figure. Beyond physics, he has transformed my life.

Statement of Originality

This thesis is based on original research published in [1–3]. It contains no material that has already been accepted, or is currently being submitted, for any degree or diploma or certificate or other qualification at the University of Oxford or another institution.

To the best of my knowledge and belief this thesis contains no material previously published or written by another person, except where due reference is made in the text.

Isabel García García 2017

Contents

Chapter 1

Naturalness

1.1 Naturalness and nature

Many of the mysteries left unanswered in the context of the Standard Model (SM), and which Beyond-the-Standard-Model (BSM) theories aim to address, have at their core an unexplained hierarchy of scales or couplings. From the smallness of the cosmological constant to the electroweak scale to the vast hierarchies in Yukawa couplings, the principle of naturalness urges us to refuse a just-so 'explanation' of these conundrums, and instead demands a dynamical mechanism behind them. Unsurprisingly, dynamical mechanisms for generating hierarchies are at the centre of much of the work done in BSM physics.

Not all of these 'hierarchy problems', however, have the same standing. If the smallness of some parameter x can be justified by the fact that in the limit $x \to 0$ the theory recovers a symmetry, then we say that x being very tiny is 'technically natural' [8]. As a result, when we take into account quantum effects, the value of x will not be destabilized from its originally small size, for its value is symmetry-protected and therefore any quantum corrections must be proportional to some power of x itself. This definition of naturalness was introduced by 't Hooft in [8]: *"At any energy scale μ, a physical parameter or set of physical parameters $\alpha_i(\mu)$ is allowed to be very small only if the replacement $\alpha_i(\mu) = 0$ would increase the symmetry of the system."*. Examples of this kind include the vast hierarchies we observe in the masses of quarks and leptons, linked to the fact that some of the Yukawa couplings are $y \ll 1$, instead of $\mathcal{O}(1)$ as one would naïvely expect from a naturalness perspective. Although such a situation may be puzzling, it is nevertheless technically natural: in the limit $y \to 0$ the theory recovers a chiral symmetry under which the left-handed (LH) and right-handed (RH) components of the corresponding massless fermion transform differently. The renormalization group (RG) evolution equations for y are then proportional to some power of y itself

and, as a result, solving such a puzzle only requires a dynamical mechanism that operates at tree-level – being symmetry-protected, quantum corrections will then respect the tiny value of the tree-level parameter. This is not to say, however, that staggering hierarchies in couplings that are technically natural are of no interest: from a model building perspective, it is clearly desirable to be able to explain tree-level hierarchies as outputs, rather than have them as inputs. This will be the focus of chapter 5, where we explore some structural aspects of a mechanism for generating hierarchies in scales and couplings – the 'clockwork' mechanism [9,10] – even though they may be considered technically natural.

Another example of a small number present in nature that is nevertheless technically natural is the ratio of the QCD confinement scale, $\Lambda_{\rm QCD} \sim 100$ MeV, to the Planck scale $m_{Pl} \sim 10^{18}$ GeV, although in this case the dynamical mechanism behind it is well know: dimensional transmutation [11]. In short, a small (and dimensionless) gauge coupling g_3 in the UV uniquely determines the value of the (dimensionful) scale of QCD confinement, defined as the IR scale at which QCD dynamics become strongly coupled, and below which the relevant degrees of freedom are no longer quarks and gluons but bound states thereof. The situation is technically natural because the β-function of g_3 is proportional to g_3 itself, so that a tiny value of the gauge coupling in the UV is not destabilized by quantum corrections. In particular, the QCD β-function at one-loop reads

$$\frac{d\alpha_3(\mu)}{d\log\mu} = -\frac{b_3\alpha_3^2}{2\pi} \ , \tag{1.1}$$

where $\alpha_3 = g_3^2/(4\pi)$, and $b_3 = 7$. Taking as boundary condition the value of α_3 at some high scale $\Lambda_{\rm UV}$, and defining the scale of confinement as $\alpha_3(\Lambda_{\rm QDC}) \equiv 1$, one finds

$$\Lambda_{\rm QCD} \approx \Lambda_{\rm UV} \exp\left(-\frac{2\pi}{b_3\alpha_3^{\rm UV}}\right) \ , \tag{1.2}$$

where $\alpha_3^{\rm UV} \equiv \alpha_3(\Lambda_{\rm UV}) \ll 1$. $\Lambda_{\rm QCD}$ is then predicted to be exponentially smaller than $\Lambda_{\rm UV}$, justifying the small ratio between the scale of QCD confinement and any other physical scale in nature, all the way up to m_{Pl}.

On the other hand, other problems stand in a particularly privileged posi-

tion for being 'neglected'. The cosmological constant problem [12] falls into this category. Whereas the energy density of the Universe has been measured to be $\Lambda_{\rm CC} \sim (10^{-12}\ {\rm GeV})^4$, quantum effects would naïvely set its natural value to be of order $m_{Pl}^4 \sim (10^{18}\ {\rm GeV})^4$ – a stunning 10^{120} factor above the experimental measurement. However, the effect of a finite vacuum energy density can only be discussed in the context of a theory of gravity, and considering quantum corrections to its value certainly invokes the presumption that gravity can consistently be made quantum. It is in this sense that particle physicists are sometimes willing to neglect the cosmological constant problem, for it is reasonable to believe that its resolution is tied to a deep understanding of a theory of quantum gravity.

Of particular acuteness are those cases that do not fit into any of the two categories discussed above, a prime example being the electroweak hierarchy problem. That the electroweak scale $v \sim 100$ GeV is so much smaller than m_{Pl} is not a technically natural statement: interactions between the Higgs and heavy particles whose masses are at some high scale Λ lead to quantum corrections to the Higgs mass-squared parameter that are quadratically sensitive to this new scale (be it at the Planck scale or below). Unlike the cosmological constant, a resolution to the electroweak hierarchy problem cannot be shamelessly deferred until the point where our understanding of quantum gravity is complete: although the fact that v is not of order m_{Pl} itself could conceivably be accounted for by a complete theory of quantum gravity, the question would remain open as to why the Higgs mass-squared appears to be insensitive to any other energy scale at which we expect some new dynamics to be present. This new dynamics could be related to the generation of a baryon asymmetry, or to a dynamical theory of flavor that explains the hierarchies in Yukawa couplings, or to the existence of a unified gauge theory. In all these cases, new dynamics at scales $\gg v$ (although they may well be below m_{Pl}) are expected to be present, and the question of why the weak scale is so much smaller than any of these remains unanswered.

Another example of a hierarchy problem involving spin-0 states was already realized in nature: the lightness of pions. Being scalars, the three pions we observe (π^0 and $\pi^\pm$) are subject, in principle, to the same type of quantum corrections that

destabilize the Higgs potential. Pions being so much lighter than any other scale present in nature would correspond to an extreme fine-tuning. This situation is however reconciled with the idea of naturalness because pions are in fact pseudo-Nambu-Goldstone bosons (pNGB's) of an approximate global symmetry. Restricting the discussion to the first generation of quarks, up and down quarks respect a global $SU(2)_L \times SU(2)_R$ chiral flavor symmetry that is broken down spontaneously to a non-chiral flavor $SU(2)_V$, as a result of the confining nature of QCD through the presence of a non-zero chiral condensate $\langle u\bar{u}\rangle = \langle d\bar{d}\rangle \sim \Lambda_{\rm QCD}^3$. This breaking leads to 3 massless NGBs, which are bound states of u and d quarks. The global $SU(2)_L \times SU(2)_R$ symmetry is further broken explicitly by non-zero quark masses. But since $m_u, m_d \ll \Lambda_{\rm QCD}$, this breaking is tiny compared to the scale of spontaneous breaking, and therefore pions remain parametrically lighter than the relevant QCD scale, $m_\pi^2 \ll (4\pi\Lambda_{\rm QCD})^2$, in a way that is perfectly natural.

In this chapter we will focus on the electroweak hierarchy problem. We review in detail the problem of electroweak naturalness in section 1.2, and discuss the requirements that any solution must fulfill. Section 1.3 is devoted to Supersymmetry – one of the best theoretically motivated of all proposed solutions to the hierarchy problem, but that nevertheless seems to be in tension with naturalness (at least in its simplest implementations) in light of negative experimental results.[1] Exploring the difficulties of Supersymmetry when it comes to reconciling naturalness and experiment will motivate our discussion of a different class of solutions to the hierarchy problem: theories of Neutral Naturalness, the prime example of which are models based on the Twin Higgs mechanism. We explore the Twin Higgs idea in section 1.4, with a particular focus on its minimal implementation, the so-called Fraternal Twin Higgs, which is the context in which the work of chapters 3 and 4 is developed.

[1] There are of course other solutions to the electroweak hierarchy problem. A prime example is the idea of compositeness, which essentially consists in making the Higgs a 'pion', i.e. the pNGB of some global symmetry that is spontaneously broken as a result of some confining dynamics (see [8,13] for the earliest work). Another well-motivated class of solutions make use of the presence of extra spatial dimensions, either warped [14] or flat [15]. We will not discuss these other possibilities in this thesis.

1.2 The electroweak hierarchy problem

The Higgs sector of the SM is effectively described by a potential of the form

$$V(|H|) = m_H^2|H|^2 + \lambda|H|^4 \ , \tag{1.3}$$

where H corresponds to the electroweak Higgs doublet. If the mass-squared parameter is $m_H^2 < 0$ then the Higgs gets a non-zero vacuum expectation value (vev)

$$\langle|H|^2\rangle = \frac{-m_H^2}{2\lambda} \equiv \frac{v^2}{2} \ , \tag{1.4}$$

which has been experimentally measured to be $v \simeq 246$ GeV from the properties of the weak interactions. This non-zero vev breaks the $SU(2)_L \times U(1)_Y$ symmetry of the SM down to $U(1)_{\rm EM}$, and, as a result, the $W^\pm$ and Z gauge bosons get masses of order ~ 100 GeV. After eletroweak symmetry breaking, one real scalar degree of freedom is left in the spectrum – the Higgs particle – with mass $m_h^2 = 2\lambda v^2 = -2m_H^2$, which has been measured to be $m_h \simeq 125$ GeV. With the experimental measurements of v and m_h we can infer the values of the parameters in eq.(1.3) as $m_H^2 \simeq -(90 \text{ GeV})^2$ and $\lambda \simeq 0.13$. The value of v is what we refer to as the weak scale, and it is set by the Higgs mass-squared parameter, m_H^2, evaluated at the weak scale itself.

An electroweak hierarchy problem arises in the context of theories *beyond* the SM, with new degrees of freedom and dynamics present at some scale $M \gg v$ that interact with the SM sector (in particular with the Higgs). In such scenarios, interactions between the Higgs and new particles with masses of order M lead to quantum corrections to the Higgs potential that, naïvely, set the value of the mass-squared parameter at large distances to be $m_H^2 \sim M^2$. The electroweak hierarchy problem is thus sometimes stated as the question of why the weak scale is so much smaller than any other scale M at which we expect new physics to appear, and which *a priori* could be as high as m_{Pl} [8, 16–18].

To illustrate this point, let's consider a complex scalar field φ, with mass $M \gg v$, that interacts with the Higgs through a quartic coupling. The relevant interaction

term in the lagrangian reads

$$\mathcal{L} \supset -\tilde{\lambda}|H|^2|\varphi|^2 \ , \tag{1.5}$$

and would result in a one-loop contribution to the Higgs two-point function given by

$i\mathcal{M}_2^{(1)}$ = 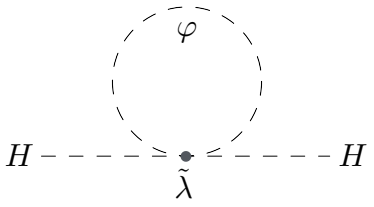

$= -i\tilde{\lambda}\int \frac{d^4k}{(2\pi)^4}\frac{i}{k^2 - M^2 + i\epsilon}$. (1.6)

The integral of eq.(1.6) is quadratically divergent, and we may use any regularization procedure to make it finite. For instance, if we use a hard cut-off Λ as a regulator we find

$$i\mathcal{M}_2^{(1)} = -\frac{i\tilde{\lambda}}{16\pi^2}\left(\Lambda^2 - 2M^2\log\frac{\Lambda}{M}\right) \ , \tag{1.7}$$

which has both a quadratic divergence and a logarithmic divergence as we take $\Lambda \to \infty$. To get rid of these divergences we may add counter-terms to the lagrangian, of the form $\mathcal{L} \supset -m^2_{H,\mathrm{c.t}}|H|^2$, with $m^2_{H,\mathrm{c.t}}$ such that the divergent terms in eq.(1.7) are cancelled. Ignoring finite pieces, this requires

$$m^2_{H,\mathrm{c.t}} = -\frac{\tilde{\lambda}}{16\pi^2}\left(\Lambda^2 - 2M^2\log\frac{\Lambda}{\mu}\right) \ , \tag{1.8}$$

where we have been forced to introduce an extra mass scale μ on dimensional grounds – the so-called renormalization scale. Now, the tree-level and counter-term pieces, together with our one-loop result, lead to a two-point function (at vanishing external momentum) given by

$$i\mathcal{M}_2 = -i\left(m_H^2 - \frac{\tilde{\lambda}}{8\pi^2}M^2\log\frac{\mu}{M}\right) \ . \tag{1.9}$$

Demanding that the result of eq.(1.9) is independent of μ, as must be the case for physical observables like n-point functions, leads to the one-loop RG equation for

the mass-squared parameter m_H^2:

$$\frac{dm_H^2(\mu)}{d\log\mu} = \frac{\tilde{\lambda}}{8\pi^2} M^2 \cdot \theta(\mu - M) \ , \tag{1.10}$$

where we have included a factor $\theta(\mu - M)$ to make it explicit that the contribution from the massive scalar is only present at scales $\mu > M$.[2]

RG equations are useful because they tell us about the properties of our theory as we move from small to large distances. In particular, if the parameters of our theory are specified as boundary conditions at some very high energy scale $\Lambda_{\rm UV} > M \gg v$, then their values in the IR are encoded in their RG flow. For instance, in our example, if the Higgs mass-squared is given in the UV as $m_H^2(\Lambda_{\rm UV})$, its value at scale $v \ll \Lambda_{\rm UV}$ reads

$$m_H^2(v) = m_H^2(\Lambda_{\rm UV}) - \frac{\tilde{\lambda}}{8\pi^2} M^2 \log\frac{\Lambda_{\rm UV}}{M} \ . \tag{1.11}$$

Now, what happens if we change the size of the UV parameter by a fractional amount $\epsilon_{\rm UV}$, such that $m_H^2(\Lambda_{\rm UV}) \to (1+\epsilon_{\rm UV}) m_H^2(\Lambda_{\rm UV})$? We can parametrize the effect of such a perturbation on the IR as $m_H^2(v) \to (1+\epsilon_{\rm IR}) m_H^2(v)$. If $\epsilon_{\rm IR} \sim \epsilon_{\rm UV}$ (i.e. changes in the properties of the theory at very small distances translate into similar changes at large distances), we say that the theory is *natural*. On the other hand, if $\epsilon_{\rm IR} \gg \epsilon_{\rm UV}$ (i.e. the properties of the theory in the IR are extremely sensitive to the UV boundary conditions), we say that the theory is *finely tuned*, with $\epsilon_{\rm IR}$ providing a measure of the degree of fine-tuning. In our example:

$$\epsilon_{\rm IR} \approx \epsilon_{\rm UV} \frac{\tilde{\lambda}}{8\pi^2} \frac{M^2}{m_H^2(v)} \log\frac{\Lambda_{\rm UV}}{M} \sim \epsilon_{\rm UV} \frac{M^2}{8\pi^2 m_H^2(v)} \ , \tag{1.12}$$

where in the last step we have assumed that both $\tilde{\lambda}$ and the log are $\mathcal{O}(1)$. Eq.(1.12) illustrates how if there is new physics at some high scale M that interacts with the Higgs with an $\mathcal{O}(1)$ coupling, the theory becomes finely tuned as soon as $M \gtrsim 1$ TeV (roughly a loop factor above the weak scale). In particular, if $M \sim m_{Pl}$, then

[2] In renormalization schemes that are independent of the mass of the particles, like the hard cut-off used here, the decoupling theorem [19] needs to be introduced 'by hand' in the RG equations in this way.

$\epsilon_{\rm IR} \sim \epsilon_{\rm UV} 10^{30}$, and we would need to specify the UV boundary condition to an accuracy of roughly 1 part in 10^{30} for the IR limit of the theory to be consistent with experimental observations. *This is the electroweak hierarchy problem.* Although we have illustrated how fine-tuning arises through an interaction with a scalar field, the form of Eqs.(1.10)-(1.12) would be the same in the case of fermions and gauge bosons, up to signs and $\mathcal{O}(1)$ factors.

It is worth emphasizing that an electroweak hierarchy problem does *not* arise in the context of the SM. If, defying expectations, the true theory of nature consisted of the SM of particle physics plus classical General Relativity, then no such problem exists. In the context of a fully renormalizable theory like the SM, quantum corrections to the Higgs mass-squared that are formally quadratically divergent are renormalized away by adding the appropriate counter-terms, as we have illustrated. Since the largest physical energy scale of the SM is the weak scale itself, the finite radiative corrections to the Higgs mass are of precisely that same order.

Any solution to the electroweak hierarchy problem must therefore (i) introduce new dynamics that remove the quadratic sensitivity of the Higgs mass-squared parameter to physics present at scales $M \gg v$, and (ii) it must do so at a scale not far from ~ 1 TeV for the solution to be natural.

In the following, we will define the degree of fine-tuning of a given theory as

$$\Delta \equiv \left| \frac{m_H^2(v)}{\delta m_H^2} \right| = \frac{1}{2} \frac{m_h^2}{|\delta m_H^2|} \sim \epsilon_{\rm IR}^{-1} \ , \tag{1.13}$$

where δm_H^2 refers to the radiative corrections to the Higgs mass-squared parameter in the IR (the second term of eq.(1.11) in our example). Intuitively, our definition of fine-tuning corresponds to the inverse of the parameter $\epsilon_{\rm IR}$ that we introduced in order to asses the sensitivity of physics at large distances to UV boundary conditions.

1.3 Supersymmetry

1.3.1 Basic structure

Supersymmetry (SUSY) is a symmetry of space-time that arises as the only possibility for a non-trivial extension of the Poincaré group if the original assumptions in the Coleman-Mandula theorem [20] are relaxed to allow for anti-commuting generators [21]. The minimum possible amount of SUSY in 4 dimensions, referred to as $\mathcal{N} = 1$, contains two two-component spinor generators Q_α and $Q^\dagger_{\dot{\alpha}}$, with commutator relations

$$[Q_\alpha, P_\mu] = 0 \qquad [Q_\alpha, M_{\mu\nu}] = (\sigma_{\mu\nu})^\beta_\alpha Q_\beta \tag{1.14}$$

$$\{Q_\alpha, Q^\dagger_{\dot{\beta}}\} = 2(\sigma^\mu)_{\alpha\dot{\beta}} P_\mu \qquad \{Q_\alpha, Q_\beta\} = 0 \ , \tag{1.15}$$

where P_μ and $M_{\mu\nu}$ are the generators of space-time translations and Lorentz transformations respectively, and $\sigma_{\mu\nu} \equiv \frac{i}{4}(\sigma_\mu \overline{\sigma}_\nu - \sigma_\nu \overline{\sigma}_\mu)$.

Irreducible representations of the SUSY algebra, known as *supermultiplets*, contain fields related to each other by the action of Q_α and $Q^\dagger_{\dot{\alpha}}$. Since these are spinors themselves, single-particle states within a given supermultiplet, known as *superpartners*, have spins that differ by 1/2. On the other hand, the SUSY generators have trivial commutation relations with P_μ, and also with the generators of any internal symmetry group, including those of gauge symmetries. As a result, superpartners have equal mass, and transform under the same representation of the gauge group. There are two types of supermultiplets relevant in $\mathcal{N} = 1$ SUSY: chiral and vector multiplets. On-shell, the former contains one two-component Weyl fermion and a complex scalar, whereas the latter is made of one massless gauge boson and a Weyl fermion – both multiplets contain two fermionic and two bosonic degrees of freedom. As a consequence of imposing SUSY as a symmetry of space-time, the number of degrees of freedom in the theory doubles, with the new states having spins that differ by 1/2 compared to those of the original particles.

Its special status as the only possible non-trivial extension of the Poincaré group provides a good motivation for considering SUSY a symmetry of nature, and it is

reinforced by the fact that it appears to be a necessary ingredient in order to build consistent string theories that contain fermions (see e.g. [22, 23]). SUSY, however, cannot be an exact symmetry of nature – if it was, the superpartners of ordinary particles would have the same mass as their SM counterparts, a possibility that is experimentally ruled out. If the scale of SUSY breaking is not far above the weak scale, and the symmetry is broken *softly*, then SUSY provides a predictive framework for gauge coupling unification [24–26], and, most importantly for our discussion, can solve the electroweak hierarchy problem [25].

To illustrate how softly broken SUSY provides a solution to the hierarchy problem, let's look at a toy example first. Consider a real scalar field ϕ, with mass-squared m_ϕ^2, two complex scalars φ_1 and φ_2, and a Dirac fermion f. The mass of the fermion is M, and we write the mass-squared of the complex scalars as $M_s^2 = M^2 + \tilde{m}^2$, with $M, M_s \gg m_\phi$. All of them have couplings to ϕ, of the form

$$\mathcal{L} \supset -\frac{\tilde{\lambda}}{2}\phi^2(|\varphi_1|^2 + |\varphi_2|^2) - \tilde{\mu}\phi(|\varphi_1|^2 + |\varphi_2|^2) - \frac{y}{\sqrt{2}}\phi\overline{f}f \ . \tag{1.16}$$

The one-loop RG equation for m_ϕ^2 due to the interactions in eq.(1.16) reads

$$\frac{dm_\phi^2(\mu)}{d\log\mu} = \frac{\tilde{\lambda}}{4\pi^2}M_s^2 + \frac{\tilde{\mu}^2}{4\pi^2} - \frac{3y^2}{4\pi^2}M^2 \ . \tag{1.17}$$

If the quartic and cubic couplings are given by $\tilde{\lambda} = y^2$, and $\tilde{\mu} = \sqrt{2}yM$, then

$$\frac{dm_\phi^2(\mu)}{d\log\mu} = \frac{y^2}{4\pi^2}(M_s^2 - M^2) = \frac{y^2}{4\pi^2}\tilde{m}^2 \ . \tag{1.18}$$

The mass-squared parameter m_ϕ^2 is only sensitive to the mass difference between scalars and fermions, and the quadratic sensitivity to the overall mass scale M that we encountered in eq.(1.10) is no longer present, due to a cancellation between the contributions from scalar and fermion degrees of freedom. The value of m_ϕ^2 in the IR will only be logarithmically sensitive to M, and even this dependence will disappear in the limit $\tilde{m}^2 \to 0$, in which fermion and scalars have the same mass.

The relations we had to impose among the different couplings ($\tilde{\lambda} = y^2$ and $\tilde{\mu} = \sqrt{2}yM$) are actually a requirement if the theory is supersymmetric. The interactions

in eq.(1.16) can then be written in a manifestly supersymmetric form as arising from terms in the superpotential, $W \supset y\Phi\Phi_1\Phi_2 + M\Phi_1\Phi_2$. ($\Phi$ refers to the chiral superfield whose scalar component has real part ϕ, and $\Phi_{1,2}$ are chiral superfields with scalar and fermion components $\varphi_{1,2}$ and $\psi_{1,2}$ respectively, the two Weyl spinors forming the Dirac fermion f.) In order to make the scalars $\varphi_{1,2}$ heavier than the fermion, we had to break SUSY. In our example, this breaking would just amount to adding an extra term in the lagrangian, of the form

$$\mathcal{L}_{\text{soft}} = -\tilde{m}^2(|\varphi_1|^2 + |\varphi_2|^2) \ . \tag{1.19}$$

We refer to this type of breaking as soft because, as we have illustrated in eq.(1.18), it does not introduce a quadratic sensitivity of m_ϕ^2 to the overall mass scale M – only a mild logarithmic dependence remains. This is in contrast to what would happen if the breaking had been *hard*: if we had instead broken SUSY by modifying the quartic coupling between scalars, by having $\tilde{\lambda} = y^2 + \delta y^2$, then the right-hand side of eq.(1.18) would now include a term $\propto \delta y^2 M^2$, and a quadratic sensitivity to M would have been reintroduced. This toy model illustrates the basics of how softly broken SUSY provides a solution to the electroweak hierarchy problem.

It is worth noting that, if M is not very large, then soft breaking and hard breaking may lead to a comparable degree of fine-tuning. However, soft breaking is advantageous from the point of view of building a UV complete theory, since we can consider physics at arbitrarily high scales while maintaining the quadratic insensitivity of the Higgs mass-squared parameter.

1.3.2 The MSSM and fine-tuning

The Minimal Supersymmetric Standard Model (MSSM) is the minimal extension of the SM that includes SUSY (for excellent reviews on the topic see e.g. [27, 28] and references therein). It consists of 4-dimensional, $\mathcal{N} = 1$ SUSY, with the particles of the SM promoted to being one of the components of a given supermultiplet. The fermions of the SM are now part of chiral multiplets, with the scalar components being referred to as *sfermions*, whereas the vector bosons are now part of vector

multiplets, with *gauginos* being their fermionic counterparts. In the MSSM, the Higgs sector needs to be somewhat extended: two Higgs chiral superfields need to be introduced, H_u and H_d, with hypercharge assingments $+1/2$ and $-1/2$ respectively. The need for two Higgs multiplets with opposite hypercharge arises from the requirement that all gauge anomalies be cancelled, and also as a model building necessity in order to write Yukawa couplings to both up-type quarks (involving H_u) and also to down-type quarks and leptons (for which H_d is required) as holomorphic couplings in the superpotential. In the MSSM, the scalar components of both H_u and H_d get non-zero vev's, subject to the condition $v_u^2 + v_d^2 = v^2 \simeq (246 \text{ GeV})^2$, and the ratio of the two vev's is typically referred to as $\tan\beta \equiv v_u/v_d$. We will focus on the limit of large $\tan\beta$, in which $v \simeq v_u$ and the discussion of electroweak fine-tuning is largely simplified.

The terms in the MSSM superpotential relevant to our discussion read

$$W_{\text{MSSM}} \supset y_t Q_3 H_u \overline{u}_3 + \mu H_u H_d \ , \tag{1.20}$$

where $Q_3 = (T_3, B_3)^T$ and $\overline{u}_3$ are the electroweak doublet and singlet superfields corresponding to the top sector, and the μ-term is required to render the fermionic partners of the Higgs, the *higgsinos*, massive. Terms in the scalar lagrangian that involve the neutral component of H_u arising from eq.(1.20) read

$$\mathcal{L} \supset -|\mu|^2 |H_u^0|^2 - y_t^2 |H_u^0|^2 (|\tilde{t}_L|^2 + |\tilde{t}_R|^2) \ , \tag{1.21}$$

where $\tilde{t}_L$ and $\tilde{t}_R$ correspond to the scalar components of T_3 and $\overline{u}_3$ respectively. From the first term in eq.(1.21) we can already see a source of trouble: the μ-term of eq.(1.20) translates into a mass-squared for H_u that is positive, therefore not allowing for electroweak symmetry breaking at tree-level.

For phenomenological reasons, the interactions encoded in the superpotential of eq.(1.20) need to be extended to include SUSY breaking. The most important terms for the discussion of electroweak naturalness in the SUSY breaking lagrangian of the

MSSM read

$$\mathcal{L}_{\text{soft}} \supset -m_{H_u}^2 |H_u|^2 - \tilde{m}_t^2 (|\tilde{t}_L|^2 + |\tilde{t}_R|^2) - \frac{1}{2}(M_3 \tilde{g}\tilde{g} + \text{h.c.}) \ . \tag{1.22}$$

The first and second terms correspond to SUSY breaking mass-squared parameters for the Higgs and stops respectively,[3] whereas the last piece is a Majorana mass term for the fermionic partners of the gluons, the so-called *gluinos*. All these terms amount to a soft breaking of SUSY.

It is clear now that the Higgs mass-squared parameter will receive contributions from different sources: from the supersymmetric $|\mu|^2$ piece, from a potential SUSY breaking contribution $m_{H_u}^2$ present at tree-level, and from radiative corrections involving the superpartners of the SM particles, the largest of which comes from the top/stop sector (due to the large Yukawa coupling $y_t \approx 1$, and the colour multiplicity factor). In order to avoid fine-tuning, all these contributions cannot be much above the weak scale. We now turn to the challenges this poses for theories with MSSM-like structure. (For detailed and extensive discussions on this topic, see [29–35].)

(*i*) **The μ-problem.** At tree level, the Higgs mass-squared parameter arising from the terms in eq.(1.20) and eq.(1.22) is given by $\mathcal{L} \supset -(|\mu|^2 + m_{H_u}^2)|H_u^0|^2$. In order to avoid fine-tuning already at tree-level, one needs $\mu \sim 100$ GeV, and of the same order as a potential SUSY breaking term m_{H_u}. However, the μ-term is a supersymmetric parameter that in principle has nothing to do with any source of SUSY breaking, and is, *a priori*, unrelated to the value of the weak scale. To avoid tuning, one therefore needs a dynamical mechanism that generates a μ-term of the required size. Although possible, see e.g. [36–38], this introduces additional model-building difficulties in MSSM-like theories.

(*ii*) **Low tuning vs. a 125 GeV Higgs.** The leading radiative correction to

[3] We could have of course written different SUSY breaking mass terms for $\tilde{t}_L$ and $\tilde{t}_R$, but the qualitative features of the discussion that follows would remain unchanged, so we focus on the case of equal stop masses for clarity.

the Higgs mass-squared parameter in the IR comes from the stop sector:

$$\frac{dm_{H_u}^2(\mu)}{d\log\mu} = \frac{3y_t^2}{4\pi^2}\tilde{m}_t^2 + \ldots \quad \Rightarrow \quad \delta m_{H_u}^2 \sim -\frac{3y_t^2}{4\pi^2}\tilde{m}_t^2 \log\frac{\Lambda_{\rm SUSY}}{\tilde{m}_t} \ , \tag{1.23}$$

where $\Lambda_{\rm SUSY}$ refers to the scale at which SUSY breaking is communicated to the SM. From eq.(1.23), it is clear that for low fine-tuning we would need light stops, as well as a low SUSY-breaking scale.

On the other hand, the tree-level quartic coupling of the Higgs is given by $\lambda_{\rm tree} = (g^2 + g'^2)/8$, and so the physical Higgs mass, in the large $\tan\beta$ limit, is given by $m_{h,\rm tree}^2 \simeq 2v^2\lambda_{\rm tree} = m_Z^2$ – well below the experimental measurement. The leading radiative contribution to the Higgs quartic coupling comes from the top/stop sector, and reads (focusing only on the leading logarithmic piece):

$$\delta\lambda \simeq \frac{3y_t^4}{16\pi^2}\log\frac{\tilde{m}_t^2 + m_t^2}{m_t^2} \approx \frac{3y_t^4}{16\pi^2}\log\frac{\tilde{m}_t^2}{m_t^2} \ , \tag{1.24}$$

leading to a change in the physical Higgs mass given by

$$\delta m_h^2 = 2v^2\delta\lambda \approx \frac{3m_t^2 y_t^2}{4\pi^2}\log\frac{\tilde{m}_t^2}{m_t^2} \ . \tag{1.25}$$

The radiative contribution to the physical Higgs mass from the top/stop sector is only logarithmically dependent on the stop mass. Thus, to achieve a phenomenologically viable Higgs, it seems like we would prefer heavy stops, well into the TeV regime (see [39–41] for detail computations and extended discussion), and in direct contradiction with the requirements of naturalness.

(*iii*) **The gluino 'sucks' problem.** Even if there were other interactions that lifted the Higgs mass to its observed value, so that the stops could remain light, such a situation would be a fine-tuned affair within the MSSM. It turns out that the stop mass-squared parameter also receives large radiative corrections from the gluino sector, of the form

$$\frac{d\tilde{m}_t^2(\mu)}{d\log\mu} = -\frac{8\alpha_s}{3\pi}|M_3|^2 + \ldots \quad \Rightarrow \quad \delta\tilde{m}_t^2 \sim \frac{8\alpha_s}{3\pi}|M_3|^2\log\frac{\Lambda_{\rm SUSY}}{|M_3|} \ , \tag{1.26}$$

which implies that $\tilde{m}_t \sim M_3$ is the natural value for the stop mass at large distances. This feature of the gluino driving the stop mass in the IR all the way up to $\sim M_3$ within a few decades of RG evolution (even if $\tilde{m}_t(\Lambda_{\rm SUSY}) = 0$) is known as the gluino 'sucks' problem [30]. Given that limits on gluino masses can be as stringent as ~ 2 TeV in the MSSM [42], this would lead to a fine-tuning of order

$$\Delta = \frac{1}{2}\frac{m_h^2}{|\delta m_H^2|} \simeq \frac{1}{2}\frac{m_h^2}{\frac{3y_t^2}{4\pi^2}\tilde{m}_t^2 \log\frac{\Lambda_{\rm SUSY}}{\tilde{m}_t}} \simeq 1\% \ , \tag{1.27}$$

where in the last step we have taken $\tilde{m}_t = 2$ TeV, and $\Lambda_{\rm SUSY} = 10\tilde{m}_t$ (only a decade above the stop mass). The fine-tuning is already at the 1% level, even for a relatively low SUSY-breaking scale.

Whereas there is nothing inconsistent with a theory that is finely-tuned at the percent level, it starts becoming disappointing. As we have seen, the bad level of fine-tuning in theories like the MSSM is directly related to the stringent bounds that experiments like the LHC set on the masses of coloured SM partners. If we could have SM partners that cancelled the quadratic sensitivity of the Higgs mass-squared to high scales but that were not charged under the SM gauge group, then experimental bounds on the masses of the new particles would not be anywhere near as stringent, which could potentially allow for a much more comfortable level of fine-tuning. This is the basic idea of Neutral Naturalness, a term that encodes theories in which the SM partners responsible for protecting the Higgs potential from large radiative corrections are neutral under SM gauge interactions. The prime example of such theories are models based on the Twin Higgs mechanism, which we explore in the remainder of this chapter.

1.4 Twin Higgs

The Twin Higgs idea is an alternative (partial) solution to the electroweak hierarchy problem, in which the Higgs is realised as a pNGB of an approximate global symmetry [43–45]. It requires the presence of a hidden sector that is an exact copy of the SM, and it is based on the idea that a discrete $\mathbb{Z}_2$ operates between the two sectors, enforcing field content and couplings to be equal. On top of the discrete $\mathbb{Z}_2$,

the scalar potential of Twin Higgs theories features an approximate global $SU(4)$, which arises as an accidental symmetry at the level of the quadratic terms as a consequence of the discrete $\mathbb{Z}_2$. This $SU(4)$ global symmetry is broken both spontaneously and explicitly, and a light pNGB remains in the spectrum, which is then identified with the Higgs particle. The role of the $\mathbb{Z}_2$ is then to ensure that radiative corrections to the mass-squared parameter in the scalar potential that are quadratically sensitive to UV scales remain $SU(4)$ symmetric, thus not contributing to the pNGB potential. In this way, Twin Higgs theories manage to solve the hierarchy problem up to scales $\Lambda \approx 5 - 10$ TeV, at which new dynamics that preserve the $\mathbb{Z}_2$ must appear to keep the theory natural. We discuss in detail the basic idea behind the Twin Higgs mechanism in section 1.4.1. In section 1.4.2 we explore its minimal realization, the so-called Fraternal Twin Higgs [46], which is the framework in which the work presented in chapters 3 and 4 was developed.

1.4.1 The Twin Higgs Mechanism

The Twin Higgs mechanism [43–45] requires the presence of a hidden sector – the *twin* sector – that mirrors the SM both in terms of field content and interactions, as enforced by the discrete $\mathbb{Z}_2$ symmetry that operates between the two sectors.[4] The Higgs doublets of the visible and twin sectors (H and H' respectively) can be arranged as $\mathcal{H} = (H, H')^T$, and the scalar potential of the theory respects a global $SU(4)$ symmetry, under which $\mathcal{H}$ transforms as a fundamental. At tree-level, the scalar potential can be written as

$$V = m_{\mathcal{H}}^2 \mathcal{H}^\dagger \mathcal{H} + \lambda (\mathcal{H}^\dagger \mathcal{H})^2 \ , \tag{1.28}$$

with $m_{\mathcal{H}}^2 < 0$. This leads to a non-zero vev $\langle |\mathcal{H}|^2 \rangle = -m_{\mathcal{H}}^2/(2\lambda) \equiv f^2/2$, that breaks the $SU(4)$ symmetry spontaneously down to $SU(3)$. As a result, 7 NGBs arise, 6 of which become the longitudinal polarizations of the Z and $W^\pm$ vector bosons of the SM and twin sectors. Two real scalar degrees of freedom then remain in the spectrum: the remaining NGB (h) that will be identified with the Higgs, and a

[4] We refer to the twin sector (both their particles and gauge group) with a prime symbol.

heavy scalar (h') with mass $\sqrt{2\lambda}f$.

The global $SU(4)$ symmetry is further broken explicitly, by the gauging of a $SU(2) \times SU(2)$ subgroup of $SU(4)$ (these $SU(2)$ components to be identified with the SM and twin gauge groups $SU(2)_L$ and $SU(2)'_L$), and by Yukawa couplings to fermions. As a result, radiative corrections lead to a quartic term in the potential that is $SU(4)$-breaking but $\mathbb{Z}_2$-preserving, of the form

$$V \supset \eta(|H|^4 + |H'|^4) \ . \tag{1.29}$$

This leads to both Higgs doublets getting a vev of the same size, $\langle|H|^2\rangle = \langle|H'|^2\rangle = f^2/4$, and the former NGB now gets a mass proportional to the $SU(4)$-breaking quartic, $m_h^2 = \eta f^2$. However, the physical mass-eigenstates are given by

$$h = \frac{1}{\sqrt{2}}(h_0 - h'_0) \qquad h' = \frac{1}{\sqrt{2}}(h_0 + h'_0) \ , \tag{1.30}$$

where h_0 (h'_0) refers to the real neutral component of the H (H') doublet – the two physical scalars are an equal admixture of visible and hidden sector states.

Since a phenomenologically viable model must have a Higgs that couples dominantly to the visible sector, a source of $\mathbb{Z}_2$-breaking must be included, that allows the two vev's to differ. We may do this by introducing a mass-squared term only for H, of the form:

$$V \supset \tilde{\mu}^2|H|^2 \ , \tag{1.31}$$

which amounts to a soft breaking of the $\mathbb{Z}_2$ symmetry. Now, carefully choosing the parameter $\tilde{\mu}^2 > 0$ allows for the two vev's to be different, such that

$$\langle|H|^2\rangle \equiv \frac{v^2}{2} \ll \frac{f^2}{2} \qquad \langle|H'|^2\rangle = \frac{1}{2}(f^2 - v^2) \simeq \frac{f^2}{2} \ , \tag{1.32}$$

which requires $\tilde{\mu}^2 = \eta(f^2 - 2v^2) \simeq \eta f^2$, and the masses of the two scalar states are now $m_h^2 \simeq 4\eta v^2$ and $m_{h'}^2 \simeq 2\lambda f^2$. The need to introduce a $\mathbb{Z}_2$-breaking term constitutes a source of fine-tuning in these kind of theories, which may be estimated

as

$$\Delta = \frac{1}{2}\frac{m_h^2}{\tilde{\mu}^2} \simeq \frac{1}{2}\frac{4\eta v^2}{\eta f^2} = \frac{2v^2}{f^2} \ . \tag{1.33}$$

The two propagating scalars are now given by

$$h = h_0 \cos\left(\frac{v}{f}\right) - h_0' \sin\left(\frac{v}{f}\right) \qquad h' = h_0' \cos\left(\frac{v}{f}\right) + h_0 \sin\left(\frac{v}{f}\right) \ , \tag{1.34}$$

so that for small v/f, h (h') is mostly made of visible (twin) gauge eigenstates. From eq.(1.34), we can see that Higgs couplings to visible sector states will be modified from the SM prediction by a factor of $\cos(v/f) \simeq 1 - v^2/(2f^2)$, whereas those to hidden sector particles are suppressed by a factor $\sin(v/f) \simeq v/f$.

The light Higgs being a small admixture of SM and twin gauge eigenstates, as specified in eq.(1.34), is crucial for experimental exploration of Twin Higgs theories – it provides the only portal of interactions between the two sectors. At colliders like the LHC, twin particles will only be produced through this 'Higgs portal', and thus their production cross sections are much smaller than those of extra states present in other solutions to the hierarchy problem in which the new particles are charged under the SM gauge group. Similarly, produced twin particles will only be able to decay back into SM degrees of freedom through their interactions with the Higgs. As a result, experimental bounds from direct searches on the masses of twin particles are basically non-existent, and definitely irrelevant regarding fine-tuning considerations [47] – in stark contrast with the situation in SUSY models as a result of the stringent bounds on coloured sparticles like gluinos, as discussed in section 1.3.2. Instead, the leading experimental constraints on these models stem from measurements of Higgs properties. In particular, precision measurements of Higgs couplings to visible sector states, as well as bounds on the Higgs invisible branching fraction, put a lower bound on $f/v \gtrsim 3$ [46], corresponding to a mild 20% tuning. Even by the end of the LHC this bound will not be larger than $f/v \gtrsim 5$, driving the level of tuning only up to around 10% [47] – still within the domain of naturalness. As we will discuss in chapters 3 and 4, the Higgs portal between SM and twin sectors will also drive most of the Dark Matter phenomenology of Twin Higgs theories.

To illustrate explicitly how the Twin Higgs mechanism solves the electroweak hierarchy problem, and to what extent it is a successful solution, let's consider two complex scalar fields φ and φ', with masses M and M' respectively (with $M, M' \gg f$), and with couplings to H and H' of the form

$$\mathcal{L} \supset -\tilde{\lambda}|H|^2|\varphi|^2 - \tilde{\lambda}'|H'|^2|\varphi'|^2 \ . \tag{1.35}$$

Radiative corrections to the quadratic terms in the scalar potential arising from these interactions read (remember eq.(1.11))

$$\Delta V \simeq -\frac{\tilde{\lambda}}{8\pi^2} M^2 \log\frac{\Lambda_{\rm UV}}{M}|H|^2 - \frac{\tilde{\lambda}'}{8\pi^2} M'^2 \log\frac{\Lambda_{\rm UV}}{M'}|H'|^2 \ . \tag{1.36}$$

Crucially, if $\tilde{\lambda}' = \tilde{\lambda}$, and $M' = M$, as would be imposed by an exact $\mathbb{Z}_2$ symmetry between the two sectors, then the above equation can be written as

$$\Delta V \simeq -\frac{\tilde{\lambda}}{8\pi^2} M^2 \log\frac{\Lambda_{\rm UV}}{M}(|H|^2 + |H'|^2) = -\frac{\tilde{\lambda}}{8\pi^2} M^2 \log\frac{\Lambda_{\rm UV}}{M}|\mathcal{H}|^2 \ , \tag{1.37}$$

i.e. radiative corrections to the mass-squared term that are quadratically sensitive to higher mass scales are fully $SU(4)$ symmetric, thanks to the discrete $\mathbb{Z}_2$, and therefore do not contribute to the Goldstone potential.[5] In essence, this is the Twin Higgs mechanism.

This example, however, also clarifies the limitations of the Twin Higgs idea. Keeping v^2 tuned to its observed value, quantum corrections to the quadratic term in the potential of the form shown in eq.(1.37) translate into a natural value of the twin vev f given by

$$\lambda f^2 \simeq |\delta m_{\mathcal{H}}^2| \simeq \frac{\tilde{\lambda}}{8\pi^2} M^2 \log\frac{\Lambda_{\rm UV}}{M} \ . \tag{1.38}$$

The natural value for f is then, roughly, no more than a loop factor below the scale at which new physics is present. Thus, for the tuning between v and f to be the only significant source of fine-tuning, and if we demand Δ to be in the $10 - 20\%$ range, then the theory needs to be UV-completed at some scale $\Lambda \approx 5 - 10$ TeV

[5] The interactions in eq.(1.35) will also generate an $SU(4)$-breaking, but $\mathbb{Z}_2$-preserving, quartic coupling, of the form of eq.(1.29). However, these will only be logarithmically sensitive to UV scales.

with some new dynamics that respect the discrete $\mathbb{Z}_2$. The Twin Higgs mechanism alone then succeeds in stabilizing the electroweak scale up to a cut-off Λ. We call this a solution to the *little* hierarchy problem, since it only maintains naturalness up to scales well below m_{Pl}.[6]

The extent to which the discrete $\mathbb{Z}_2$ symmetry is broken when it comes to interactions involving heavy states constitutes an additional source of fine-tuning – on top of the 'v/f-tuning' of eq.(1.33), and the 'f-tuning' of eq.(1.38). Such breaking could happen softly, for instance by having $M' \neq M$ in our example, or it could be a hard breaking, as would happen if $\tilde{\lambda}' \neq \tilde{\lambda}$. Although we expressed a preference for soft versus hard breaking of a symmetry in our discussion of SUSY, in theories with a relatively low cut-off, as is the case for Twin Higgs models, a hard breaking may still be consistent with naturalness.

In the following, we explore the minimal implementation of the Twin Higgs idea that allows for a low level of fine-tuning – the so-called Fraternal Twin Higgs [46]. This minimal senario precisely exploits the fact that, since the theory only provides a solution to the little hierarchy problem, a hard breaking of the $\mathbb{Z}_2$ by not mirroring all the particles of the SM in the twin sector is still compatible with a low level of tuning.

1.4.2 Fraternal Twin Higgs

The Fraternal Twin Higgs scenario corresponds to the minimal realization of the Twin Higgs idea, as far as naturalness is concerned, and it is based on the observation that a low level of tuning does not require a twin sector that is a complete copy of the SM, with partial matter and gauge content sufficing. The philosophy behind the Fraternal Twin Higgs idea is thus to include only those degrees of freedom that, if absent, would lead to an unacceptably large level of tuning, assuming the theory is UV-completed at scales $\Lambda \approx 5 - 10$ TeV. The Fraternal Twin Higgs was introduced in [46], and apart from a twin Higgs doublet, whose presence is at the core of the

[6] Several UV completions of Twin Higgs theories have been explored, either by invoking SUSY [48–50], compositeness [51–54], or other more exotic possibilities [55,56]. In this work, we will only be concerned with the effective theory below scale Λ, where the relevant degrees of freedom are just the SM particles plus their twin sector counterparts.

Twin Higgs mechanism, it also requires a twin top sector, twin $SU(2)'_L$ interactions, and a twin $SU(3)'$ gauge group.

The requirement of a twin top sector (both an $SU(2)'_L$ doublet $Q'_3 = (t'_L, b'_L)^T$ and singlet t'_R), can be readily understood by considering radiative corrections to the Higgs mass-squared parameter from new heavy states related to the top sector of the SM. Such new degrees of freedom could be the extra partners arising from whatever UV-completion takes over at scale Λ. In order to parametrize the form of such contributions, we can use a hard cut-off when computing the one-loop correction to the Higgs two-point function from the SM top itself – the quadratically divergent piece will be, parametrically, indicative of the size of the contributions arising from whatever new states are present at scale Λ. One finds

$$\Delta V \simeq -\frac{3y_t^2}{8\pi^2}\Lambda^2|H|^2 \ . \tag{1.39}$$

Eq.(1.39) reflects how the absence of a twin top sector corresponds to a hard breaking of the $\mathbb{Z}_2$, since the $SU(4)$-breaking mass-squared term is now quadratically senstive to the UV scale Λ. This would lead to a level of fine-tuning

$$\Delta \simeq \frac{1}{2}\frac{m_h^2}{\frac{3y_t^2}{8\pi^2}\Lambda^2} \lesssim 1\% \left(\frac{5 \text{ TeV}}{\Lambda}\right)^2 \ , \tag{1.40}$$

i.e. worse than 1% for a cut-off of just 5 TeV!

Such fine-tuning is clearly unacceptable, therefore requiring the presence of a twin top, with twin Yukawa coupling $y_{t'}$. Now, radiative corrections to the quadratic term in the scalar potential from hypothetical new states present at the cut-off take the form

$$\Delta V \simeq -\frac{3{y_{t'}}^2}{8\pi^2}\Lambda^2|\mathcal{H}|^2 + \frac{3({y_{t'}}^2 - y_t^2)}{8\pi^2}\Lambda^2|H|^2 \ . \tag{1.41}$$

Whereas the first term in this equation is $SU(4)$ symmetric, the last one is not, as a result of the hard $\mathbb{Z}_2$-breaking we have introduced by allowing the two top Yukawa couplings to differ, and will contribute to the level of fine-tuning. If we demand this source of tuning be better than $\sim 20\%$ (so that it is subleading to the v/f-tuning of eq.(1.33)), then the value of the two Yukawa couplings at the cut-off scale must

be rather similar. In particular, for $\Lambda \approx 5$ TeV, we find

$$\frac{|y_{t'}(\Lambda) - y_t(\Lambda)|}{y_t(\Lambda)} \lesssim 1\% \ , \tag{1.42}$$

i.e. they must be within 1% of each other.

Similarly, only gauging the $SU(2)_L$ group of the SM would lead to an unacceptable level of fine-tuning, and even two-loop corrections involving gluons are large enough that a twin QCD gauge group is also required by naturalness. Low tuning thus requires $SU(2)_L$ and $SU(3)$ gauge interactions be mirrored in the twin sector, and, for a 5 TeV cut-off, the corresponding twin gauge couplings in the UV must be within 10% and 20% of those in the SM, respectively. Moreover, once the $SU(2)'_L$ and $SU(3)'$ groups are gauged, anomaly cancellation requires the presence of a coloured $SU(2)'_L$ singlet b'_R, and a lepton $SU(2)'_L$ doublet $L'_3 = (\nu'_L, \tau'_L)^T$. RH leptons ν'_R and τ'_R may be added to the theory in order to render twin leptons massive, although they are not required by anomaly cancellation or naturalness arguments.

Gauging twin hypercharge is not required by naturalness either, although it would remain an accidental global symmetry of the twin sector. Similarly, the smallness of all other Yukawa couplings compared to y_t, means that first and second generation fermions need not be mirrored in the twin sector. Moreover, naturalness only requires Yukawa couplings of the twin fermions present (other than the twin top) to be $\ll y_t \approx 1$, but otherwise they largely remain free parameters of the effective theory.

In summary, the Fraternal Twin Higgs scenario contains: twin $SU(2)'_L$ and $SU(3)'$ interactions, a twin Higgs doublet H', twin tops and bottom quarks (Q'_3, t'_R, and b'_R), and a twin lepton doublet L'_3. This is the framework in which the work described in chapters 3 and 4 is realised, although we will also consider the presence of twin RH leptons for convenience.

The presence of a twin colour gauge group, as required by naturalness, is a particularly interesting feature of Fraternal Twin Higgs models, and it drives much of their phenomenology [46, 57]. With only two quark flavors (t' and b'), the $SU(3)'$ gauge group will confine in the IR, just as happens in the SM, but the smaller

matter content of the twin sector leads to a more negative β-function coefficient for the twin gauge coupling g'_3. In the UV, far above any particle thresholds, the one-loop β-function for the twin gauge coupling reads

$$\frac{d\alpha'_3(\mu)}{d\log\mu} = -\frac{b'_3{\alpha'_3}^2}{2\pi} \ , \tag{1.43}$$

with $b'_3 = 29/3 > b_3 = 7$ (remember eq.(1.1)). As a result, even if the two gauge couplings are approximately equal in the UV, i.e. $g'_3(\Lambda) \approx g_3(\Lambda)$, g'_3 will run towards larger values faster (i.e. within less decades of RG evolution), and the twin colour sector will reach the regime of strong coupling at higher scales than its SM counterpart. The prediction of a confining gauge group with a twin confinement scale $\Lambda'_{\rm QCD} > \Lambda_{\rm QCD}$ is an inevitable consequence of Fraternal Twin Higgs theories, with the exact size of $\Lambda'_{\rm QCD}$ fixed by the requirements of minimality and naturalness alone [46].

Figure 1.1 illustrates the one-loop RG evolution of the colour gauge couplings in the SM and twin sectors, assuming $g'_3(\Lambda) = g_3(\Lambda)$ for $\Lambda = 5$ TeV. Although we have taken $f/v = 3$ and $y_{b'} = y_b$ in figure 1.1, changing the f/v ratio by an $\mathcal{O}(1)$ amount within the regime allowed by naturalness makes a negligible difference, and similarly small effects arise if one increases the value of $y_{b'}$ so long as it remains $\ll 1$. As one can appreciate from figure 1.1, the twin confinement scale $\Lambda'_{\rm QCD}$ is larger than $\Lambda_{\rm QCD}$ by around an order of magnitude. The exact value of $\Lambda'_{\rm QCD}$ is however rather sensitive to the value of g'_3 in the UV: varying the value of g'_3 in the UV by $\sim 10\%$ compared to the SM coupling results in $\Lambda'_{\rm QCD}$ changing from ≈ 1 GeV to a few 10's of GeV. (More careful calculations including two-loop effects only make an $\mathcal{O}(1)$ difference to these statements [46].)

The presence of a confining gauge group in the twin sector leads to a spectrum of bound states. If all twin quarks have masses above the scale of confinement $\Lambda'_{\rm QCD}$, then the low energy dynamics of the twin colour sector are those of a pure gauge theory, and the lightest states are glueballs. As has been made apparent by lattice studies [58–60], a rich spectrum of glueballs exists, with different J^{PC} quantum numbers, the lightest one being a scalar state with $J^{PC} = 0^{++}$, and mass

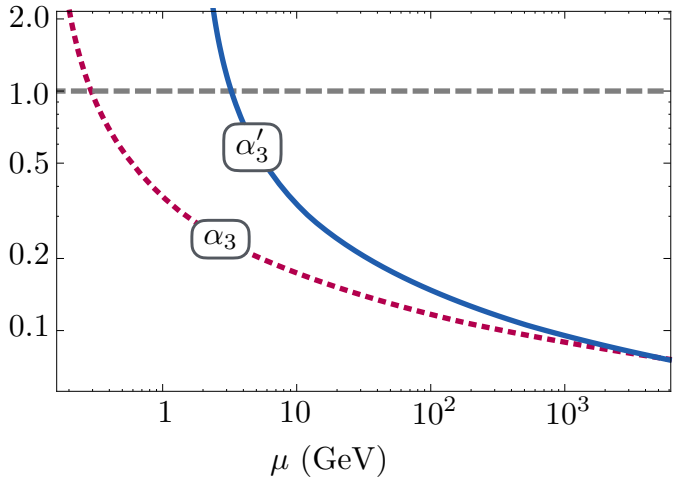

Figure 1.1: One-loop RG evolution of the SM and twin colour gauge couplings, α_3 and α_3', assuming they are equal at scale $\Lambda = 5$ TeV. Faster running of the twin gauge coupling results in a higher confinement scale, understood as the scale at which α_3' becomes unity (indicated with a horizontal dashed line).

$m_0 \simeq 6.8\Lambda'_{\rm QCD}$ [58,59]. Figure 1.2 shows the masses of some of the lightest glueballs, which can be found in terms of m_0 from computations on the lattice. Given that m_0 is fixed by the confinement scale, the value of $\Lambda'_{\rm QCD}$ is then the only ingredient necessary to specify the spectrum of twin bound states.

With the lightest glueball having the same quantum numbers as the Higgs, the two states can mix, and they indeed do so as a result of the effective coupling between the Higgs and twin gluons, arising at one-loop order through the usual triangle diagram involving quarks (mainly the top quark), but now with those of the twin sector instead. This mixing provides a decay channel for the lightest glueball, which now can decay into SM states by mixing with the Higgs, as well as for some of the heavier glueballs that may decay first to the lightest one. At colliders, this feature of Fraternal Twin Higgs models can lead to striking signatures, including displaced vertices depending on the exact value of the 0^{++} mass (equivalently, depending on the exact value of $\Lambda'_{\rm QCD}$), as was thoroughly explored in [46,57]. The mixing between the Higgs and the confining twin sector will also be of crucial importance for the Dark Matter phenomenology of this class of theories, and we discuss the relevant details in chapters 3 and 4.

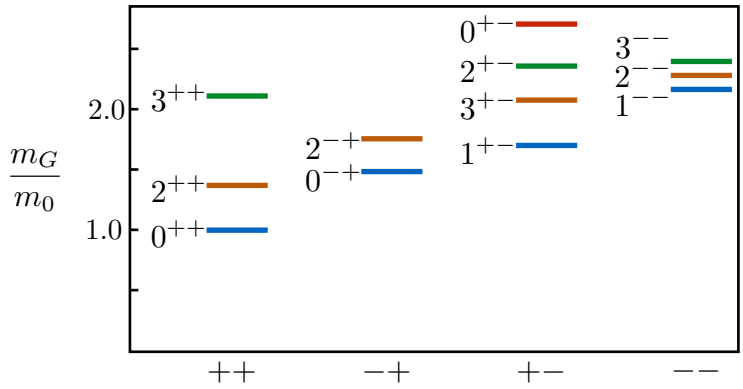

Figure 1.2: Spectrum of glueballs present in the confining phase of an $SU(3)$ pure gauge theory [58–60]. States are labelled by their J^{PC} quantum numbers, and their masses are specfied with respect to that of the lightest bound state, the 0^{++} glueball.

Chapter 2

Dark Matter

That Dark Matter (DM) accounts for roughly 25% of the content of the Universe is a claim well supported by a wide range of experimental evidence, both at galactic and cosmological scales. Moreover, it is known that the nature of this exotic form of matter must be non-baryonic, with the familiar baryonic matter only accounting for around 5% of our Universe's energy budget. However, the nature of the DM remains an unresolved mystery, and is one of the most important open problems in physics. In this chapter, we review what is known about DM, how it may have been produced in the early Universe, potential DM candidates, and the kind of experiments that are carried out to try and detect it. In following chapters, the emphasis will be on how DM may be accounted for in the context of BSM theories that provide a solution to the electroweak hierarchy problem, rather than on the details of DM detection and phenomenology.

2.1 What we know about DM

2.1.1 Observational evidence for DM

As early as the 1930s, Fritz Zwicky noticed that the radial velocities of galaxies in the Coma Cluster were much larger than would be predicted by taking into account the gravitational effects of visible matter in the Cluster [61, 62]. Although a good part of that missing matter was actually accounted for by a halo of hot gas (only observed many years later thanks to X-ray telescopes), some of it was what we refer to today as DM, and Zwicky's work provided the first hint of its existence at the scale of galaxy clusters.

On galactic scales, the most solid evidence of the existence of DM comes from measurements of rotation curves of galaxies, a work pioneered in the 1970s by Rubin and collaborators [63, 64]. If only visible matter accounted for the total mass of a

galaxy, at distances r far away from the centre of the galaxy (where the bulk of its mass concentrates), stars would move with orbital velocities $v \approx \sqrt{G_N M_{bulk}/r}$. But instead of a $v \propto r^{-1/2}$ behaviour, observations show that v remains essentially flat for very large r [65, 66]. This indicates that the amount of matter in galaxies keeps growing even very far from where most of the visible matter concentrates, leading to the conclusion that an approximately spherical halo of DM exists. Attempts to explain this 'missing mass' problem in galaxies without invoking DM have also been made, by positing that Newtonian dynamics must break down at low accelerations. This paradigm, known as Modified Newtonian Dynamics [67–69] is successful at accommodating the observed galaxy rotation curves, but seems to fail on the scale of galaxy clusters [70, 71].

Another powerful method that allows for the determination of the total mass in galaxies and galaxy clusters is gravitational lensing. Combined with observations of their visible amount of matter, gravitational lensing measurements help determine that the dominant component in these objects is in fact DM (see [72] for a review). Gravitational lensing even enables the mapping of the distribution of visible matter versus DM, the most famous example being that provided by the Bullet Cluster [73], which enables us to set constraints on the strength of the DM self-interactions, as we will discuss in section 2.1.2.

A further argument supporting the presence of DM has to do with the evolution of large scale structure. The net of galaxies and galaxy clusters we observe today has its origin in the density perturbations present at the time of recombination, when photons started to stream freely and a hotter version of the Cosmic Microwave Background (CMB) we see today was formed. After recombination took place in the early Universe, baryons could then fall into overdense regions as a result of the effects of gravity. To account for the structure we observe today, taking density perturbations at the time of recombination as our initial conditions, numerical simulations show that some form of non-baryonic matter (invisible to photons) must be present [74, 75].

This argument is further reinforced by detailed measurements of the CMB carried out by the Planck satellite, which provide the strongest piece of evidence for the

existence of DM on cosmological scales. Temperature anisotropies on the CMB carry information about the density perturbations present at the time of recombination, when the CMB was formed, and therefore about the amount of baryonic and non-baryonic matter in the Universe. Planck measurements have established that the fraction of the Universe's energy budget in the form of baryonic and DM is $\Omega_b \simeq 0.048$ and $\Omega_{\rm DM} \simeq 0.26$ respectively [76]. This result is in keeping with the value of Ω_b that can be inferred from measurements of light elements abundances (like those of D, ^{4}He, ^{7}Li) produced during Big Bang Nucleosynthesis (BBN) [77].

2.1.2 Properties of DM

All the evidence supporting the existence of DM, discussed in section 2.1.1, is of gravitational origin. So although we know that DM behaves as regular matter as far as gravity is concerned, we do not know whether it is subject to any other kind of interaction with the SM sector – albeit we hope it is, for otherwise any attempt at detecting DM in non-gravitational experiments would be doomed. We also do know that the DM must be stable on cosmological timescales, with a lifetime much larger than the age of the Universe (at least a factor of $\sim 10^8$ larger than a Hubble time [78, 79]), and very close to being electromagnetically non-interacting [80].

Another rather well-established property of the DM is that most of it must be 'cold' DM, which means it was already non-relativistic at the time of matter-radiation equality. This allows the DM to form clumps before recombination takes place, when photons start to stream freely and baryons can then surrender to gravitational collapse. If most of the DM had been relativistic at matter-radiation equality (so-called 'hot' DM), it would have washed-out density perturbations, affecting the subsequent formation of structure in a way incompatible with current observations. Constraints from DM free-streaming suggest a lower bound $m_{\rm DM} \gtrsim 1$ keV (for instance, see [81]). Notice that this lower bound on the DM mass rules out SM neutrinos as potential DM candidates, since their masses are known to be below ~ 1 eV. Therefore, explaining the origin of DM requires new degrees of freedom beyond those of the SM. Arguably, the existence of DM is the most solid piece of evidence for BSM physics.

As opposed to baryons, the DM halo structure that we observe in galaxies suggests that most of the DM must be non-dissipative. Otherwise, emission of some light state would allow the DM to cool down and collapse to a disk, in the same way that baryonic matter collapses through emission of photons. Not all of the DM, however, needs to be of this non-dissipative nature, and it is believed that a fraction of around $5-10\%$ of all the DM could have some kind of dissipative dynamics [82]. Models in which a component of the DM is dissipative arise, for example, in theories with rich dark sectors featuring a dark photon that interacts with the DM particle. Such a situation arises naturally in the context of Twin Higgs models in which the hypercharge gauge group of the SM is mirrored in the twin sector, as we will mention in chapter 4.

That the DM has to be (mostly) non-dissipative does not imply that it cannot be self-interacting. The strongest constraints on DM self-interactions are derived from studies on colliding galaxy clusters (like the Bullet Cluster), which leads to an upper bound $\sigma_{self}/m_{\rm DM} \lesssim 0.5\ {\rm cm}^2\ {\rm g}^{-1} \approx 10^{-24}\ {\rm cm}^2\ {\rm GeV}^{-1}$ [83]. Notice this is in fact a rather weak bound: in comparison, the cross section for nucleon-nucleon interactions is, parametrically, $\sigma_{\rm QCD} \sim \Lambda_{\rm QCD}^{-2} \sim 10^{-26}\ {\rm cm}^2$ – i.e. the DM may be subject to interactions even stronger than those of QCD. Suggestively, DM self-interactions towards the allowed upper bound seem to ameliorate apparent disagreement between the observed shape of galactic halos and the results of numerical simulations, as first noted in [84, 85].

2.2 DM production and candidates

Any successful DM candidate must have been produced in the early Universe in a way such that it accounts for the present DM relic abundance, $\Omega_{\rm DM} \simeq 0.258$, or, more precisely, that it does not exceed that amount.[1] A common and well-motivated assumption is that the DM was in equilibrium with the SM thermal plasma at very early times. In this work, we will assume this is indeed the case, and will focus on two possibilities for DM production that arise in this context: freeze-out production

[1] Stable states whose present relic abundace fall below $\Omega_{\rm DM} \simeq 0.258$ will still account for a fraction of all the DM. The remaining fraction will be due to some other particle species, leading to a multicomponent DM scenario.

of DM and Asymmetric DM. We review the former in section 2.2.1, following [81], and the latter in section 2.2.2. Section 2.2.3 briefly reviews other possible DM candidates.

2.2.1 Freeze-out production of DM

The assumption of thermal equilibrium between the DM and the thermal plasma implies that, at some very high temperature, annihilation and production of DM occurred efficiently as the Universe expanded. If Γ_{ann} is the rate for the annihilation process, then the assumption of thermal equilibrium holds so long as $\Gamma_{ann}(T) > H(T)$.

The DM annihilation rate is given by $\Gamma_{ann} = n_{\mathrm{DM,eq}}\langle\sigma_{ann}v\rangle$, with σ_{ann} the annihilation cross-section, $n_{\mathrm{DM,eq}}$ the equilibrium number density of the DM particles, v their velocity, and the brackets denote thermal averaging. At temperatures $T \gg m_{\mathrm{DM}}$, the DM is relativistic, $n_{\mathrm{DM,eq}} \sim T^3$ and thus the requirement $\Gamma_{ann}(T) > H(T)$ is easily satisfied. But at temperatures $T \sim m_{\mathrm{DM}}$, the DM becomes non-relativistic, and its number density is now given by

$$n_{\mathrm{DM,eq}} = g_{\mathrm{DM}} \left(\frac{m_{\mathrm{DM}}T}{2\pi}\right)^{3/2} e^{-m_{\mathrm{DM}}/T} \ , \tag{2.1}$$

i.e. it decreases exponentially as the temperature drops. As a result, $\Gamma_{ann}(T)$ eventually becomes smaller than $H(T)$ – the DM falls out of equilibrium with the thermal plasma and the annihilitation/production of DM stops.

This departure from equilibrium is known as *freeze-out*, and the temperature T_F at which $\Gamma_{ann}(T_F) = H(T_F)$ is the freeze-out temperature. For temperatures $T < T_F$, the number density (per comoving volume) of the DM remains approximately constant.

The transition from equilibrium to out-of-equilibrium dynamics is captured by the Boltzmann equation:

$$\frac{dn_{\mathrm{DM}}}{dt} + 3Hn_{\mathrm{DM}} = \langle\sigma_{ann}v\rangle(n^2_{\mathrm{DM}} - n^2_{\mathrm{DM,eq}}) \ , \tag{2.2}$$

which may be more conveniently written as, defining $Y \equiv n_{\rm DM}/T^3$, and $x \equiv m_{\rm DM}/T$,

$$\frac{dY}{dx} = -\frac{\alpha}{x^2}(Y^2 - Y_{\rm eq}^2) \ , \tag{2.3}$$

where α is given by

$$\alpha = \frac{3}{\pi}\sqrt{\frac{10}{g_*(T)}} m_{\rm DM} m_{Pl} \langle \sigma v \rangle \ . \tag{2.4}$$

For temperatures $T \ll T_F$, the value of Y stays approximately equal to

$$Y_\infty \approx \frac{x_F}{\alpha} \ , \tag{2.5}$$

where $x_F = m_{\rm DM}/T_F$.

From Y_∞ it is now straightforward to obtain the current DM energy density, $\rho_{\rm DM,0}$, and thus its relic abundance, which is given by

$$\Omega_{\rm DM} \equiv \frac{\rho_{\rm DM,0}}{\rho_{c,0}} \approx 0.26 \ \frac{x_F}{25} \ \sqrt{\frac{g_*(m_{\rm DM})}{100}} \ \frac{1.7 \cdot 10^{-9} \ {\rm GeV}^{-2}}{\langle \sigma_{ann} v \rangle} \ , \tag{2.6}$$

where $\rho_{c,0} = 3 m_{Pl}^2 H_0^2$ is the present value of the critical density. Numerically, for DM in the GeV $-$ TeV range, one typically finds that $x_F \sim 10$ and $g_* \sim 100$ are good approximations. The value of $\langle \sigma_{ann} v \rangle$ can be computed within the context of a given particle physics model, and will determine the viability of a given DM candidate.

WIMP's

Weakly interacting massive particles (WIMP's) have been, by far, the most studied DM candidates. Their popularity stems from the fact that a DM particle interacting with the SM sector with a strength equal to that of the weak interactions (set by the Fermi constant $G_F = 1/(\sqrt{2}v^2) \sim 10^{-5}$ GeV^{-2}) leads to, parametrically,

$$\langle \sigma_{ann} v \rangle \sim \frac{1}{4\pi} G_F^2 m_{\rm DM}^2 \sim 10^{-9} \ {\rm GeV}^{-2} \left(\frac{m_{\rm DM}}{10 \ {\rm GeV}} \right)^2 \ , \tag{2.7}$$

which is the right cross-section to account for the observed DM abundance (see eq. (2.6)) for a DM mass of $\sim$ 10 GeV (not too far from the weak scale) – an

observation that has been referred to as the 'WIMP miracle' [86]. Although once worthy of its name, current direct detection constraints (to be discussed in section 2.3) put the simplest version of the WIMP paradigm well under tension.

However, the term WIMP has been broadened to include any DM candidate whose mass is not too far from the weak scale, and with an annihilation cross-section similar to that of the SM weak interactions. In fact, WIMP-like candidates for DM remain exceptionally well motivated in the context of theories concerned with electroweak naturalness: in order to address the electroweak hierarchy problem, new particles not too far above the weak scale must be present in the theory, with interactions whose strength is not too different from that of the SM electroweak sector.[2] Chapter 3 will be concerned with an example of this kind, in which a WIMP-like DM candidate arises naturally in the context of Fraternal Twin Higgs models.

2.2.2 Asymmetric DM

Within the assumption that the DM had been in equilibrium with the thermal plasma in the early Universe, a second possibility for DM production that arises very naturally is that of Asymmetric DM (ADM) [87–99]. In ADM, the final DM abundance is not set by the energy density after freeze-out, but rather by a primordial asymmetry between the number density of DM and anti-DM particles, given by

$$\eta_{\rm DM} \equiv \frac{n_{\rm DM} - \overline{n}_{\rm DM}}{n_\gamma} \ . \tag{2.8}$$

For a scenario of ADM to work, thermal equilibrium between the DM and the visible sector needs to hold for long enough such that essentially all of the anti-DM annihilates (i.e. the remaining freeze-out abundance is essentially zero), and only the asymmetric population of DM particles, which could not find anti-DM to annihilate with, remains.

[2] Crucially, in theories with extended dark sectors, as naturally occurs in Twin Higgs models, the DM annihilation cross section can be similar in size to that of eq.(2.7) without being in conflict with direct detection constraints, so long as the dominant annihilation channels proceed through particles of the dark sector, and interactions with the SM feature much smaller scattering cross sections.

Although this scenario may sound more involved than that of simple freeze-out, it is worth remembering that our very baryon relic abundance was not set by freeze-out dynamics, but precisely by an asymmetry between the number of baryons and anti-baryons, $\eta_b \sim 10^{-10}$. In fact, one of the strongest motivations for ADM is that it enables an explanation (or at least proceeds in the direction of explaining) of why the ratio $\Omega_{\rm DM}$ to Ω_b is an $\mathcal{O}(1)$ number, $\Omega_{\rm DM} \simeq 5\Omega_b$. Without a common origin, one would expect these two quantities to differ by orders of magnitude. In the context of ADM, the ratio of energy densities is given by

$$\frac{\Omega_{\rm DM}}{\Omega_b} = \frac{m_{\rm DM}}{m_N}\frac{\eta_{\rm DM}}{\eta_b}. \tag{2.9}$$

Hence, if the two asymmetries are of a similar size, $\eta_{\rm DM} \sim \eta_b$, then a DM mass of size $m_{\rm DM} \approx 5m_N \approx 5$ GeV would account for the experimentally observed ratio. In chapter 4, we discuss an example of ADM that arises in the context of Fraternal Twin Higgs theories.

2.2.3 Other DM candidates

It is also possible for the DM to have been produced through a mechanism that did not require thermal equilibrium with the SM sector. Examples of such non-thermal production of DM include axions (for a review see [100,101]), and primordial Black Holes. Black Holes (BH's) formed in the early Universe (before ~ 1 s) are referred to as primordial BH's (pBH's), and could be potential DM candidates for BH masses above 10^{15} g (pBH's with mass $m_{\rm BH} < 10^{15}$ g would have evaporated by now). Experimental constraints on pBH's with masses $m_{\rm BH} \gtrsim 10^{15}$ g arise from a variety of sources: evaporation (even if they have not evaporated completely by now, partial evaporation from pBH's with masses $10^{15} - 10^{17}$ g would lead to detectable γ-ray emission), gravitational lensing, accretion effects, etc. (see [102,103] for a comprehensive review). As a result, the possibility of pBH's of a given mass accounting for all of the DM abundance seems in high tension with observations. However, pBH's in several mass ranges could still account for around 10% of the DM (and in some cases that fraction is somewhat larger), chiefly pBH's with masses

$10^{17} - 10^{18}$ g, $10^{24} - 10^{28}$ g, and $10 M_\odot - 10^2 M_\odot$ [102].

The most likely scenario is that the DM is actually made of different components. For instance, even if pBH's did not account for most of the DM, it seems reasonable that they may account for some fraction of it, with the remaining fraction being accounted for by, for instance, WIMP-like particles, or axions. Scenarios of multicomponent DM, in which the DM is made of different particle species, also arise in the context of models with enough symmetry content so that two or more states remain stable. Chapters 3 and 4 explore explicit examples, in the context of Fraternal Twin Higgs models, in which the DM is naturally of this multicomponent form.

2.3 Detection of DM

In this section, we briefly comment on two methods for DM detection that are most relevant for the models of DM we discuss in chapters 3 and 4: direct and indirect detection experiments. Collider searches for DM also provide useful constraints (the best in some regions of parameter space, e.g. for masses below ~ 1 GeV where direct detection experiments lack sensitivity), but they will not be relevant for the work presented in this thesis, so we will not discuss them further. (For a recent review of the status of DM searches at the LHC, see [104].)

Direct Detection

The idea behind DM direct detection experiments is that some density of DM must be present at our position in the Galaxy, from the galactic DM halo. These experiments then aim to detect DM particles by measuring the recoil energy they would produce when scattering off target nuclei. A comprehensive review on the principles of DM direct detection, which we discuss below, can be found in [105].

If the DM density distribution is approximately static in the galactic rest frame, and taking into account that the Sun moves around the centre of the Galaxy with velocity $v_\odot \approx 200$ km s^{-1}, the relative velocity of the DM halo with respect to the Earth is of roughly the same size – from the Earth, we observe a DM 'wind' moving towards us with speed $v \approx 200$ km s^{-1} $\sim 10^{-3}$. The maximum recoil energy that

a DM particle with mass $m_{\rm DM}$ and velocity v would generate when scattering off a target nucleus with mass M_N is given by

$$E_R^{max} = \frac{2\mu^2 v^2}{M_N} \tag{2.10}$$

where $\mu = m_{\rm DM} M_N/(m_{\rm DM} + M_N)$ is the reduced mass of the DM-nucleus system. For $M_N \sim 10$ GeV, E_R^{max} varies between a few keV for light DM ($m_{\rm DM} \sim$ GeV), and a few 10's of keV for heavy DM ($m_{\rm DM} \gg M_N$). These small recoil energies make it very challenging for experiments to be able to detect a DM signal above background arising from, for instance, cosmic rays (to reduce the levels of background, DM direct detection experiments are typically built underground). However, one feature of a potential DM signal that would make it potentially distinguishable from background events is that it must show an annual modulation: during the summer (when the velocity of the Earth around the Sun is aligned with that of the Sun itself), the relative velocity of the DM particles is a bit larger, so a few more scattering events should be observed (due to the increase in effective DM flux); whereas the oppostive effect occurs during the winter [106].

The differential rate of scattering events with a given nuclear recoil energy E_R, per unit mass of target nuclei, is given by

$$\frac{{\rm d}R}{{\rm d}E_R} = \frac{1}{M_N}\frac{\rho_0}{m_{\rm DM}}\int_{v_{min}}^{\infty} {\rm d}v v f(v) \frac{{\rm d}\sigma}{{\rm d}E_R} \ , \tag{2.11}$$

where ρ_0 refers to the local DM density, and σ is the scattering cross section for interactions between the DM and the nucleus. Direct detection experiments measure the number of scattering events as a function of the recoil energy, and then derive bounds on the size of the scattering cross section between the DM and a single nucleon. However, in deriving those bounds several assumptions need to be made. First, notice how ρ_0 enters eq. (2.11). The typical value used for this paramter is $\rho_0 \simeq 0.3$ GeV cm^{-3}, but, as discussed in [107], that value is subject to significant uncertainties, and so the bounds on the interaction cross section would be stronger (weaker) if we happened to live in a region of the Galaxy with a larger (smaller) DM density. Second, it is important to consider the nature of the interactions between

the DM and the nucleus, which can be classified in two basic types: spin-independent (SI) and spin-dependent (SD). In the case of SI interactions, the differential cross section may be written as (assuming the DM interacts equally with all nucleons)

$$\frac{\mathrm{d}\sigma^{\mathrm{SI}}}{\mathrm{d}E_R} = A^2 F(E_R)^2 \frac{M_N}{2\mu^2 v^2} \sigma_n^{\mathrm{SI}} \ , \tag{2.12}$$

where A is the total number of nucleons in the nucleus, σ_n^{SI} the interaction cross-section between the DM particle and a single nucleon, and $F(E_R) \leq 1$ is a nuclear form factor, such that $F(0) = 1$.[3] SD interactions, on the other hand, do not present this A^2 enhancement, and so constraints on them are weaker.

To date, no direct detection experiment has found unambiguous evidence for the existence of DM.[4] The strongest constraints on σ_n^{SI} come from the PandaX [109] and LUX [110] experiments, with the latter ruling out cross sections as small as 10^{-46} cm^2 for a DM mass around 50 GeV. Notice this upper bound is almost 10 orders of magnitude smaller than the value of 10^{-9} GeV^{-2} $\sim$ 10^{-37} cm^2 required by the 'WIMP miracle', if DM annihilation proceeds mainly through SM degrees of freedom. For DM masses below $\sim$ 10 GeV, direct detection experiments start losing sensitivity due to the small recoil energies involved. On the other hand, for heavy DM ($m_{\mathrm{DM}} \gg M_N$), the nuclear recoil energy produced by a DM particle stays constant, in the 10's of keV regime, but the flux of DM particles that reaches the detector ($\dot{n}_{\mathrm{DM}} = v\rho_0/m_{\mathrm{DM}}$) decreases, and so the bounds on the cross section decrease linearly for large masses (remember eq. (2.11)). Direct detection experiments are thus ideal to look for DM candidates with mass in the 10 GeV $-$ 1 TeV range. Next-generation experiments such as LZ [111] may be operative in a few years, and will be able to improve on current limits by several orders of magnitude. In chapters 3 and 4, we

[3] The role of the nuclear form factor is to account for the non-trivial structure of the nucleus, that may be probed by the DM-nucleus interactions if the momentum transferred in the interaction, q, is large enough. For very small momentum transfer, $q^{-1} \gg R_N$, where R_N is the nuclear radius, the nucleus can be treated as a point particle, and thus $F(E_R) \simeq 1$. If, on the other hand, $q^{-1} \sim R_N$, the interaction may probe the nuclear structure, and the final cross section will deviate from the point-like case.

[4] Famously, the DAMA collaboration claims they have found evidence for DM with mass $\sim$ 10 GeV, with an annual modulation in their signal, with a significance of 9σ [108]. However, the fact that these claims have not been reproduced by any other detectors, combined with the fact that the relevant region of parameter space has already been ruled out by several other experiments, makes a DM interpretation of these anomalies dubious.

comment on current bounds and how they affect our proposed DM candidates.

Indirect Detection

DM indirect detection methods aim to detect the final products that would be produced by DM annihilating or decaying today. Of particular interest are those cases where the final state includes γ-rays and highly energetic neutrinos, but also positrons and antiprotons.

High energy γ-rays produced in DM annihilation or decay would provide a very clean signature – photons travel from their sources in straight lines, suffering very little disruption (see [112] for a review). The most sophisticated instrument trying to detect high energy γ-rays arising from DM annihilation or decay is Fermi LAT – a γ-ray telescope covering the energy range 0.2 - 300 GeV. At the moment, the most stringent limits on the γ-ray flux are set by Fermi, from observations of dwarf spheroidal galaxies in the outskirts of the Milky Way [113], which are some of the most DM-dominated astrophysical objects. The Fermi LAT collaboration reported an excess in γ-rays in the GeV range from the galactic centre [114], although the strength of the excess depends strongly on the details of how the γ-ray background is modelled – an endeavour that becomes particularly complicated close to the centre of the Galaxy. Although this mild excess does not amount to strong evidence of the existence of DM, we briefly comment on a possible DM origin in chapter 3.

Another potential final state in the process of DM annihilation is highly energetic neutrinos – even if the DM does not annihilate into neutrinos directly, they will likely be produced from the decay of heavier SM particles. More specifically, as the Sun moves around the galactic halo, DM particles will scatter off baryons in the Sun. Such scattering events will cause the DM particles to lose some of their momentum, and potentially become gravitationally bound to the star. The more DM particles get captured, the more annihilations will take place, until an equilibrium is reached such that $\Gamma_{ann} = \Gamma_C/2$, where Γ_{ann} and Γ_C refer to the annihilation and capture rates respectively. The neutrinos produced in the annihilation process will have energies of order the DM mass – in particular, DM in the GeV range will produce neutrinos with such high energies that no other process in the Sun could mimic such

an event. Because of their small scattering cross section with all other particles, neutrinos escaping from the Sun will reach the Earth essentially unimpeded, and, if detected, would provide unambiguous evidence for the presence of DM. The most competitive instrument aimed at trying to detect such highly energetic neutrinos coming from the Sun is the IceCube telescope, which has set stringent bounds on the DM scattering cross section [115].

In a Universe made of matter, sources of anti-matter are scarce, yet annihilating DM would produce equal fractions of matter and anti-matter in the final state. This effect could be observed as an excess in the positron and antiproton fractions of cosmic rays. In the absence of primary sources of positrons and antiprotons, these are only produced in the collision of cosmic rays with the interstellar material. This secondary production provides a background for primary positron and antiproton searches. Dedicated detectors like PAMELA and AMS-02 are designed to study the composition of cosmic rays, and could provide indirect hints of the existence of annihilating DM. Unlike photons, however, positrons and antiprotons interact with the interstellar material and magnetic fields, which affect their propagation until they reach the detector. Uncertanties in both secondary production mechanisms and propagation strongly affect the possible constraints on annihilating DM that can be set using these final states [116, 117]. In 2008, the PAMELA collaboration reported an observed increase in the cosmic ray positron fraction for energies between 10 GeV and a few 100 GeV [118], later confirmed by Fermi [119] and AMS-02 [120]. Although at first sight the data seems incompatible with secondary positrons only, it is now believed that properly taking propagation uncertainties into account could make these observations consistent with the expected background [121]. We will not comment further on a possible positron excess with a DM origin in this work. Regarding antiprotons, a $\overline{p}/p$ ratio larger than expected from secondary emission was reported by AMS-02 [122], although production and propagation uncertainties are also believed to play a major role in the compatibility between background and observations [123]. We will briefly discuss DM constraints from antiproton injection in the context of the DM models explored in chapter 3.

Chapter 3

Twin WIMP Dark Matter

Based on work done in collaboration with Robert Lasenby and John March-Russell [1].

3.1 Introduction

This chapter explores the possibilities for DM candidates in the context of Twin Higgs models, with a focus on the Fraternal Twin Higgs scenario described in section 1.4.2. We consider the case where there is no asymmetry present in the twin sector, and where $U(1)'_Y$ remains a global symmetry (not gauged, in the spirit of the most economical version of the Fraternal Twin Higgs model). The very different scenarios that arise when a twin asymmetry is present, and when $U(1)'_Y$ is gauged, are explored in chapter 4.

The twin and SM sectors remain in thermal equilibrium well below the UV cutoff as a result of the interactions between the two sectors that take place via the Higgs portal, with a strength set by the ratio f/v – a fact that is at the heart of the Twin Higgs mechanism. This observation allows for the possibility of twin DM with a relic abundance that is set purely by freeze-out dynamics (as described in section 2.2.1), and makes unambiguous predictions regarding DM direct detection signatures, as we explore in section 3.4. We show that the most attractive DM candidates are twin leptons (τ' and ν'), whose relic abundance is determined by twin weak interactions, with a strength set by $g'_2 \simeq g_2$ and $G'_F = (v/f)^2 G_F$, and directly related to that of SM weak interactions purely by naturalness arguments – a *twin-WIMP miracle*.

We focus on the most natural case where $y_{b'} \approx y_b$ and $y_{t'} \approx y_t$, and we take $\Lambda'_{\rm QCD} = 3$ GeV as our default value (a discussion as to why much smaller values of $\Lambda'_{\rm QCD}$ may not be desirable can be found in section 3.8). For the values of $f/v \gtrsim 3$ that are phenomenologically allowed, this realises the heavy quark limit in the twin QCD sector (i.e. $m_{b'}, m_{t'} \gg \Lambda'_{\rm QCD}$). As a result, the lightest states in the QCD$'$ sector are twin glueballs, which will not account for a significant fraction of the DM

but nevertheless lead to very interesting phenomenology, as we discuss in section 3.6.

3.2 Stable and metastable states

The twin sector in the Fraternal Twin Higgs scenario we are concerned with features three $U(1)$ global symmetries: twin baryon number B′, twin lepton number L′ (in the absence of Majorana mass terms for RH leptons, as we will assume is the case),[1] and twin 'charge' Q′ (in the case where the $U(1)'_Y$ symmetry is not gauged). If these global symmetries remain unbroken, the lightest states in the theory carrying B′, L′, and Q′ charge will be stable, making them automatic DM candidates. We are aware that higher dimensional operators (HDO's), perhaps connected to the UV completion of the theory, may break these global symmetries. However, in this work we will assume that those effects are small enough so that the lightest states charged under these symmetries remain stable on timescales $\gtrsim 10^8 H_0^{-1}$ [78, 79].

In the naïvely most natural case where $m_{\nu'} < m_{\tau'}$, and $m_{\nu'}, m_{\tau'} < m_{W'}$, both ν' and τ' are stable (protected by L′ and Q′ respectively), and thus potential DM candidates. Although we will focus on the regime $m_{\tau'} \gtrsim m_h/2$ (to avoid collider constraints from the invisible Higgs width), we allow ν' to be heavy or essentially massless. In the former case, it contributes to the final DM abundance, whereas in the latter it behaves as dark radiation (DR) and will contribute to the number of effective neutrino species $\Delta N_{\rm eff}$, as discussed in section 3.8. If $m_{\tau'} + m_{\nu'} > m_{W'}$, $W'^{\pm}$ gauge bosons are also stable, and could contribute significantly to the DM energy density (although the amount of fine-tuning required in this case approaches an unpleasant regime, as we discuss in section 3.5).

In the quark sector, one obvious stable state is the spin-3/2 baryon Δ', made of three b' quarks, which is the lightest state with B′ charge. However, twin QCD interactions lead to efficient annihilation of $\bar{b}'b'$ pairs into twin gluons (or glueballs and quarkonia if the freeze-out temperature of the b' quark is below that of the QCD′ phase transition), rendering them irrelevant as potential DM candidates unless

[1] Both B′ and L′ may be considered good global symmetries at scales well below the temperature of the $SU(2)'_L$ phase transition, where anomaly effects that violate both B′ and L′ are exponentially suppressed. This is an appropriate assumption in our case, since the freeze-out temperatures of our DM candidates are well below this scale, as will become apparent in section 3.4 and 3.5.

$m_{b'} \gtrsim 1$ TeV, a possibility we comment on in section 3.5.

Concerning the twin QCD sector, in the heavy quark regime we are considering, the lightest states are twin glueballs, the spectrum of twin quarkonia being heavier. The lightest such glueball is a scalar state, with quantum numbers 0^{++} and mass $m_0 \simeq 6.8\Lambda'_{\rm QCD}$ [58,59], and therefore mixes with the Higgs before decaying into light SM fermions, the mixing angle given by [46]

$$\theta = \frac{\alpha'_3 v \mathcal{F}_0}{6\pi f^2 (m_h^2 - m_0^2)} \approx \frac{v m_0^3}{8\pi^2 f^2 m_h^2} \,, \tag{3.1}$$

where $\mathcal{F}_0 = 3.06 m_0^3/(4\pi\alpha'_3)$ [59] is the 0^{++} glueball decay constant, and in the final step we have assumed $m_h^2 \gg m_0^2$. As a result, the 0^{++} glueball decays quickly into SM states ($\tau_{0^{++}} \sim 4 \times 10^{-10}$ s for $\Lambda'_{\rm QCD} = 3$ GeV and $f/v = 3$). In the case of massless ν', all other glueballs decay to some number of 0^{++} glueballs and $\overline{\nu'}\nu'$ pairs in some appropriate angular momentum state, leaving no stable twin glueballs that could be the DM.

When the ν' as well as the τ' are heavy (heavier than the mass splittings between glueballs, which are of order $\Lambda'_{\rm QCD}$), then two other glueballs become worthy of consideration, for they can be stable or very long-lived metastable states:[2] a 0^{-+} glueball, with mass $m_{0^{-+}} \approx 1.5 m_0$ [58, 59], and a 1^{+-} glueball, with mass $m_{1^{+-}} \approx 1.7 m_0$ [58, 59]. Nevertheless, as we discuss in section 3.6, the relic abundance of these glueballs would only amount to a $\sim 10^{-10}$ fraction of the DM. Such a tiny contribution to the final DM abundance would render glueballs irrelevant as far as their gravitational effects are concerned, but if they happened to decay around the time of recombination or later, they could be subject to constraints from CMB and cosmic ray observations, providing interesting indirect signals of this scenario beyond those of the DM itself, as we discuss in section 3.7.

Finally, notice that twin discrete symmetries P and C are maximally violated by $SU(2)'_L$, but twin CP may remain conserved. We concentrate on the case where twin CP is unbroken, although we note that twin CP-breaking would have important

[2] As we thoroughly discuss in section 3.6, the (meta)stability of these glueballs depends strongly on the UV completion of the theory and on whether twin CP remains unbroken, as well as on the exact values of the IR parameters of the theory.

phenomenological consequences – we mention where this would make a difference.

3.3 Twin QCD phase transition

Before we continue to compute the relic abundances of the stable twin states that might account for the DM, it is important to consider the nature of the twin QCD phase transition, expected to take place at a temperature $T \sim \Lambda'_{\rm QCD}$. Since $\Lambda'_{\rm QCD} = \mathcal{O}(1\text{ GeV})$, the temperature at which the phase transition takes place will fall below the freeze-out temperature of our DM candidates (since their masses are ~ 100 GeV). Thus, it is crucial to assess whether entropy production during a potentially first order QCD$'$ phase transition could have led to the dilution of the DM relic abundance.

It is well known that in the regime of only one light flavour, the QCD$'$ phase transition between the unconfined and confined phases proceeds as a smooth cross-over (with no non-equilibrium dynamics), and remains so as long as the quark mass satisfies $m_{b'} \lesssim 8\Lambda'_{\rm QCD}$ [124–126]. The transition becomes second order for $m_{b'} \sim 8\Lambda'_{\rm QCD}$, and above such value the pure gauge case is recovered, in which the phase transition is of a weak first order kind, as shown by both analytical arguments [124, 127] and lattice computations [128]. Our default choices $y_{b'} \simeq y_b$, $f/v \simeq 3$, and $\Lambda'_{\rm QCD} \simeq 3$ GeV, lead to $m_{b'} \simeq 12\text{ GeV} < 8\Lambda'_{\rm QCD}$, well within the smooth cross-over regime, but larger values of f/v will quickly drive the value of $m_{b'}$ into the weakly first order region. We therefore dedicate the rest of this section to the details of the weakly first order case, in which the phase transition takes place via nucleation of bubbles of the confined phase.

The rate of bubble nucleation at finite temperature per unit volume is given by $\Gamma(T) \sim T^4 e^{-\Delta F_c/T}$ [129], where ΔF_c is the free energy cost of nucleating a bubble of critical size (i.e. a bubble just big enough such that its free energy cost decreases as it grows). If the unconfined phase is supercooled to a temperature $T = T_c(1-\delta) < T_c$, with $\delta \ll 1$ (as one would expect for a weakly first order transition), a difference in pressure between the two phases will arise, and bubbles of the confined phase could grow if this pressure was large enough to overcome their wall tension. The

free energy cost of nucleating a bubble with radius R is given by

$$\Delta F = -\frac{4\pi}{3} R^3 |\Delta V| + 4\pi^2 R^2 \sigma \ , \tag{3.2}$$

where $|\Delta V|$ is the free energy density difference between the unconfined and confined phases (i.e. the difference between the finite temperature effective potential between the two vacua), and σ the bubble wall tension. The radius of a critical bubble is then defined as $\frac{\partial \Delta F}{\partial R}\Big|_{R_c} \equiv 0$, which yields $R_c = \frac{2\sigma}{|\Delta V|}$, and the free energy cost for a critical bubble

$$\Delta F_c = \frac{16\pi}{3} \frac{\sigma^3}{|\Delta V|^2} \ . \tag{3.3}$$

On the other hand, $\Delta V = -\Delta P$, where ΔP is the pressure difference between the two phases, which for small δ is approximately given by

$$\Delta P \simeq \Delta T \ \frac{\rho_L}{T} \simeq \delta \cdot \rho_L \ , \tag{3.4}$$

where $\Delta T = T - T_c = \delta \cdot T_c$, and ρ_L is the latent heat per unit volume. This leads to

$$\frac{\Delta F_c}{T} \simeq \frac{16\pi}{3} \frac{\sigma^3}{T_c \rho_L^2} \ \delta^{-2} \approx 3 \cdot 10^{-5} \ \delta^{-2} \ , \tag{3.5}$$

where in the last step we have used the results from lattice studies, which yield $\rho_L \simeq 1.4 T_c^4$ and $\sigma \simeq 0.0155 T_c^3$ [130]. (Lattice computations also show that the critical temperature for a pure gauge QCD$'$ phase transition is $T_c \simeq 1.26 \Lambda_{\rm QCD}^{\prime \overline{\rm MS}}$ [131], and so $T_c \sim \Lambda'_{\rm QCD}$ as one would expect.)

We define the nucleation temperature T_n as the temperature at which the probability of nucleating a bubble in a Hubble volume in a Hubble time becomes of order unity, i.e. $\Gamma(T_n) \approx H(T_n)^4$, and we find $\delta_n \approx 4 \cdot 10^{-4}$, where $T_n \equiv T_c(1 - \delta_n)$. Thus, a small supercooling $\delta \gtrsim \delta_n$ easily leads to a large bubble nucleation rate: a drop in $\log T$ by only 10^{-6} results in Γ increasing by a factor of e, which confirms the validity of our $\delta \ll 1$ approximation. Notice that this extremely large nucleation rate that arises as soon as the temperature decreases ever so slightly below T_c has to do with the smallness of the bubble wall tension $\sigma \sim 10^{-2} \ T_c^3$ (as computed on the lattice), parametrically smaller than the naive T_c^3 value one would have expected,

which makes it easier for the bubbles to expand, and therefore to nucleate bubbles of critical size.

Regarding the entropy produced during the phase transition, its maximum possible value corresponds to the case in which the out-of-equilibrium dynamics (when the pressure difference between phases drives bubble expansion) is responsible for converting all the volume occupied by the unconfined phase into confined phase, i.e. all the difference in free energy density between the two vacua goes into entropy increase:

$$\Delta s \simeq \frac{\Delta P}{T_c} \simeq \frac{\delta \cdot \rho_L}{T_c} \sim \text{few} \times \frac{\delta_n \rho_L}{T_c} \sim 10^{-3}\ T_c^3 \ll T_c^3\ . \tag{3.6}$$

Since the maximum possible value of the entropy density generated by the phase transition is much smaller than the entropy density due to the thermal plasma ($s \sim T_c^3$), we can confidently neglect the effects of the QCD$'$ phase transition on the calculation of the relic abundance of our DM candidates.

3.4 Twin τ DM

After having shown in section 3.3 that entropy injection due to a potentially (weak) first order QCD$'$ phase transition would lead to no significant dilution of relics, we can now compute the final abundance of our DM candidates. First, we consider the simplest case in which twin τ leptons account for all of the DM, and so we assume the ν' to be effectively massless. (Notice the situation in which ν' was the DM and τ' was very light would be exactly the same, given that $U(1)'_Y$ is not gauged, as long as a ν' Dirac mass arose through a Yukawa coupling.) Annihilation of $\overline{\tau'}\tau'$ pairs proceeds mostly via $SU(2)'_L$ interactions into $\overline{b'}b'$ and $\overline{\nu'}\nu'$ pairs (predominantly the former due to the colour factor). Annihilation via SM Higgs exchange (through a coupling of the form $\frac{y'_\tau}{\sqrt{2}}\frac{v}{f}h\overline{\tau'}\tau'$) gives a subleading effect, except in a small window around the resonance region $m_{\tau'} \sim m_h/2$.

Figure 3.1 shows the ratio of the present energy density of τ' species to the observed DM density, for several values of f/v.[3] For $f/v \approx 3$, the observed DM density is achieved for a mass $m_{\tau'} \approx 63$ GeV, whereas larger values of this ratio necessi-

[3]The calculation of this and other relic densities in this work are carried out using the dedicated software MicrOMEGAs [132].

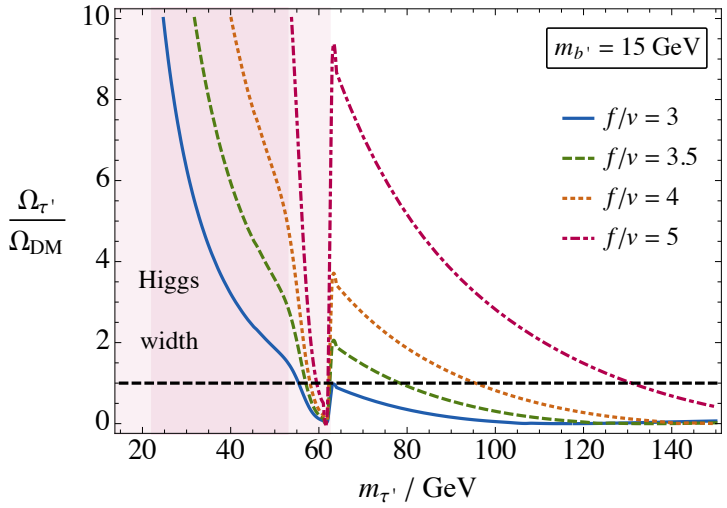

Figure 3.1: Ratio of τ' energy density to the observed DM density, as a function of $m_{\tau'}$ for several values of f/v. The light (dark) pink region indicates the 2-sigma bounds from invisible Higgs width constraints and modified couplings to SM states for $f/v = 3$ (3.5) ($f/v \gtrsim 4$ remains unconstrained). Notice that in the light $m_{\tau'}$ region, annihilations would receive important non-perturbative corrections if $\Lambda'_{\rm QCD}$ was so large that $m_0 \gtrsim 2m_{b'}$, but since this regime leads to overproduction of DM it is not our concern in this work.

tate heavier DM. The calculation is performed taking $m_{b'} \approx 15$ GeV (a value that naturally arises for $y_{b'} \simeq y_b$ and $f/v \simeq 3$), which saturates the experimental bound from constraints on the Higgs width for $f/v \approx 3$. (Notice $y_{b'}$ is only constrained by naturalness arguments to be $y_{b'} \ll y_{t'}$, which is perfectly satisfied in this case.) We emphasize that a different value of $m_{b'}$ would not affect our results as long as $m_{b'} \ll m_{\tau'}$ (and $\Lambda'_{\rm QCD} \ll m_{\tau'}$), for in that regime the τ' relic density is essentially independent of the exact value of $m_{b'}$.

As anticipated in section 3.1, the relic density of our (successful) DM candidate is set by the strength of the twin weak interactions, whose gauge coupling $g'_2 \simeq g_2$ and gauge boson masses $m_{W'} \simeq (f/v)m_W$ are linked to those of the SM sector purely by naturalness arguments, giving rise to a *twin-WIMP miracle*.

Regarding direct detection signatures, scattering of τ' off SM nuclei takes place at tree-level via Higgs exchange. Figure 3.2 shows the SI scattering cross section per nucleon for τ' DM, as a function of its mass and for the values of f/v that yield the correct DM abundance. At the time [1] was written, all values of $f/v \gtrsim 3$ were below existing bounds set by LUX [133]. Now, more stringent constraints [110] rule out values of $f/v \lesssim 6$, constraining the level of fine-tuning in this scenario to be at the 5% level at best, and the DM mass to be $m_{\tau'} \gtrsim 165$ GeV. Ratios $f/v \gtrsim 6$ will

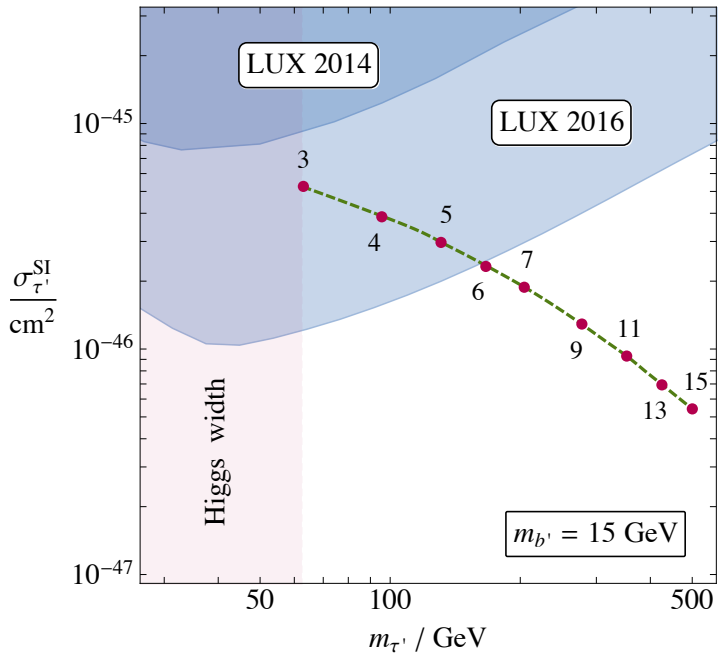

Figure 3.2: Dashed green line: SI scattering cross section per nucleon for τ' DM as a function of $m_{\tau'}$, and for values of f/v such that the correct DM density is obtained, with red dots pointing out particular values of f/v; blue areas: LUX 2014 [133] and LUX 2016 [110] bounds; pink area: region ruled out by bounds on the invisible Higgs width and modified couplings to visible sector particles [46].

be probed by next-generation experiments such as LZ [111].

3.5 Multicomponent, W', and Δ' DM

If $m_{\tau'} + m_{\nu'} > m_{W'}$, W' gauge bosons cannot decay. Moreover, in the regime $m_{\tau'} \sim m_{\nu'}$ and $m_{\tau'}, m_{\nu'} < m_{W'}$, all three states are stable and may contribute significantly to the DM energy density, opening a possibility for a three-component DM scenario.

In figure 3.3 we show the contribution to the DM energy density from these three particle species (τ', ν' and W'), normalized to $\Omega_{\rm DM}$, for several values of the $SU(2)'_L$ gauge coupling (we allow a deviation by 10% from its central value $g'_2 = g_2 \approx 0.64$). For concreteness, we take $m_{\tau'} = m_{\nu'} \approx 0.55\ m_{W'}$, with $m_{W'} = g'_2 f/2$. As can be appreciated, the correct DM abundance is only obtained for rather large values of f/v, leading to a fine-tuning between 5% and 1%. The reason why larger values of f/v are needed (compared to the pure τ' DM case) is that since both τ' and ν' are now required to be heavier (for the W' to be stable), their annihilation cross sections $\propto m^2_{\tau',\nu'}/f^4$ are also larger, and thus f needs to be increased accordingly to

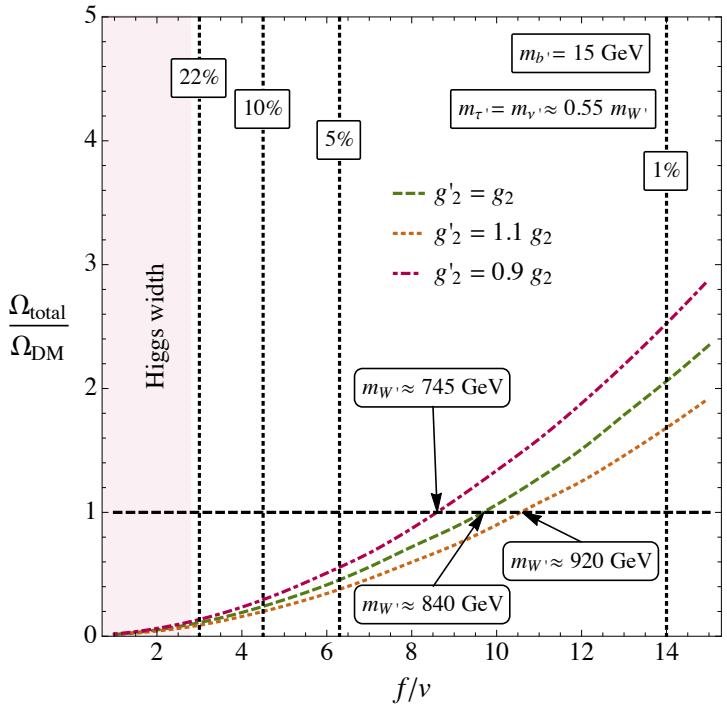

Figure 3.3: Contribution to the energy density of the Universe from τ', ν' and W', species normalized to the observed DM energy density, as a function of f/v and for different values of the twin weak coupling g'_2. Vertical lines represent tuning contours. We indicate the W' mass for the three different values of g'_2 considered when the right DM density is achieved.

compensate. As can be seen from figure 3.3, the correct DM abundance is obtained for $f/v \approx 9$, which drives the fine-tuning to the 2% level. In this particular case, W' species contribute roughly 25% to the DM, with τ' and ν' making for the remaining 75%.

With respect to direct detection signatures, the prediction for the SI scattering cross section per nucleon is of order $\sim 10^{-46}$ cm^2 for all three particle species involved, and for the range of masses that lead to the correct DM abundance. This is well below current bounds, leaving next-generation direct detection experiments such as LZ [111] as the only hope for probing this scenario.

Small variations of $m_{\tau'}$ and $m_{\nu'}$ do not make a significant difference to our results, except when $m_{\tau'} + m_{\nu'} < m_{W'}$, in which case the W' is no longer stable and only τ' and ν' species contribute to the DM. Enough annihilation in this two-component scenario requires $m_{\tau'}, m_{\nu'} \gtrsim m_h/2$, which automatically evades invisible Higgs width constraints. The different contribution to the DM from the two particle species would depend solely on the ratio of their masses: if $m_{\tau'} = m_{\nu'}$, both components

would contribute equally, whereas if they differ by approximately 10 GeV the right DM abundance requires $m_{\nu'} \approx 70$ GeV (therefore $m_{\tau'} \approx 80$ GeV) and ν' and τ' species would make for 65% and 35% of DM respectively. Regarding the strength of direct detection signals, this two-compononent case is completely analogous to the single-component scenario discussed in section 3.4.

Finally, we comment briefly on the potential DM candidate from the twin quark sector, the Δ' baryon. In this case, annihilation of $\bar{b}'b'$ pairs into twin gluons occurs so efficiently in the early Universe that the remaining freeze-out density of Δ' baryons would be irrelevantly small unless $m_{b'} \gtrsim 1$ TeV $\gg \Lambda'_{\rm QCD}$. To estimate the Δ' relic density, we consider the case where the b' freeze-out temperature is well above $\Lambda'_{\rm QCD}$, (in that regime, quarks and gluons are the appropriate degrees of freedom), and compute the abundance of the b' species after the annihilation rate into a pair of gluons, whose cross section scales as $\sigma v \sim (\alpha'_3/m_{b'})^2$, has frozen out. By numerically evaluating the annihilation rate, we find a freeze-out temperature $T_f \sim m_{b'}/30$, and a non-negligible freeze-out density of the b' species only for $m_{b'} \gtrsim 1$ TeV, which in turn requires $f/v \gtrsim 30$ and thus an extreme level of fine-tuning (this statement applies if we insist on keeping $y_{b'} \lesssim 0.2$ so as not to introduce yet further tuning at 1-loop). We can therefore conclude that the Δ' baryon is a rather unattractive DM candidate in the Fraternal Twin Higgs model.[4]

3.6 Stable and metastable twin glueballs

As mentioned in section 3.2, the lightest states in the QCD$'$ sector are twin glueballs, with the lowest lying one being a 0^{++} state that mixes with the SM Higgs and quickly decays to SM final states (mainly to $\bar{b}b$ pairs, as long as $m_{0^{++}} > 2m_b$). Most other glueballs will be able to decay to some number of 0^{++} glueballs, in some appropriate angular momentum state, that later decay into SM degrees of freedom. However, in the absence of other light states in the twin sector (e.g. massless ν'), two other glueballs become worthy of attention: those with quantum numbers 0^{-+} and 1^{+-},

[4]Notice that our estimate of the Δ' relic abundance is an optimistic one (and thus the lower bound on $m_{b'}$ is equally optimistic), for the number density of Δ' baryons does certainly not correspond to 1/3 the number density of b' quarks. After the QCD$'$ phase transition takes place, many of the remaining b' quarks would combine with $\bar{b}'$ into mesons. The fraction of b' quarks that actually combine into Δ' baryons escapes our knowledge.

with mass $m_{0^{-+}} \approx 1.5 m_{0^{++}}$ and $m_{1^{+-}} \approx 1.7 m_{0^{++}}$ respectively, as mentioned already in section 3.2.

The pseudoscalar 0^{-+} glueball is the lightest (twin) CP-odd state in the twin sector. Thus, if CP remains a good symmetry of the twin sector, this state would be completely stable. However, new interactions between the two sectors arising from a UV completion of the theory could render the 0^{-+} glueball unstable. For example, the lowest HDO's that would allow the decay of the 0^{-+} glueball directly into SM states, conserving the product of CP in both sectors but violating them individually, are of dimension 7, parametrically given by

$$\mathcal{L} \sim \frac{1}{M^3} \overline{q} \gamma^5 q \times \mathrm{tr}(G' \tilde{G}') \ , \tag{3.7}$$

where q refers to SM fermions, G' represents the QCD$'$ field strength, and M is some UV mass scale, at least as high as the cutoff of the theory. If the operator of eq. (3.7) were indeed present, the lifetime of the 0^{-+} glueball would be

$$\tau_{0^{-+}} \sim 10^{-12} \text{ s } \left(\frac{M}{5 \text{ TeV}} \right)^6 \left(\frac{3 \text{ GeV}}{\Lambda'_{\text{QCD}}} \right)^7 \ , \tag{3.8}$$

which is cosmologically safe (well before BBN as long as $M \lesssim 500$ TeV), but potentially interesting for displaced vertices at the LHC.

Regarding the 1^{+-} glueball, the lowest HDO's that would make it decay are of dimension 10, parametrically

$$\mathcal{L} \sim \frac{1}{M^6} \overline{q} \gamma_\mu \gamma^5 q \times \partial^\mu G' G' G' \ , \tag{3.9}$$

which would lead to a lifetime

$$\tau_{1^{+-}} \sim 10 \text{ s } \left(\frac{M}{5 \text{ TeV}} \right)^{12} \left(\frac{3 \text{ GeV}}{\Lambda'_{\text{QCD}}} \right)^{13} . \tag{3.10}$$

If, on the other hand, only IR operators are to be relevant regarding the 1^{+-} glueball decay, then its decay could proceed to two 0^{++} glueballs in an angular momentum $L = 1$ state, one of them necessarily being off-shell and therefore mixing with the

Higgs before decaying to SM states. Since the final state has quantum numbers 1^{-+}, it is clear that although CP is conserved in this process, both C and P are violated. Hence, this decay must proceed via $SU(2)'_L$ interactions involving both axial and vector currents. Notice this can only happen through a $\overline{b}'b'$ pair formed inside the glueballs, and thus we need to know the QCD corrections to the axial and vector weak currents that arise in the heavy quark limit we are concerned with. These were computed in [134, 135], and are given by

$$\delta J^{\rm V}_\mu = \frac{g_3'^3}{16\pi^2 {m_{b'}}^4}\partial_\alpha \ {\rm Tr}\left(\frac{1}{7}G_{\sigma\tau}\{G^{\sigma\tau}, G_{\alpha\mu}\} - \frac{14}{45}G_{\mu\sigma}\{G^{\sigma\tau}, G_{\tau\alpha}\}\right) \ , \tag{3.11}$$

and

$$\delta J^{\rm A}_\mu = \frac{g_3'^2}{48\pi^2 {m_{b'}}^2}\epsilon_{\mu\rho\tau\sigma}{\rm Tr}(G^{\alpha\rho}\partial_\alpha G^{\tau\sigma} + 2G^{\tau\sigma}\partial_\alpha G^{\alpha\rho}), \tag{3.12}$$

for the vector and axial currents respectively. This leads to a decay rate

$$\Gamma_{1^{+-}} \sim \frac{1}{32\pi^3}\left(\frac{g_3'^3}{16\pi^2 m_{b'}^4}\frac{g_3'^2}{16\pi^2 m_{b'}^2}\right)^2\left(\frac{g_2'^2}{16 m_{Z'}^2}\right)^2\left(\frac{\theta}{m_0^2}\right)^2 \Gamma_{h\to{\rm SM}}(m_0^*)\times \tilde{m}^{20} \ . \tag{3.13}$$

The first numerical factor comes from 3-body-decay phase space, the second from QCD corrections to the vector and axial weak currents, the third from s-channel exchange of a Z' gauge boson, the fourth from the off-shell 0^{++} glueball mixing with the Higgs, the factor of $\Gamma_{h\to{\rm SM}}(m_0^*)$ corresponds to the decay width of the SM Higgs with a mass equal to that of the off-shell glueball, and the final factor (of mass dimension 20) accounts for dimensions ($\tilde{m}$ will typically be either $m_{1^{+-}}$ or $\sqrt{m_{1^{+-}}^2 - m_0^2} \approx 1.4 m_0$). The lifetime of the 1^{+-} glueball is then, parametrically

$$\tau_{1^{+-}} \sim 10^2 \text{ s } \left(\frac{y_{b'}}{y_b}\right)^{12}\left(\frac{f/v}{3}\right)^{20}\left(\frac{3 \text{ GeV}}{\Lambda'_{\rm QCD}}\right)^{23} \ . \tag{3.14}$$

Notice the strong dependence of $\tau_{1^{+-}}$ on the value of $y_{b'}$, the ratio f/v, and the twin confinement scale $\Lambda'_{\rm QCD}$. For example, whereas $\tau_{1^{+-}} \sim 10^2$ s for $\Lambda'_{\rm QCD} = 3$ GeV, it is $\sim 10^9$ s for $\Lambda'_{\rm QCD} = 1.5$ GeV, and $\sim 10^{-5}$ s for $\Lambda'_{\rm QCD} = 6$ GeV – a factor of 2 change in $\Lambda'_{\rm QCD}$ changes $\tau_{1^{+-}}$ by 7 orders of magnitude! In view of this, all one can say is that, for some resonable values of the parameters involved, the 1^{+-} glueball

may have a lifetime long enough to be of cosmological interest.

If these two glueballs are indeed metastable, one should be concerned about their relic abundance after freeze-out, either to find out what fraction of the DM they account for (if their lifetime was larger than the age of the Universe), or to assess the strength of the constraints coming from energy injection into the thermal plasma after BBN. In order to compute their relic abundace, we note that the last number-changing interactions to fall out of equilibrium will be two-to-two scattering processes, like $0^{-+}0^{-+} \to 0^{++}0^{++}$ or $1^{+-}1^{+-} \to 0^{++}0^{++}$. The strength of this interaction would be characterized by the twin confinement scale, and thus $\langle \sigma v \rangle \sim \Lambda'^{-2}_{\rm QCD}$, which would lead to a relic abundance

$$\frac{\Omega_{\rm glue}}{\Omega_{\rm DM}} \sim 10^{-10} \left(\frac{\Lambda'_{\rm QCD}}{3 \text{ GeV}} \right)^2 . \tag{3.15}$$

If the metastable glueballs only accounted for a 10^{-10} fraction of the DM, they would have no observable gravitational consequences, and all other effects would be negligible if they decayed before the time of recombination ($t \sim 10^{13}$ s), since they would not have enough energy to disrupt BBN or the CMB spectrum [136–138]. However, an energy injection of $\gtrsim 10^{-10}$ of the DM energy density can, depending on the injection time and channels, have observational consequences if it occurs around recombination time or later, either through CMB effects, or via cosmic ray observations [78,138]. Thus, it may be a requirement that the meta-stable glueballs have lifetimes shorter than $\sim 10^{13}$ s.

3.7 Indirect detection

DM annihilating today may lead to observable signatures in indirect detection experiments, since the Higgs portal interaction between SM and twin sectors will result in some of the DM annihilation products finally decaying into light SM degrees of freedom. In particular, for τ' and ν' DM, arguably the most attractive DM candidates as discussed in section 3.4, the dominant annihilation channel is to $\overline{b}'b'$ pairs proceeding via Z' exchange. Given the confining nature of the QCD$'$ sector, the final $\overline{b}'b'$ pair will then fragment into some number of twin glueballs and quarkonia,

albeit we expect dominantly glueballs in the heavy quark limit.

If twin neutrinos are effectively massless (and thus only τ' is the DM), then heavier glueballs will decay to the lightest 0^{++} state and $\overline{\nu}'\nu'$ pairs, with the scalar glueball then decaying via mixing with the Higgs. If, on the other hand, the ν' were heavy (and therefore contributed to the DM), then some of the annihilation products would be the 0^{-+} and 1^{+-}, which in this scenario may be extremely long-lived, while all other glueballs would still be able to decay to some number of 0^{++} states. Either way, the final annihilation products will contain some invisible fraction (either massless $\overline{\nu}'\nu'$ pairs or (meta)stable glueballs), and a number of off-shell SM Higgs states h^*, with off-shell masses determined by the glueball mass splittings ($\sim \Lambda'_{\rm QCD}$) and the details of the QCD$'$ fragmentation process. For the values of $\Lambda'_{\rm QCD}$ considered in this work, most of these h^* will decay into $\bar{b}b$ pairs, although some fraction of them may not be above the $\bar{b}b$ threshold and would decay into $\overline{\tau}\tau$ pairs instead. Final SM annihilation products will be a spectrum of $\bar{b}b$, and $\overline{\tau}\tau$ to a lesser extent, with energies determined by the hadronization process of the twin sector. For the range of DM masses considered here ($m_{\rm DM} \sim 100$ GeV), the most sensitive probes of this kind of energy injection are cosmic ray antiprotons, and gamma-rays.

The most stringent constraints on antiproton injection from annihilating DM come from the AMS-02 detector. In [122], this experiment reported that the measured $\overline{p}/p$ ratio was somewhat larger than expected for kinetic energies larger than ~ 20 GeV (the measured ratio stayed constant at higher energies rather than decrease), a behaviour that could not be explained by antiprotons arising from cosmic ray collisions. Taking AMS-02 data at face value, DM annihilating into $\bar{b}b$ pairs with a thermal freeze-out cross section would be ruled out for DM masses $m_{\rm DM} \lesssim 100$ GeV. However, the background against which AMS-02 compares their data depends strongly on the parameters chosen for modelling the production of secondary antiprotons and their propagation through the interstellar medium, as thoroughly discussed in [123]. Taking these uncertainties into account, the upper bound on the cross section of DM annihilating into $\bar{b}b$ pairs may change by up to an order of magnitude, which might considerably weaken (or strengthen) the lower

bound on the DM mass.

Regarding highly energetic gamma-ray emission from annihilating DM into $\bar{b}b$ or $\overline{\tau}\tau$ pairs, the most stringent constraints come from measurements of the Fermi-LAT instrument. By looking at 15 dwarf spheroidal galaxies that are satellities of the Milky Way, Fermi observations seem to disfavour the existence of DM with mass $\lesssim 100$ GeV annihilating into $\bar{b}b$ or $\overline{\tau}\tau$ pairs with a thermal freeze-out cross section [113]. However, although dwarf spheroidal galaxies are known to be the most DM dominated astrophysical objects, their DM distribution is rather uncertain, and taking these uncertainties into account could weaken the lower bound on the DM down to around 20 GeV. Similar measurements performed by Fermi in the Milky Way halo region also render similar constraints, i.e. $m_{\rm DM} \gtrsim 20$ GeV, for DM annihilating into $\bar{b}b$ or $\overline{\tau}\tau$ pairs [139].

In our particular case, the fact that the fraction of invisible annihilation products is rather unknown, together with the uncertainty in the off-shell Higgs spectrum of masses, means we cannot make detailed predictions that could be compared with current bounds from either AMS or Fermi data. However, the fact that we are already considering DM masses $\gtrsim 100$ GeV, together with the existence of a significant fraction of invisible decay products, means that the models discussed here are certainly not currently ruled out, but may be probed in the near future (especially for the lowest possible values of the ratio f/v, for which the coupling between twin and SM sectors is strongest).

On a more speculative note (but nevertheless worth considering), future measurements that would help clarify the nature of the gamma-ray excess in the few GeV range seen by Fermi would be of special interest [114]. Although the excess is mild, and seems to depend strongly on the model of interstellar emission used to interpret the gamma-ray background, it has been claimed that DM particles with $m_{\rm DM} \sim 40$ GeV annihilating to quarks with roughly thermal freeze-out cross sections (or ~ 10 GeV DM annihilating to leptons) could account for the excess [140,141]. In the models discussed here, although the mass of the DM is larger than these values, the masses of the off-shell Higgs states that finally decay into SM fermions are much smaller than the DM mass, and could potentially give a good fit to the observed

excess. Unfortunately, a more detailed assessment of this possibility would require a thorough understanding of the fragmentation process in the twin sector, as well as a more precise determination of the fraction of invisible decay products.

Finally, another indirect signature of these models may arise (in the case of heavy ν') if a significant fraction of metastable glueballs are produced when the DM annihilates. These long-lived states could travel for very long distances, perhaps very far from the centre of the Galaxy where most of the DM accumulates, before decaying into light SM states. This could lead to striking signatures for indirect detection experiments: the products of annihilating DM would seem to proceed less from the centre of the Galaxy, and more from its outskirts. For this effect to be relevant, glueball lifetimes would need to be of order the size of the Milky Way ($\sim$ kpc $\approx 10^{11}$ sec), a theoretical possibility as discussed in section 3.4.

3.8 Equilibration of sectors

In the case where the ν' are light, they will not contribute to the DM abundance, and we expect all glueballs to decay with short lifetimes. On the other hand, light twin neutrinos will result in a contribution to DR, and constraints on the number of effective neutrino species, $\Delta N_{\rm eff}$, may apply.

Direct couplings between ν' and the SM sector are so weak that they fail to maintain equilibrium between the two sectors below temperatures of order $m_{b'} \gg \Lambda'_{\rm QCD}$ at best, a scenario that would typically lead to a small contribution to $\Delta N_{\rm eff}$. However, the twin QCD sector will maintain equilibrium with the ν' sector down to temperatures presumably close to $\Lambda'_{\rm QCD}$, through the decay of heavier glueballs to lighter ones, accompanied by emission of a $\overline{\nu}'\nu'$ pair in some appropriate angular momentum state. If most of the entropy in the QCD$'$ sector degrees of freedom goes into the ν' sector and remains decoupled from the SM, then a potentially large contribution to $\Delta N_{\rm eff}$ may arise. The situation leading to the smallest contribution to $\Delta N_{\rm eff}$ arises when both interactions between the QCD$'$ sector and ν', and between QCD$'$ and the SM plasma remain in thermal equilibrium until after the QCD$'$ phase transition, and have been so for long enough such that the ν' and SM sectors reached

full thermal equilibrium.

Regarding $\nu' \leftrightarrow \text{QCD}'$ interactions, the latest to freeze-out would be the decay of the 0^{-+} glueball, taking place as $0^{-+} \to 0^{++}\overline{\nu}'\nu'$ (with angular momentum $L = 1$ in the final state). Notice the final state has quantum numbers 0^{-+} (both P and C are conserved in this decay), and so although the decay needs to proceed through s-channel exchange of a Z' gauge boson, it can do so via two axial currents. The decay rate for this process is, parametrically

$$\Gamma_{\nu' \leftrightarrow \text{QCD}'} \sim \frac{1}{32\pi^3} \left(\frac{g_3'^2}{16\pi^2 m_{b'}^2} \frac{g_2'^2}{16 m_{Z'}^2} \right)^2 m_{0^{-+}}^9 \ , \tag{3.16}$$

and this remains larger than $H(T)$ so long as

$$\frac{T}{\Lambda'_{\text{QCD}}} \lesssim 7 \cdot 10^2 \left(\frac{\Lambda'_{\text{QCD}}}{3 \text{ GeV}} \right)^{7/2} \left(\frac{3}{f/v} \right)^4 \left(\frac{100}{g_*(T)} \right)^{1/4} \ , \tag{3.17}$$

which is larger than 1 for $\Lambda'_{\text{QCD}} \gtrsim 0.5$ GeV. So for all the values of Λ'_{QCD} of interest, interactions $\nu' \leftrightarrow \text{QCD}'$ remain in thermal equilibrium until after the QCD$'$ phase transition.

The question is then whether QCD$' \leftrightarrow$ SM interactions are also fast enough to be in thermal equilibrium until temperatures $T \sim \Lambda'_{\text{QCD}}$. The most efficient process is the decay of the 0^{++} glueball into SM degrees of freedom by mixing with the Higgs, whose rate is given by [46]

$$\Gamma_{0^{++}} \approx 1.6 \cdot 10^{-15} \text{ GeV} \left(\frac{\Lambda'_{\text{QCD}}}{3 \text{ GeV}} \right)^7 \left(\frac{3}{f/v} \right)^4 \ , \tag{3.18}$$

and this remains larger than $H(T)$ so long as

$$\frac{T}{\Lambda'_{\text{QCD}}} \lesssim 1 \left(\frac{\Lambda'_{\text{QCD}}}{1 \text{ GeV}} \right)^{5/2} \left(\frac{3}{f/v} \right)^2 \left(\frac{100}{g_*(T)} \right)^{1/4} \ , \tag{3.19}$$

which is larger than 1 for $\Lambda'_{\text{QCD}} \gtrsim 1$ GeV.

So it seems that, as long as $\Lambda'_{\text{QCD}} \gtrsim 1$ GeV, there will be some range of temperatures above Λ'_{QCD} where the rate of interactions $\nu' \leftrightarrow \text{QCD}'$ and QCD$' \leftrightarrow$ SM are fast enough to maintain equilibrium. (This justifies our choice of $\Lambda'_{\text{QCD}} \approx 3$ GeV,

somewhat larger than the lower bound of 1 GeV to account for the fact that equilibration between sectors does not happen instantaneously.) Under the assumption of thermal equilibrium between the ν' and SM sectors down to $\Lambda'_{\rm QCD}$, it becomes then straightforward to estimate the temperature of the ν' background compared to that of the ν background. Using conservation of entropy per comoving volume, one finds

$$T_{\nu'} \approx \left(\frac{g_*(1\text{ MeV})}{g_*(\Lambda'_{\rm QCD})}\right)^{1/3} T_\nu \approx \left(\frac{10.75}{75}\right)^{1/3} T_\nu \approx 0.53\ T_\nu\ , \tag{3.20}$$

where $g_*(1\text{ MeV}) \approx 10.75$ is the effective number of relativistic degrees of freedom at the time of neutrino decoupling (which happens at ~ 1 MeV), and $g_*(\Lambda'_{\rm QCD})$ the same quantity at temperatures $T \approx \Lambda'_{\rm QCD}$, which is approximately 75 for $\Lambda'_{\rm QCD} = \mathcal{O}(1\text{ GeV})$.

If we define the contribution from the ν' sector to the energy density in DR as

$$\rho^{\rm DR}_{\nu'} \equiv \Delta N_{eff,\nu'}\ \rho_{\nu,\rm SM}\ , \tag{3.21}$$

where $\rho_{\nu,\rm SM}$ refers to the energy density of a single neutrino species, then we have

$$\Delta N_{eff,\nu'} = \left(\frac{T_{\nu'}}{T_\nu}\right)^4 \simeq \left(\frac{10.75}{75}\right)^{4/3} \simeq 0.075\ . \tag{3.22}$$

Given that the contribution form the SM itself is $\Delta N_{eff,\rm SM} \simeq 0.046$, and Planck has measured $\Delta N_{\rm eff} = 0.15 \pm 0.2$ [142], a contribution to $\Delta N_{eff,\nu'}$ of this size is consistent with current observations, and potentially in reach of future measurements.

3.9 Conclusions

In this chapter, we have considered the possibility of DM candidates arising in the context of the Fraternal Twin Higgs model [46]. We have shown that twin states may account for the observed DM abundance, and although a weak first order phase transition in the twin QCD sector may take place in the early Universe, the amount of entropy produced in such event would be insignificant.

The most attractive DM candidate is the twin tau lepton, with a mass $m_{\tau'} > m_h/2$ in order to account for the observed relic abundance and evade constraints

from Higgs invisible width measurements. Interactions with SM nuclei proceed via the Higgs portal, and current bounds on the SI cross section per nucleon from the LUX experiment [110] already rule out ratios $f/v \lesssim 6$ (driving the level of fine-tuning to around 5% at best), which requires DM masses $m_{\tau'} \gtrsim 165$ GeV. Larger values of f/v will only be accesible to next-generation experiments [111].

Scenarios of multicomponent DM seem to arise naturally in the context of Fraternal Twin Higgs models: as soon as $m_{\tau'} \sim m_{\nu'}$, both particle species will contribute significantly to the DM energy density. (Admittedly, the phenomenology of this two-component case is very similar to the single-component scenario, except for the absence of a contribution to $\Delta N_{\rm eff}$.) Moreover, as soon as $m_{\tau'} + m_{\nu'} > m_{W'}$, W' gauge bosons also become stable, and all three species of twin particles will typically contribute to the DM energy density, albeit the large value of f/v required in this case drives the fine-tuning to the few percent level – worse than the single-component case.

The case in which the DM is made of twin baryons (Δ' baryon made of three b' quarks, the lightest state carrying twin baryon number) is a possibility, but only a viable one in a rather extreme region of parameter space, requiring masses $m_{b'} \gtrsim$ 1 TeV, and ratios $f/v \gtrsim 30$ for $y_{b'} \approx 0.2$, which drives the fine-tuning to the 0.5% level.

With respect to indirect detection signatures, annihilation of twin DM particles proceeds mostly into $\overline{b}'b'$ pairs, which in turn hadronize and result in some number of twin sector glueballs. These glueballs will then decay into light SM states and some fraction of invisible (twin) states (either $\overline{\nu}'\nu'$ pairs for the case of massless ν', or (meta)stable twin glueballs). SM products will mostly consist of $\overline{b}b$ pairs, and also $\overline{\tau}\tau$ pairs to some extent, which means that bounds from experiments like AMS-02 and Fermi-LAT are applicable, although a direct comparison with existing data is not possible given the lack of knowledge about how the fragmentation process in the twin sector takes place. Given the masses of our DM candidates ($m_{\rm DM} \gtrsim 165$ GeV), it is clear that the models described here are completely consistent with current bounds, but may be probed in the coming future. In those versions of the model where metastable glueballs exist, decays of these states far from the galactic centre

could also provide striking signatures for indirect detection experiments, although the extreme dependence of glueball lifetimes on parameters like $\Lambda'_{\rm QCD}$, the exact value of $m_{b'}$, and potential contributions from HDO's, makes it impossible to make concrete predictions.

Although a vanishing contribution to $\Delta N_{\rm eff}$ is possible for large ν' masses, a massless twin neutrino will give $\Delta N_{\rm eff} \approx 0.075$ at least. A prediction of this size, albeit compatible with current measurements, will certainly be probed in the near future.

Finally, we note that similar investigations of DM in Twin Higgs models have been carried out by other groups [143] and [144].

Chapter 4

Twin Asymmetric Dark Matter

Based on work done in collaboration with R. Lasenby and J. March-Russell [2].

4.1 Introduction

This chapter explores the possibility of ADM in the context of Fraternal Twin Higgs theories. As discussed in section 2.2.2, the paradigm of ADM provides a context in which the $\mathcal{O}(1)$ ratio between the DM and baryon relic abundances, $\Omega_{\rm DM}/\Omega_b \simeq 5$, can be explained. A true explanation, however, requires a rationale for having $\eta_{\rm DM} \sim \eta_b$, and also $m_{\rm DM} \sim m_N$. Here, we will assume that the two asymmetries are of the same order, but we will see that $m_{\rm DM} \sim m_N \sim$ GeV is in fact a feature of this class of Twin Higgs models, and it is fixed by the requirements of naturalness alone.

Unlike in chapter 3, we work in the regime $m_{b'} \lesssim \Lambda'_{\rm QCD}$, where the twin QCD$'$ theory is determined by a single scale – the scale of twin QCD confinement $\Lambda'_{\rm QCD}$. In section 4.2, we study potential stable states in the twin sector, and argue that the baryon $\Delta' \sim b'b'b'$ arises as a natural DM candidate. We study its characteristics, and direct detection phenomenology, in section 4.3. In section 4.4 we deviate from the most minimal version of Fraternal Twin Higgs, and consider the case in which $U(1)'_Y$ is gauged. Now, an atomic bound state made of Δ' and $\overline{\tau'}$ can be the DM.

4.2 Stable and relativistic twins

Within the Fraternal Twin Higgs scenario, the twin sector respects three accidental global symmetries: twin baryon number B$'$, lepton number L$'$ and 'charge' Q$'$. If these are not too badly broken by HDO's, as we will assume, then the lightest twin particles carrying these quantum numbers will be cosmologically stable states. Twin CP could be a good discrete symmetry of the twin sector, although both P and C are violated by $SU(2)'_L$ interactions.

We consider massive τ' but allow for heavy or massless ν', usually with $m_{\tau'} + m_{\nu'} < m_{W'}$ so that $W'^{\pm}$ gauge bosons decay, although a possibly interesting scenario arises if $m_{\tau'} + m_{\nu'} > m_{W'}$ and $W'^{\pm}$ are stable. For $m_{b'} \lesssim \Lambda'_{\rm QCD}$, the lowest QCD$'$ states are $\overline{b}'b'$ mesons, the lightest being a pseudoscalar $\hat{\eta}$ and a scalar $\hat{\chi}$ with masses $m_{\hat{\eta}} \approx (2-3)\Lambda'_{\rm QCD}$ and $m_{\hat{\chi}} \approx 1.5 m_{\hat{\eta}}$ [145]. (A distinctive feature is the absence of pNGB's due to the chiral anomaly.) The glueball spectrum is heavier and only weakly mixed with the mesons, with the lightest being a 0^{++} state of mass $m_0 \simeq 6.8\Lambda'_{\rm QCD}$ [58,59]. Meson/glueball states decay quickly via $SU(2)'_L$ interactions to $\overline{\nu'}\nu'$ pairs if $m_{\nu'} \approx 0$ (and multi-γ' states if $U(1)'_Y$ is gauged) and lighter mesons/glueballs, or to SM states via twin-scalar$-$Higgs mixing [46, 135]. Independently of $m_{\nu'}$, the lightest twin meson $\hat{\eta}$ may decay very fast via dimension-6 HDO's that preserve total CP, of the form $\sim (\overline{q}\gamma^5 q\ \overline{b}'\gamma^5 b')/M^2$, where q denotes SM quarks (for $M \sim 10$ TeV, this gives a lifetime $\tau_{\hat{\eta}}^{-1} \sim 10^{-14}$ s).

The spin-3/2 twin Δ' baryon with mass $m_{\Delta'} \approx 5\Lambda'_{\rm QCD}$ [145] and Q$'$ charge -1, is naturally extremely long-lived since it is the lightest B$' \neq 0$ object. Moreover, the leading HDO violating SM and twin baryon numbers but preserving a linear combination is dimension-12, resulting in a lifetime $\tau_{\Delta'} \sim 10^{26}$ s for $m_{\Delta'} \sim 10$ GeV and $M \sim 10$ TeV. Thus even in the presence of HDO's, Δ' can be stable on cosmological timescales. For the purposes of this chapter we assume that the Δ' is the only B$'$-carrying state with a cosmologically relevant lifetime. (The presence of heavier stable twin baryon states would not qualitatively change our conclusions.)

DR contributions to the number of effective neutrino species, $\Delta N_{\rm eff}$, can arise from light twin neutrinos, and twin photons when $U(1)'_Y$ is gauged. Due to the extremely fast decay of the lightest twin meson $\hat{\eta}$ into SM states naturally present via HDO's, we expect the ν' and γ' sectors to remain in equilibrium with the SM after the QCD$'$ phase transition, even for values of $\Lambda'_{\rm QCD}$ as small as ~ 0.5 GeV. As a result, in the case of $m_{\nu'} \approx 0$ and *no* gauged $U(1)'_Y$ we expect a contribution to $\Delta N_{\rm eff}$ of ≈ 0.075 (as argued in section 3.8) and of ≈ 0.16 when twin photons are also present. Notice these are the minimum possible contributions to $\Delta N_{\rm eff}$ and are compatible with the current measured value $\Delta N_{\rm eff} - \Delta N_{\rm eff,SM} \simeq 0.1 \pm 0.2$ [142], although future experiments may achieve an accuracy of ~ 0.05 [146, 147] and therefore probe these

two scenarios.

4.3 Twin baryon and W' DM

The ADM scenario necessarily has a linked asymmetry in SM- and twin-sector quantum numbers. The generation of such an asymmetry is a UV issue — here we simply assume that it is present. In addition, ADM requires efficient annihilation of the symmetric component of stable DM states, so that the final DM abundance is dominantly set by the asymmetry. In our case, annihilation of the symmetric component of the twin baryon states happens efficiently via twin strong interactions. Sufficiently heavy τ' and ν' species also annihilate efficiently, mainly to $\overline{b}'b'$ states (see figure 2 in [148]). The QCD$'$ phase transition for $m_{b'} \lesssim \Lambda'_{\rm QCD}$ is a smooth crossover [124–126], so we expect neither significant non-equilibrium dynamics nor entropy production affecting relic densities.

A twin baryon number asymmetry implies an asymmetric relic population of Δ' baryons. If $\eta_{\rm Q'} = 0$, then the (ungauged) charge density of the Δ' population must be balanced by a population of twin charged states. So, if the Δ' baryons are to be the only significant DM component, either $m_{\tau'} \approx 0$ so that an asymmetric abundance of these can exist as DR, or we must have a compensating asymmetry in (global) twin charge, $\eta_{\rm Q'} \simeq -\eta_{\rm B'}$. Depending on UV dynamics there may be a non-zero twin lepton asymmetry setting an asymmetric ν' DR relic density (the τ' density is fixed by $\eta_{\rm B'}$ and $\eta_{\rm Q'}$).

As anticipated in section 4.2, $m_{\Delta'} \approx 5\Lambda'_{\rm QCD}$ [145], which translates into $\eta_{\rm B'}/\eta_b \approx m_N/\Lambda'_{\rm QCD}$, with $\Lambda'_{\rm QCD} = 0.5 - 20$ GeV [46]. Thus this framework allows for a successful realisation of ADM in which the mass of the DM particle is not *tuned* to be $\sim 1-10$ GeV, but rather is set by the confinement scale of the DM sector, whose range is restricted directly by naturalness arguments. The value of $y_{b'}$ is irrelevant for the DM mass as long as $m_{b'} \lesssim \Lambda'_{\rm QCD}$ is realised. DM in this framework is then made of *individual* Δ' baryons. Bound states, if they exist in the spectrum, will not form in the early universe, since the only states parametrically lighter that could be emitted in the binding process are ν' or light SM states, but these both only

interact via tiny sub-weak interactions. Moreover, we find that even in the presence of twin photons, radiative capture is not fast enough to give a significant population of $\Delta' - \Delta'$ bound states as the electric and magnetic dipole radiative capture rates vanish. (This situation can be significantly different when lighter generations are present, in which case bound states may form allowing for a scenario of nuclear DM [149, 150].)

Regarding Δ' self-interaction bounds we have, parametrically, $\sigma_{\Delta'}/m_{\Delta'} \sim (\Lambda'_{\rm QCD})^{-3} \sim 10^{-3} - 10^{-8}$ cm^2 g^{-1} for $\Lambda'_{\rm QCD} = 0.5 - 20$ GeV, well below the current experimental upper bound of ~ 0.5 cm^2 g^{-1} [151].

Finally, in the case where $m_{\tau'} + m_{\nu'} > m_{W'}$, $W'^{\pm}$ are also stable states, and even if $\eta_{\rm B'} = -\eta_{\rm Q'}$, an asymmetric population of τ' ($\overline{\tau'}$) states could survive, whose charge is balanced by an equal number of asymmetric W'^{+} (W'^{-}) states. Notice that for small values $f/v \approx 3 - 5$ (see figure 4 in [148]), annihilation of the symmetric populations of τ', ν' and $W'^{\pm}$ occurs very efficiently. For this latter possibility to be realised without introducing significant extra tuning, one would need $m_{\tau'}, m_{\nu'} \sim 10^2$ GeV (since $m_{W'} \approx (f/v) m_W$), above the mass range where ADM scenarios work most naturally.

4.3.1 Direct detection

Scattering of Δ' baryons off SM nucleons happens via Higgs exchange or by exchanging a twin scalar state ($\hat{\chi}$ meson or 0^{++} glueball) that mixes with the Higgs. Couplings between scalar mesons/glueballs and a pair of twin baryons are unknown and require dedicated lattice computation. We find that within a reasonable range for the couplings and mixing angles either Higgs exchange or meson/glueball exchange can dominate the scattering. We therefore separately consider the two processes (ignoring interference effects) to give an idea of the possible scattering cross sections.

In the case where Higgs exchange dominates, the SI scattering cross section is given by

$$\sigma_h^{\rm SI} \approx \frac{1}{\pi} \mu_{N\Delta'}^2 \frac{(f_N m_N)^2}{m_h^4 v^4} \frac{(m_{\Delta'} f_{\Delta'})^2}{(f/v)^4} \ , \tag{4.1}$$

where $\mu_{N\Delta'} = m_N m_{\Delta'}/(m_N + m_{\Delta'})$ is the reduced mass of the Δ'-nucleon system. $f_N \approx 0.32$ [152–154] and $f_{\Delta'} = (2+87f_{b'})/31$ (following [155]) are the effective Higgs couplings to nucleons and Δ' baryons, respectively, where $f_{b'}$ is the dimensionless part of the matrix element of b' in Δ'. In the light b' case, one expects $f_{b'} \ll 1$ albeit its exact value requires dedicated lattice study. In the case where the dominant process is meson exchange, the cross section can be written as

$$\sigma^{\rm SI}_{\hat{\chi}} \approx \frac{1}{\pi}\mu^2_{N\Delta'}\frac{(f_N m_N)^2}{m^4_{\hat{\chi}}v^2}\lambda'^2\theta'^2 \ , \tag{4.2}$$

where λ' is the coupling between $\hat{\chi}$ and a pair of Δ' baryons and θ' is the Higgs-$\hat{\chi}$ mixing angle

$$\theta' = \frac{f_{\hat{\chi}} m_{\hat{\chi}}}{2f(f/v)}\frac{\mathcal{F}_{\hat{\chi}}}{m_h^2 - m^2_{\hat{\chi}}} \ , \tag{4.3}$$

with $\mathcal{F}_{\hat{\chi}}$ the 0^{++} meson decay constant that we define as $\mathcal{F}_{\hat{\chi}} \equiv a' m^2_{\hat{\chi}}$ (with a' an unknown dimensionless constant) and $f_{\hat{\chi}} = (2 + 58\tilde{f}_{b'})/31$ accounts for the effective coupling between meson and Higgs. Numerical evaluation shows that for $\lambda' \lesssim 1$ Higgs exchange dominates, whereas for $\lambda' \gtrsim 4\pi$ meson exchange provides the leading interaction. In the event of glueball exchange being the dominant process, the scattering cross section is given by eq.(4.2) after performing the appropriate substitutions.

Figure 4.1 shows these SI scattering cross sections for particular choices of the unknown parameters. To illustrate the range possible we have chosen the minimum Higgs-exchange cross section (i.e. $f_{b'} = 0$), while for meson exchange we have selected reasonably large values of the parameters. Note that different choices allow Higgs or glueball exchange to dominate. A significant portion of parameter space is covered by the neutrino floor, in particular the region $m_{\Delta'} \approx 5$ GeV that would allow for $\eta_{\rm B'} \approx \eta_b$. For values $m_{\Delta'} \approx 10 - 50$ GeV, which correspond to $\eta_{\rm B'}/\eta_b \approx 0.5 - 0.1$, predicted cross sections escape the neutrino background and sit close to (or within) the region that will be probed by next-generation experiments such as LZ [156].

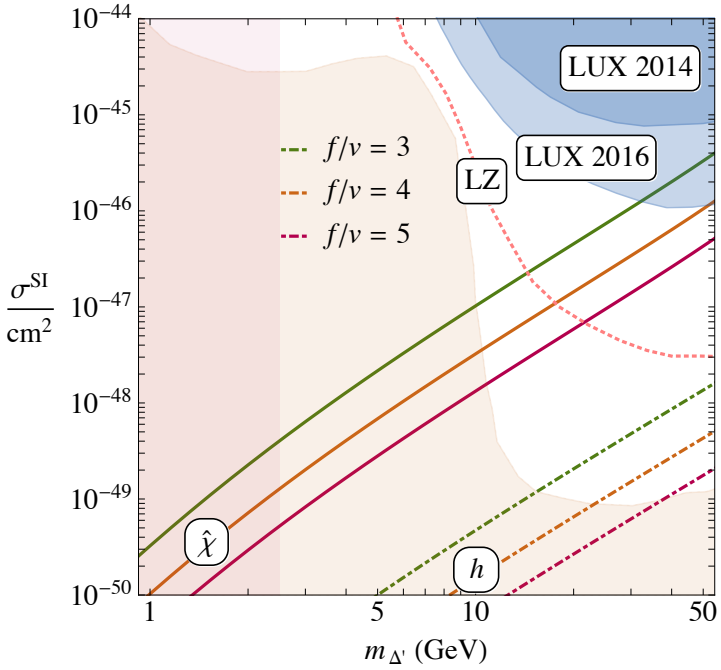

Figure 4.1: Illustrative range of possible SI scattering cross sections of Δ' baryons off SM nucleons when either Higgs or $\hat{\chi}$ meson exchange dominates (dashed and thick lines respectively). We take $m_{\hat{\chi}} = 3\Lambda'_{\rm QCD}$, $\lambda' = 4\pi$, $a' = 1$, $f_{b'} = 0$ and $\tilde{f}_{b'} = 0.1$ for illustration. Dark blue region: LUX bounds at the time [2] was written [133]; light blue: current region of parameter space excluded by LUX [110]; orange: neutrino background [156]; pink dotted line: LZ sensitivity [156]; pink: values of $m_{\Delta'}$ (equivalently, of $\Lambda'_{\rm QCD}$) that imply extra tuning [46].

4.4 Twin atoms

Once the $U(1)'_Y$ group is gauged, the physics becomes substantially richer. Twin-charge neutrality of the Universe requires $\eta_{Q'} = 0$, which means that a B$'$ asymmetry resulting in a non-zero asymmetric population of Δ' baryons must be balanced by an L$'$ asymmetry, such that an equal asymmetric population of $\overline{\tau'}$ is present (we here assume that $W'^{\pm}$ are unstable). Due to twin electromagnetic interactions, the asymmetric populations of Δ' and $\overline{\tau'}$ states may form bound states. In fact, the late-time DM population *must* consist of overall-neutral 'twin atoms', rather than a plasma of charged states, for values of the twin electromagnetic coupling α' that are not extremely small; otherwise, the long-range interactions between DM particles result in plasma instabilities that strongly affect Bullet Cluster-like collisions [157, 158]. Requiring that efficient twin recombination takes place imposes non-trivial constraints on the sizes of α' and the mass of the twin atom $\hat{H}$ [159]. Further constraints are present due to DM self-interactions: low energy atom-atom scattering processes have cross sections $\sigma \approx 10^2 (a'_0)^2$ where $a'_0 = (\alpha' \mu_{\hat{H}})^{-1}$ is the atomic Bohr radius and $\mu_{\hat{H}}$ the reduced mass of the atomic system, although the exact value of σ depends strongly on the ratio $R \equiv m_{\Delta'}/m_{\tau'}$ for values $R \gtrsim 15$ [160]. We impose the constraint $\sigma/m_{\hat{H}} \lesssim 0.5$ cm^2 g^{-1} [151] applicable to contact-like DM scattering, since the effect of hard scatterings generally dominates over soft or dissipative processes for atom-atom scattering in the regimes we consider. Figures 4.2 and 4.3 show constraints from recombination [159] and DM self-interactions, for ratios $R \equiv m_{\Delta'}/m_{\tau'} = 1$ and 10 respectively.

For values of α' and $m_{\hat{H}}$ satisfying recombination and self-interaction constraints, and for the parameter ranges we consider, annihilation of the symmetric populations of Δ' and τ' happens very efficiently. As can be seen from figures 4.2 and 4.3, the minimum value of α' consistent with all constraints is $\alpha' \approx 10^{-2}$, in which case the twin atom mass is constrained to be $m_{\hat{H}} \approx 20,\ 40$ GeV for $R = 1, 10$ respectively. This results in binding energies of order $\sim 10^2$ keV, and a hyperfine splitting of the first atomic energy level of order $\Delta E \sim 10$ eV.

Before twin sector recombination occurs, the Δ' and $\overline{\tau'}$ are coupled to the twin

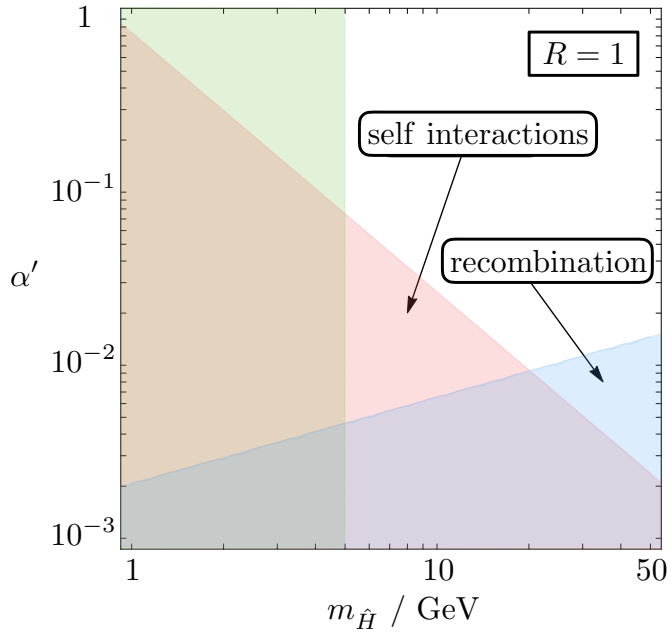

Figure 4.2: Constraints in the $\alpha', m_{\hat{H}}$ plane, for a ratio $R = m_{\Delta'}/m_{\tau'} = 1$. Blue: twin recombination is inefficient, an ionised fraction $\gtrsim 0.1$ remaining; pink: self-interaction cross section is $\gtrsim 0.5$ cm^2 g^{-1}; green: twin atom masses small enough that significant extra tuning is present.

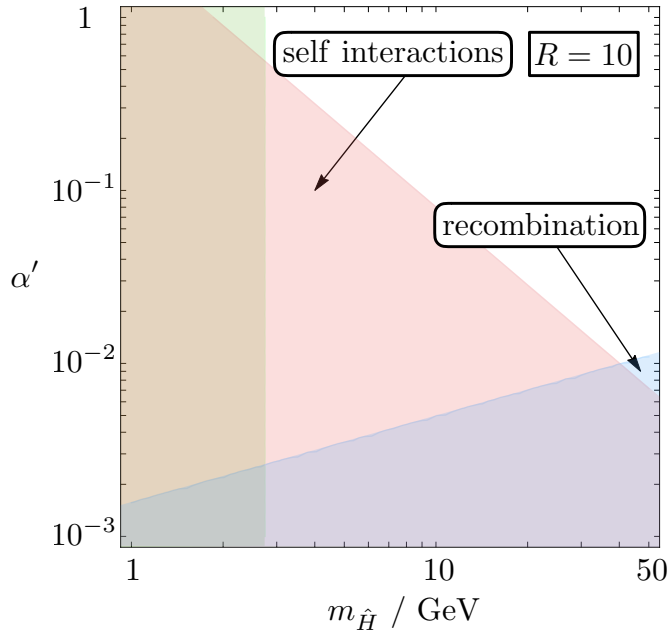

Figure 4.3: As figure 4.3 but for a ratio $R = m_{\Delta'}/m_{\tau'} = 10$.

photon bath, constituting a dark plasma that can undergo 'dark acoustic oscillations' [159]. If twin sector recombination is late enough, these oscillations can leave an imprint in the power spectrum of baryonic matter. However, since $\alpha' \gtrsim 10^{-2}$ in our allowed regions, the binding energy of our twin atoms is sufficiently high ($\gg 10$ keV) that twin recombination is always too early to realise this possibility.

Another possibility is that, after dark recombination, molecular bound states may form at lower temperatures. However, radiative capture of two neutral atoms to a 'dark hydrogen molecule' is very suppressed [161], with molecule formation requiring that there is an abundance of charged particles to catalyse the reactions. Given the constraints that must already be satisfied, our estimates indicate that a significant proportion of molecules will not be formed, either in the early universe, or in halos.

We remark that most of the physics discussed in this section is not specific to Fraternal Twin Higgs models, relying only on asymmetric DM charged under a dark $U(1)$ gauge group. There is a large body of literature on the physics of such 'dark atoms', e.g. [162–165], which in particular can arise in many 'mirror world' models [166, 167].

4.4.1 Direct detection

We first neglect the impact of kinetic mixing between the twin and SM photons on direct detection signatures and concentrate on the process of scattering purely via Higgs exchange or by exchange of a twin scalar that mixes with the Higgs. An interesting situation arises for $R \approx 1$. In this case, $m_{\Delta'} \approx m_{\tau'}$ and therefore the Higgs couples to both states with equal strength. On the other hand, the typical size of the atom is set by $a_0' = (\alpha' \mu_{\hat{H}})^{-1}$, which is ≈ 4 fm for $\alpha' \approx 10^{-2}$ and $m_{\hat{H}} \approx 20$ GeV, values consistent with all constraints (see figure 4.2). The size of the atomic system is thus comparable to that of SM nuclei relevant for direct detection experiments, and the possibility of a detectable 'dark form factor' arises (with the form factor approximately given by the Fourier transform of the ground state atomic wavefunction squared). While such a signal would be degenerate with modifications to the DM halo velocity distribution for data from a single direct

detection experiment [168], multiple experiments with different SM target nuclei could allow the dark form factor contribution to be disentangled [169].

Alternatively, if $R \gg 1$ then the atom's coupling to the Higgs is dominantly through the Δ', whose structure is on smaller scales than SM nuclei, since $\Lambda'_{\rm QCD} > \Lambda_{\rm QCD}$. Thus, in this case, we would have a basically momentum-independent dark form factor, and SI cross sections would be like those shown in figure 4.1.

Finally, kinetic mixing between the two sectors can arise via the operator $\frac{\epsilon}{2} F_{\mu\nu} F'^{\mu\nu}$. This results in twin sector particles acquiring SM-sector electric charges of size $\sim \epsilon e'$, with $e' = \sqrt{4\pi\alpha'}$. Low-energy radiative contributions to the kinetic mixing parameter appear to be absent up to three-loop order [43,46], and therefore one can expect $\epsilon \sim (16\pi^2)^{-4} \sim 10^{-9}$ *if* a non-vanishing four-loop contribution to ϵ indeed exists (UV contributions to kinetic mixing can be present depending on the completion). Notice that our DM atoms are neutral under both visible and twin sector electromagnetism and have vanishing permanent electric dipole moments, due to their spherical distribution of charge. Nevertheless, twin atoms have magnetic dipole moments under both sectors, with the visible sector moment suppressed by a factor of ϵ. Experimental constraints on ϵ arise from a combination of astrophysical, accelerator, and direct detection considerations [170–174]. The nature of the dominant constraint depends strongly on the values of α', $m_{\hat{H}}$ and R, but for the range of parameters considered here, values of $\epsilon \lesssim 10^{-9}$ are likely to satisfy all current bounds.

4.5 Conclusions

We have shown that for the values of $\Lambda'_{\rm QCD}$ allowed by naturalness, and in the ungauged $U(1)'_Y$ case, the twin hadron $\Delta' \sim b'b'b'$ is a successful ADM candidate, with mass $\sim 1 - 10$ GeV – automatically in the most attractive regime for ADM theories to explain the $\mathcal{O}(1)$ ratio of DM-to-baryon energy densities. If $U(1)'_Y$ is gauged, an asymmetric population of Δ' baryons is balanced by an equal number of asymmetric $\overline{\tau'}$. In significant regions of parameter space, twin atoms are formed and are successful DM candidates consistent with all current constraints, although modified halo dynamics and direct detection signals are possible.

Chapter 5

Disassembling the Clockwork Mechanism

Based on work done in collaboration with Nathaniel Craig and Dave Sutherland [3].

5.1 Introduction

The problems of the SM remain as striking as ever, but their solutions — if they indeed exist — have yet to make themselves apparent. From the electroweak hierarchy problem to the DM puzzle to the inflationary paradigm, experimental data largely disfavors solutions involving mass scales and couplings commensurate with those seen elsewhere in nature.

Perhaps this is a sign that the degrees of freedom solving the problems of the SM are in some way sequestered from us, interacting feebly due to small dimensionless couplings or the suppression by vast dimensionful scales. Indeed, extensions of the SM operating along these lines are among the most compatible with existing data: cosmological observations are accommodated by inflationary potentials that are flat on trans-Planckian scales; the electroweak hierarchy problem may be solved by the evolution of fields across similarly trans-Planckian distances [175]; and DM may be explained by light particles carrying infinitesimal electromagnetic charges. Recent attempts to test these feebly-interacting degrees of freedom have led to a proliferation of novel experiments across the energy, intensity, and cosmic frontiers.

Such feeble interactions require large parametric hierarchies with respect to the couplings and scales of the SM and quantum gravity. These parametric hierarchies are challenging to understand from the perspective of naturalness, which prefers $\mathcal{O}(1)$ dimensionless couplings and degenerate scales in the fundamental theory. Even parameters that are technically natural or otherwise radiatively stable beg for deeper explanation if they are infinitesimally small. Beyond questions of field-theoretic naturalness, extremely weak couplings are challenging to reconcile with generic properties of quantum gravity [176].

To this end, there has recently been considerable progress in generating large effective hierarchies from theories whose fundamental parameters are all natural in the conventional sense. These include models of inflation with sub-Planckian intrinsic scales and super-Planckian effective couplings [177–179], as well as more general theories realizing exponential hierarchies in the decay constants of pseudo-goldstone bosons [9,10]. Such "clockwork" models involve a linear quiver with $N+1$ sites, where each site possesses a global $U(1)$ symmetry acting on a complex scalar field. The $U(1)^{N+1}$ symmetry of the quiver is explicitly broken by asymmetric nearest-neighbour interactions that preserve a single $U(1)$. When the scalars acquire vacuum expectation values, the resulting goldstone boson is a linear combination of fields from each site whose weights follow a geometric sequence, and the unbroken symmetry is asymmetrically distributed among sites. As a result, any coupling of additional fields to the scalar at a specific site gives rise to an exponentially-suppressed and site-dependent coupling of those fields to the goldstone boson. This provides a natural mechanism for generating exponential hierarchies in a theory whose fundamental parameters are all of comparable size, and leads to a variety of model-building possibilities [180–182].

In [183], the clockwork mechanism was generalized to include states of higher spin, giving rise to exponentially small fermion masses, gauge millicharges, and gravitational couplings. Even more ambitiously, the authors of [183] also conjecture a continuum counterpart to four-dimensional clockwork in the form of five-dimensional linear dilaton models, which in turn are holographically related (with the addition of two more compact dimensions) to little string theory [184]. If true, this would open the door to a wider variety of constructions in both four and five dimensions [185, 186].

Given the potentially vast applications of clockwork to questions of phenomenological interest, it is crucial to precisely determine the scope of clockwork. As such, in this chapter we systematically answer two questions:

1. *What theories can be clockworked in four dimensions?*

2. *What are their higher-dimensional continuum counterparts?*

To answer these questions, we must take care to carefully define the features of a clockwork theory. In particular, the definition must distinguish genuine "clockwork" phenomena from already-familiar hierarchies arising from volume suppression [15] or curvature-induced localization [14] in extra dimensions (or their deconstructed counterparts [187–189]). For our purposes, we will take clockwork to involve the salient features of the original models [9, 10], namely

> **Clockwork:** *A four-dimensional quiver theory with no exponential hierarchies in fundamental parameters that gives rise to exponentially suppressed (and site-dependent) couplings to a symmetry-protected zero mode.*

These are not merely incidental properties of clockwork, but essential ones. In particular, site-dependent exponentially suppressed couplings are a hallmark of the asymmetric distribution of the unbroken symmetry among different sites. This clearly distinguishes the clockwork theories of [9, 10] in four dimensions from, say, deconstructions of extra dimensions with flat or bulk AdS metrics. For example, deconstructions of flat extra dimensions involve no hierarchies in fundamental parameters, but only give rise to site-independent zero mode couplings suppressed by $\sim \sqrt{N}$ factors. Similarly, deconstructions of Randall-Sundrum and other warped models can give rise to exponentially-suppressed (albeit position-independent) zero mode couplings, but necessarily involve exponential hierarchies in the vacuum expectation values of the link fields. The genuine novelty of clockwork is that it furnishes exponential and site-dependent effective couplings from a fundamental theory with no large parametric hierarchies or multiplicity of sites. To the extent that these properties arise from the asymmetric distribution of an unbroken symmetry subgroup, in what follows we will refer to the localization of fields in the space of appropriate symmetry generators as 'symmetry-localization.' Such symmetry-localization controls the couplings of fields dictated by gauge or global symmetries. As we will see, this symmetry-localization differs in important ways from localization of fields propagating in a non-trivial geometry with respect to a 5D metric.

As we will show, the answers to these questions are:

1. *Clockwork is a strictly abelian phenomenon.* In particular, there is no clock-

work for Yang-Mills theories, non-linear sigma models, or gravity.

2. *Geometry alone cannot clockwork bosonic fields.* Zero modes of massless bosonic bulk fields are flat, regardless of apparent features of the metric. In particular, higher-dimensional models with massless bulk fields on linear dilaton backgrounds do not furnish continuum counterparts of clockwork. Successful continuum clockwork requires bulk and brane masses to symmetry-localize the zero mode.

These conclusions are consistent with the original clockwork proposals [9, 10], but they are in tension with the results of [183], applications thereof [185], and subsequent attempts to clockwork non-abelian global symmetries [186]. Insofar as it is not possible to clockwork gravity in the sense of generating an asymmetrically-distributed general coordinate invariance, clockwork offers no new solution to the electroweak hierarchy problem. Moreover, in those cases where clockwork is possible, namely for spin-0 and abelian spin-1 fields, we argue that — appropriately interpreted — deconstructions of five-dimensional linear dilaton models do not exhibit clockwork phenomena.

We emphasize that our statement about the lack of a clockwork solution to the hierarchy problem stems solely from the fact that gravity cannot be consistently clockworked, as we prove in section 5.2.4. This is *not* a statement about the potential of linear dilaton theories for solving the hierarchy problem — that they do is well-known [190, 191]. In these theories exponential hierarchies are generated by a linear profile for the dilaton, whose exponential coupling gives rise to the desired hierarchies. When deconstructed, they do not lead to four-dimensional theories with a clockwork graviton in which the surviving general coordinate invariance is asymmetrically distributed among different sites.[1]

More optimistically, we construct five-dimensional theories with bulk and brane masses that exhibit clockwork phenomena. These are the continuum counterparts of clockwork theories, in the sense that discretizing them gives four-dimensional theories whose spectra and couplings match those of a uniform four-dimensional

[1] Very much in the same way that other extra dimensional solutions, like Randall-Sundrum [14] or large flat extra dimensions [15], do not lead to a clockwork graviton when deconstructed.

clockwork up to appropriately small $1/N$ corrections. The emergence of meaningful clockwork phenomena in the deconstruction of higher-dimensional theories with bulk and brane masses opens the door to a variety of promising model-building possibilities.

We stress that further model building opportunities may arise if the definition of clockwork is significantly relaxed. In particular, if we do not require that the zero-mode be symmetry protected, it is possible to construct a quiver of non-linear sigma models whose zero-mode has exponentially suppressed, and site-dependent, couplings [192]. Whilst such a zero-mode is necessarily massive, it may be parametrically lighter than the other modes of the quiver — a fact which is mirrored in the quiver's 5D analog as the fifth component of a non-Abelian gauge field in AdS. However, in keeping with the original clockwork model, we will insist on a symmetry-protected, massless zero-mode.

The chapter is organized as follows: in section 5.2 we review the essential features of the discrete clockwork mechanism, following the arguments of [183], and illustrate how effective clockworking arises only for goldstone bosons of spontaneously broken abelian global symmetries, and gauge bosons of abelian gauge symmetries. We explicitly show how an analogous mechanism cannot be built for non-abelian gauge bosons and gravitons. In section 5.3 we turn to the conjectured continuum counterpart of viable four-dimensional clockwork. We show that the couplings between the zero mode of a massless bulk scalar or vector and matter localized at some point in the fifth dimension do not reproduce the properties of clockwork models when deconstructed – a statement that holds for a general class of warped metrics, and includes linear dilaton theories. Given the failure of geometry alone to produce clockwork, in section 5.4 we show that genuine clockwork arises in the deconstruction of extra dimensions with a flat metric and suitably-chosen bulk and brane mass terms that preserve a massless zero mode. In section 5.5 we explicitly show how the deconstruction of a gravitational extra dimension does not lead to a graviton clockwork, in keeping with our results of section 5.2. We summarize our conclusions in section 5.6.

5.2 Discrete clockwork

In this section, we discuss the basic features of the discrete clockwork mechanism using the framework introduced in [183]. Sections 5.2.1 and 5.2.2 focus on the spin-0, and abelian spin-1 scenarios, in which a finite amount of clockworking may be successfully generated in a consistent fashion (as defined in section 5.1). On the other hand, sections 5.2.3 and 5.2.4 illustrate how an analogous clockwork mechanism cannot be consistently constructed in the non-abelian spin-1 and spin-2 cases. We summarize these results from the perspective of the clockwork symmetry in section 5.2.5.

5.2.1 Scalar clockwork

The discrete scalar clockwork mechanism involves $N+1$ real scalar fields, together with N charge and mass-squared parameters, q_j and m_j^2 ($j = 0, ..., N-1$), such that the lagrangian of the scalar sector is given by[2]

$$\mathcal{L}_4 = -\frac{1}{2}\sum_{j=0}^{N}(\partial_\mu \phi_j)^2 - \frac{1}{2}\sum_{j=0}^{N-1} m_j^2(\phi_j - q_j\phi_{j+1})^2 \ . \tag{5.1}$$

The $N+1$ scalar fields ϕ_j may be conveniently thought of as the Goldstone bosons of a global $U(1)^{N+1}$ symmetry, spontaneously broken at some high scale f. Eq.(5.1) can then be regarded as the effective lagrangian of the Goldstone sector, valid at scales $\ll f$, and with the mass-squared parameters m_j^2 introducing an explicit breaking of N of the $N+1$ global symmetries. As a result, the effective theory of the Goldstone sector features only one massless state.

The parameters m_j^2 may arise from the vacuum expectation values (vev's) of N additional scalar fields charged under the $U(1)_j$ and $U(1)_{j+1}$ global subgroups, with charges $+1$ and $-q_j$ respectively, as discussed in [183]. This allows for the effective theory defined through eq.(5.1) to be UV completed in a way such that all sources of symmetry breaking are spontaneous.

The profile of the massless mode corresponding to the single Goldstone that

[2]Throughout this chapter, implicit contraction of Greek indices denotes contraction with $\eta_{\mu\nu} = (-1, +1, +1, +1)$.

remains in the spectrum is given by $\phi_{(0)} = \sum_{j=0}^{N} c_j \phi_j$, with

$$c_j = c_0 \prod_{k=0}^{j-1} \frac{1}{q_k} \quad (\text{for } j \geqslant 1) \ , \quad \text{and} \quad c_0 = \left(1 + \sum_{j=1}^{N} \prod_{k=0}^{j-1} \frac{1}{q_k^2} \right)^{-1/2} \ , \tag{5.2}$$

where the expression for c_0 comes from demanding the kinetic term of $\phi_{(0)}$ be canonical. In particular, in the case of equal clockwork parameters ($m_j^2 \equiv m^2, q_j \equiv q \; \forall \; j = 0, ..., N-1$) considered in [183], one finds $c_j \simeq q^{-j}$ (for $q > 1$ and large N). The massless mode therefore has a profile that is exponentially localized towards the $j = 0$ site.

The clockwork mechanism as a means of generating large hierarchies comes into play when we introduce an axion-like coupling between one of the scalar fields (e.g. the scalar field of the k-th site), and a non-abelian gauge theory, of the form

$$\mathcal{L}_4 \supset -\frac{1}{4\overline{g}^2} G_{\mu\nu} G^{\mu\nu} + \frac{\phi_k}{16\pi^2 f} G_{\mu\nu} \tilde{G}^{\mu\nu} \ . \tag{5.3}$$

The term in the above equation involving only the scalar zero mode reads[3]

$$\mathcal{L}_4 \supset \frac{c_k \phi_{(0)}}{16\pi^2 f} G_{\mu\nu} \tilde{G}^{\mu\nu} \equiv \frac{\phi_{(0)}}{16\pi^2 f_0} G_{\mu\nu} \tilde{G}^{\mu\nu} \ , \tag{5.4}$$

where we have defined an effective axion coupling scale

$$f_0 = \frac{f}{c_k} = \frac{f q^k}{c_0} \simeq q^k f = q^k M_{Pl} \left(\frac{f}{M_{Pl}} \right) \ . \tag{5.5}$$

(We have restricted ourselves to the case of equal charges, $q_j \equiv q > 1$, for illustration.) An effective axion coupling that is hierarchically larger than the symmetry breaking scale f is dynamically generated if the gauge theory is coupled to one of the scalar fields towards the end of the array of sites.

The clockwork mechanism for scalars then allows for exponentially different effective axion couplings depending on where the gauge theory is localized, as a result of the symmetry-localization of the massless scalar field along the lattice, and in the

[3]Notice that since $\mathbb{M}^2$ is a real symmetric matrix (therefore it can be diagonalized by an orthogonal matrix), the scalar field of the j-th site may be written in terms of mass eigenstates as $\phi_j = c_j \phi_{(0)} + ...$, where the dots denote strictly massive modes.

absence of site-dependent hierarchies in the decay constants of the $N+1$ axions in the unbroken phase. In particular, for two non-abelian gauge theories localized on opposite sites, but otherwise identical (with the same gauge coupling, and therefore the same physical properties like their confinement scales), the clockwork mechanism leads to a hierarchy of effective axion couplings:

$$\frac{f_{0,k=0}}{f_{0,k=N}} = q^{-N} \ll 1 \ . \tag{5.6}$$

Finally, notice that f_0 can be super-Planckian in a natural fashion, in the sense that it is achieved with parametrically few lattice sites, each of which may have a sub-Planckian symmetry breaking scale f.

5.2.2 Abelian vector clockwork

In analogy with the scalar mechanism described in section 5.2.1, the abelian vector clockwork [193] consists of $N+1$ $U(1)$ gauge theories, each with its own gauge coupling g_j, together with N charge and mass-squared parameters, q_j and v_j^2 ($j = 0, ..., N-1$), such that the lagrangian of the vector sector is given by

$$\mathcal{L}_4 = -\sum_{j=0}^{N} \frac{1}{4g_j^2} F_{j\mu\nu}^2 - \frac{1}{2}\sum_{j=0}^{N-1} v_j^2 (A_{j\mu} - q_j A_{j+1\mu})^2 \ . \tag{5.7}$$

The mass terms have the same form as those in eq.(5.1) for the scalar case, and, as before, may be regarded as arising from the vev's of N scalar fields Φ_j ($j = 0, ..., N-1$) with charges $+1$ and $-q_j$ under $U(1)_j$ and $U(1)_{j+1}$ respectively. As a result, N of the $N+1$ abelian gauge symmetries are broken spontaneously, with a single unbroken $U(1)$ factor remaining. Eq.(5.7) then corresponds to the effective lagrangian describing the vector sector, in unitary gauge. The terms involving the only massless vector that remains in the spectrum are given by the substitutions $A_{j\mu} = c_j A_{\mu(0)} + \ldots$, with c_j as in eq.(5.2) and the dots denoting strictly massive modes, yielding an effective gauge coupling

$$\frac{1}{g_{(0)}^2} = \sum_{j=0}^{N} \frac{c_j^2}{g_j^2} \simeq \frac{c_0^2}{g^2} \ , \tag{5.8}$$

where in the last step we have assumed $q_j \equiv q > 1$ and $g_j \equiv g \; \forall \; j$ for simplicity.[4]

If we now consider a scalar field φ with charge Q_φ under the $U(1)_k$ gauge group, then its kinetic term reads

$$\mathcal{L}_4 \supset -|(\partial_\mu + iQ_\varphi A_{k\mu})\varphi|^2 \simeq -|(\partial_\mu + iQ_\varphi c_0 q^{-k} A_{(0)\mu} + ...)\varphi|^2 \; , \tag{5.9}$$

where the dots denote strictly massive modes, and in the second equality we have again considered the case of $q_j \equiv q > 1$. The effective coupling strength between φ and the massless vector is then given by $\sim g_{(0)} Q_\varphi c_0 q^{-k} \simeq g Q_\varphi q^{-k}$. In particular, for two scalar fields, φ_0 and φ_N, charged under the gauge groups at opposite sites with the same charge Q_φ, the clockwork mechanism leads to an effective hierarchy of charges under the unbroken gauge group:

$$\frac{Q_{0,k=N}}{Q_{0,k=0}} = q^{-N} \ll 1 \; . \tag{5.10}$$

As in the scalar case, the exponential difference in effective couplings arises as a consequence of the symmetry-localization of the massless vector along the lattice, and in the absence of site-dependent hierarchies in the gauge couplings of the $N+1$ vectors in the unbroken phase.

5.2.3 (No) Non-abelian vector clockwork

The difficulties for constructing a non-abelian version of the discrete clockwork mechanism become apparent after having reviewed the abelian case. By analogy, we might choose the N scalar link fields, responsible for spontaneously breaking the non-abelian G^{N+1} group down to G, to transform under different representations of adjacent gauge groups. However, as we show below, such a symmetry breaking pattern would not leave a single non-abelian symmetry group intact (the N vev's would break all $N+1$ copies of G). The only viable lagrangian, which retains a G symmetry after the link fields acquire vev's, has link fields transforming as bifundamentals, in which case it is clear that no clockworking can be generated, as this

[4]Strictly speaking, in the gauge $U(1)$ case we consider here the coefficients c_j are equal to those in eq.(5.2) for $j \geq 1$ with $c_0 = q^N$, so that charge quantization in the N-th site in units of g corresponds to charge quantization of the unbroken gauge theory in units of $g_{(0)} \simeq g q^{-N}$.

would be analogous to the abelian case discussed in section 5.2.2 with all $q_j = 1$.

To illustrate this situation, consider $N+1$ copies of a non-abelian gauge group $SU(n)$, and N scalar fields Φ_j $(j = 0, ..., N-1)$ transforming as bifundamentals under $SU(n)_j$ and $SU(n)_{j+1}$. After spontaneous symmetry breaking of N of the $N+1$ $SU(n)$ gauge symmetries due to the non-zero vev's of the scalar fields, the effective lagrangian of the vector sector, in unitary gauge, is that of eq.(5.7) after setting $q_j \equiv 1$, and with the obvious replacements $A_{j\mu} \to A^a_{j\mu}$ and $F_{j\mu\nu} \to F^a_{j\mu\nu}$. The massless vector lagrangian is then obtained by the substitutions $A^a_{j\mu} = A^a_{\mu(0)} + \ldots$, and the effective gauge coupling of the unbroken non-abelian gauge theory is given by

$$\frac{1}{g^2_{(0)}} = \sum_{j=0}^{N} \frac{1}{g^2_j} \ . \tag{5.11}$$

Consider now a scalar field φ transforming under a representation $\mathcal{R}$ of the gauge group $SU(n)_k$. Its kinetic term reads

$$\mathcal{L}_4 \supset -|(\partial_\mu + iA^a_{k\mu}T^a_{\mathcal{R}})\varphi|^2 = -|(\partial_\mu + iA^a_{(0)\mu}T^a_{\mathcal{R}} + ...)\varphi|^2 \ , \tag{5.12}$$

where $T^a_{\mathcal{R}}$ are the generators of $SU(n)$ in the appropriate representation, and the dots denote strictly massive modes. The field φ then transforms under representation $\mathcal{R}$ of the unbroken $SU(n)$ factor, with an effective gauge coupling $g_{(0)}$ independent of the position of the k-th site.[5]

Moreover, notice from eq.(5.11) that it is not possible to generate a parametrically small effective gauge coupling in a natural fashion. In particular, eq.(5.11) has two ineffective limits. One, we may set all $g_j = g$, such that $g_{(0)} \simeq g/\sqrt{N}$, and so an unnaturally large number of sites N would be required to generate a meaningful hierarchy between $g_{(0)}$ and g_j. Two, the individual g_j may be of parametrically different sizes, the smallest of which determines the size of $g_{(0)} \sim \min_j g_j$.

We can be more general, and prove that the lack of symmetry-localization of the massless vector mode along the different sites is in fact a requirement if its mass is to be protected by gauge invariance.[6] To illustrate this, consider the case in which

[5] This is a hardly surprising result, for our construction is manifestly gauge invariant, and a massless state with different effective gauge couplings to different matter fields would violate gauge invariance explicitly.

[6] Above, we have only shown that non-abelian clockwork cannot arise if the N scalar fields

the vector field on every site is given by $A^a_{j\mu} = c_j A^a_{(0)\mu} + ...$, with the dots denoting massive modes as usual, and let's remain agnostic about the dynamical origin of the coefficients c_j. The kinetic terms of the $N+1$ non-abelian gauge theories read

$$\begin{aligned}\mathcal{L}_{4,\text{kin}} &= -\sum_{j=0}^{N} \frac{1}{4g_j^2} \left(F^a_{j\mu\nu}\right)^2 \\ &= -\sum_{j=0}^{N} \frac{1}{g_j^2} \left\{ \frac{1}{4} \left(\hat{F}^a_{j\mu\nu}\right)^2 + f^{abc} \partial_\mu A^a_{j\nu} A^{b\mu}_j A^{c\nu}_j + \frac{1}{4} f^{abc} f^{ars} A^b_{j\mu} A^c_{j\nu} A^{r\mu}_j A^{s\nu}_j \right\} ,\end{aligned} \tag{5.13}$$

where $\hat{F}^a_{j\mu\nu} \equiv \partial_\mu A^a_{j\nu} - \partial_\nu A^a_{j\mu}$. Substituting $A^a_{j\mu} = c_j A^a_{(0)\mu} + ...$, the terms in eq.(5.13) involving the massless mode $A^a_{(0)\mu}$ only read

$$\begin{aligned}\mathcal{L}_{4,\text{kin}} \supset &-\frac{1}{4} \left(\sum_{j=0}^{N} \frac{c_j^2}{g_j^2} \right) \hat{F}^{a\ 2}_{(0)\mu\nu} - \left(\sum_{j=0}^{N} \frac{c_j^3}{g_j^2} \right) f^{abc} \partial_\mu A^a_{(0)\nu} A^{b\mu}_{(0)} A^{c\nu}_{(0)} \\ &- \frac{1}{4} \left(\sum_{j=0}^{N} \frac{c_j^4}{g_j^2} \right) f^{abc} f^{ars} A^b_{(0)\mu} A^c_{(0)\nu} A^{r\mu}_{(0)} A^{s\nu}_{(0)} \ .\end{aligned} \tag{5.14}$$

Gauge invariance of the massless mode lagrangian requires all three sums in the equation above be equal,[7] and they define the effective gauge coupling of the unbroken theory, i.e.

$$\frac{1}{g^2_{(0)}} \equiv \sum_{j=0}^{N} \frac{c_j^2}{g_j^2} = \sum_{j=0}^{N} \frac{c_j^3}{g_j^2} = \sum_{j=0}^{N} \frac{c_j^4}{g_j^2} \ . \tag{5.15}$$

The above equalities are only satisfied if $c_j \in \{0, 1\}\ \forall j$, and the terms in eq.(5.14) are then manifestly invariant under infinitesimal gauge transformations of the usual form $A^a_{(0)\mu} \to A^a_{(0)\mu} + \partial_\mu \alpha^a - f^{abc} \alpha^b A^c_{(0)\mu}$.

This general argument addresses, in particular, the case in which the scalar fields Φ_j are chosen to transform under inequivalent representations of the gauge groups at sites j and $j+1$, as well as more intricate constructions in which the Φ_j are chosen to transform non-trivially under non-contiguous gauge groups. Either

transform as bifundamentals. However, one could ask whether a more complicated construction (for instance, the case in which each Φ_j transforms under inequivalent representations of contiguous gauge groups, or a construction that is not restricted to nearest neighbour interactions) could lead to consistent non-abelian clockwork.

[7] Gauge invariance requires both the terms in eq.(5.14), and interaction terms between the massless mode and massive modes (omitted from eq.(5.14)) be gauge invariant independently. However, focusing on the terms in eq.(5.14) will be sufficient to prove that it is not possible to build non-abelian clockwork.

way, the resulting effective lagrangian describing the vector sector will not have a clockworked non-abelian gauge boson.

Thus, although it is possible to build constructions leading to $c_j \notin \{0, 1\}$, and in which the lowest lying vector mode is massless at tree-level (e.g. by writing a mass term for the non-abelian gauge sector as in eq.(5.7) with $q_j > 1$), the masslessness of this mode will not be protected by gauge invariance. We can therefore conclude that a meaningful clockwork mechanism is impossible to engineer in the context of a non-abelian gauge theory. As we discuss next in section 5.2.4, this statement straightforwardly generalizes to the graviton case – an unsurprising result, for gravity is a non-abelian theory itself.

5.2.4 (No) Graviton clockwork

After having discussed the scalar and vector cases, one could wonder whether a spin-2 version of the clockwork mechanism may be consistently built. As before, the starting point would consist of $N+1$ sites, each of them with its own metric $g_{j\mu\nu}$ and general coordinate invariance symmetry GC_j. Allowing for gravitational interactions of varying strength on each site, the Einstein-Hilbert part of the lagrangian simply reads

$$\mathcal{L}_{4,\mathrm{EH}} = \sum_{j=0}^{N} \frac{M_j^2}{2} \sqrt{|g_j|} R_j \ , \tag{5.16}$$

where R_j is the Ricci scalar corresponding to the metric $g_{j\mu\nu}$, and M_j the reduced Planck mass at site j. Eq.(5.16) is manifestly invariant under all $N+1$ copies of GC_j. If we expand the metric on every site as a perturbation around flat space, i.e. $g_{j\mu\nu} = \eta_{\mu\nu} + h_{j\mu\nu}$, then the expansion of eq.(5.16) up to $\mathcal{O}(h_j^2)$ takes the familiar form

$$\mathcal{L}_{4,\mathrm{EH}} = \sum_{j=0}^{N} \frac{M_j^2}{2} \left\{ -\frac{1}{4}(\partial_\mu h_{j\rho\sigma})^2 + \frac{1}{4}(\partial_\mu h_j)^2 + \frac{1}{2}(\partial_\mu h_j^{\mu\nu})^2 - \frac{1}{2}\partial^\mu h_j \partial^\nu h_{j\mu\nu} + ... \right\} \ , \tag{5.17}$$

where $h_j \equiv \eta_{\mu\nu} h_j^{\mu\nu}$.

Subtleties arise when trying to write a mass term that would render N of the gravitons massive in a way that allows for the full general coordinate invariance of

the theory to be restored at some high scale. This was thoroughly explored in [194], where it is argued that this may be achieved by introducing N 'link' fields Y_j^μ ($j = 0, ..., N-1$), which transform non-trivially under GC_j and GC_{j+1}, in complete analogy with the scalar fields Φ_j introduced in the vector case. As discussed in [194], each field Y_j^μ corresponds to a map between a set of coordinates x_j^μ at site j and coordinates $Y_j^\mu(x_j)$ at site $j+1$, and defines a pullback map from site $j+1$ to site j. For instance, using this map we can pullback the metric $g_{j+1\mu\nu}$, which is defined at site $j+1$ and transforms non-trivially under GC_{j+1}, to find an object

$$G_{j\mu\nu}(x_j) \equiv \frac{\partial Y_j^\alpha}{\partial x_j^\mu}\frac{\partial Y_j^\beta}{\partial x_j^\nu} g_{j+1\alpha\beta}(Y_j(x_j)) \ , \tag{5.18}$$

which is now defined at site j, and transforms as a metric under GC_j. In particular, it is now possible to add a term to the lagrangian that respects the full general coordinate invariance of the theory, of the form [194]

$$\mathcal{L}_4 \supset \frac{1}{2}\sum_{j=0}^{N-1}\sqrt{|g_j|}\frac{M_j^2 m_j^2}{4}(g_{j\mu\nu} - G_{j\mu\nu})(g_{j\alpha\beta} - G_{j\alpha\beta})(g_j^{\mu\nu}g_j^{\alpha\beta} - g_j^{\mu\alpha}g_j^{\nu\beta}) \ , \tag{5.19}$$

where the mass parameters m_j will set the mass scale of the N massive graviton excitations, and are analogous to the mass parameters introduced in the scalar and vector cases.

Since we are interested in expanding the metric on every site around the same flat space background, unitary gauge corresponds to $Y_j^\mu = x_j^\mu \ \forall \ j = 0, ..., N-1$.[8] In this gauge, the terms in eq.(5.19) that are quadratic in the perturbation lead to a mass term

$$\mathcal{L}_{4,\mathrm{mass}} = \frac{1}{2}\sum_{j=0}^{N-1}\frac{M_j^2 m_j^2}{4}\left\{(h_j - h_{j+1})^2 - (h_{j\mu\nu} - h_{j+1\mu\nu})^2\right\} \ . \tag{5.20}$$

As in the non-abelian case, the massless graviton lagrangian can be obtained by the substitutions $h_{j\mu\nu} = h_{(0)\mu\nu} + ...$, where the dots denote strictly massive states, and

[8] This is not necessarily the case in general, but it holds if we are expanding around flat space in each site, since in this case the pullback of the background metric acting at site $j+1$ must be equal to the background metric acting at site j.

eq.(5.17) then defines an effective 4D Planck scale

$$M_{(0)} = \left(\sum_{j=0}^{N} M_j^2 \right)^{1/2} \quad . \tag{5.21}$$

This expression clearly illustrates how an effective scale $M_{(0)}$ much larger than the fundamental scale M_j of the individual sites is not possible to engineer in this context. In particular, in the simplest case $M_j \equiv M \; \forall \; j$, $M_{(0)} \simeq M\sqrt{N}$, and so a large hierarchy between $M_{(0)}$ and M would require an even larger value of N, frustrating any attempt to build a solution to the electroweak hierarchy problem in a natural fashion.

If we now consider a stress energy tensor defined on the k-th site, its leading coupling to the metric perturbation is of the form

$$\mathcal{L}_4 \propto h_{k\mu\nu} T^{\mu\nu} = h_{(0)\mu\nu} T^{\mu\nu} + ... \; , \tag{5.22}$$

where the dots denote strictly massive graviton modes. We see how the massless graviton couples with the same strength to a given stress-energy tensor, independently of the position of the site in which $T^{\mu\nu}$ is defined, in keeping with the Equivalence Principle.

As in the non-abelian case of section 5.2.3, we can be more general and prove that the flatness of the massless graviton mode across the different sites is again a requirement if its mass is to be protected by diffeomorphism invariance.[9] In order to do this, it is crucial to consider terms in the expansion of eq.(5.16) that involve higher-order terms in the metric perturbation. Schematically, such an expansion has the form

$$\mathcal{L}_{4,\mathrm{EH}} \sim \sum_{j=0}^{N} M_j^2 \left\{ \partial^2 h_j^2 + \sum_n \partial^2 h_j^{2+n} \right\} \; . \tag{5.23}$$

Now, if we allow ourselves to write $h_{j\mu\nu} = c_j h_{(0)\mu\nu} + ...$, without prejudice about the

[9] So far, we have only shown that a term like that of eq.(5.19) does not lead to an asymmetrically distributed massless graviton. However, one could ask whether a more complicated version of eq.(5.19) could lead, at quadratic order, to an effective mass term like that in eq.(5.20) but with asymmetric couplings in front of the h_j and h_{j+1} terms.

origin of the c_j coefficients, then the previous equation reads

$$\mathcal{L}_{4,\text{EH}} \sim \left(\sum_{j=0}^{N} M_j^2 c_j^2\right) \partial^2 h_{(0)}^2 + \sum_n \left(\sum_{j=0}^{N} M_j^2 c_j^{2+n}\right) \partial^2 h_{(0)}^{2+n} + \dots \,, \tag{5.24}$$

where the dots denote terms involving massive graviton modes only, but also interaction terms between the massless and massive gravitons. As in the non-abelian case, that the terms in the effective lagrangian involving the massless graviton be diffeomorphism invariant requires that all the sums in the equation above be equal,[10] and define an effective Planck scale, i.e.

$$M_{(0)}^2 \equiv \sum_{j=0}^{N} M_j^2 c_j^2 = \sum_{j=0}^{N} M_j^2 c_j^{2+n} \quad \forall\ n \geq 1 \ . \tag{5.25}$$

As in section 5.2.3, these equalities are only satisfied for $c_j \in \{0, 1\}$. The terms in eq.(5.24) are then invariant under infinitesimal diffeomorphism transformations of the usual form

$$h_{(0)\mu\nu} \to h_{(0)\mu\nu} + \partial_\mu \epsilon_\nu + \partial_\nu \epsilon_\mu + f_{\mu\nu}^{\rho\sigma} \partial_\rho \epsilon^\alpha h_{(0)\alpha\sigma} + \epsilon^\alpha \partial_\alpha h_{\mu\nu} \ , \tag{5.26}$$

where $f_{\mu\nu}^{\rho\sigma} \equiv \delta_\mu^\rho \delta_\nu^\sigma + \delta_\nu^\rho \delta_\mu^\sigma$.[11] Hence, any construction that leads to $c_j \notin \{0, 1\}$ will feature a lowest-lying graviton excitation whose mass is not protected by diffeomorphism invariance, even if it is engineered to be massless at tree-level.

In analogy with the results of section 5.2.3 for non-abelian gauge fields, we conclude that it is not possible to build a 4D effective theory in which a massless spin-2 particle is symmetry-localized and, at the same time, retains diffeomorphism invariance. Moreover, in the absence of exponential hierarchies among the values of the different scales M_j, the effective Planck scale only depends on the number of sites as $\sim \sqrt{N}$. Consequently, it is apparent that there is no such thing as a clockwork

[10] Again, we emphasize that diffeomorphism invariance requires both the terms explicitly written in eq.(5.24), and interaction terms between massless and massive modes be invariant independently. However, focusing on the terms in eq.(5.24) will be enough to rule out the possibility of building a clockwork graviton.

[11] We remind the reader that eq.(5.26) is the way in which the metric perturbation $h_{\mu\nu}$ changes under an infinitesimal diffeomorphism transformation, which in a coordinate basis is given by $Y^\mu = x^\mu + \epsilon^\mu$, regardless of the size of $h_{\mu\nu}$. The last term in eq.(5.26) captures the non-abelian nature of gravity, and must be taken into account if we want to assess whether the masslessness of the graviton is indeed symmetry-protected.

graviton, and, by extension, no such thing as a clockwork solution to the hierarchy problem. (In section 5.5 we explicitly show how a clockwork graviton does *not* arise when deconstructing a gravitational extra dimension.)

As an aside, we note that it is sometimes common, and convenient, to rescale the metric perturbation as $h_{j\mu\nu} \to 2h_{j\mu\nu}/M_j$, so that the kinetic terms in eq.(5.17) are canonical. In this rescaled basis, eq.(5.20) now reads

$$\mathcal{L}_{4,\text{mass}} = \frac{1}{2}\sum_{j=0}^{N-1} m_j^2 \left\{ \left(h_j - \frac{M_j}{M_{j+1}} h_{j+1} \right)^2 - \left(h_{j\mu\nu} - \frac{M_j}{M_{j+1}} h_{j+1\mu\nu} \right)^2 \right\} , \qquad (5.27)$$

and the massless graviton mode is just given by $h_{(0)\mu\nu} = \sum_{j=0}^{N} (M_j/M_{(0)}) h_{j\mu\nu}$.[12] The graviton coupling to matter in eq.(5.22) is now

$$\mathcal{L}_4 \propto \frac{h_{k\mu\nu}}{M_k} T^{\mu\nu} = \frac{h_{(0)\mu\nu}}{M_{(0)}} T^{\mu\nu} + \dots , \qquad (5.28)$$

which again makes it explicit how the strength of gravitational interactions between matter and the massless graviton mode is just set by $M_{(0)}$, as given in eq.(5.21).

5.2.5 When does clockwork not work?

The results of the previous sections can also be understood clearly from the perspective of the unbroken clockwork symmetry, both in the low-energy effective theory and in possible UV completions. For simplicity we will focus here on abelian vector clockwork, for which the role of the clockwork symmetry is particularly clear, though the conclusions apply equally well to all spins, and clarify the cases in which meaningful clockwork is possible.

The abelian vector clockwork of eq.(5.7) arises from a UV theory of $N+1$ $U(1)$ gauge bosons connected by N link scalar fields Φ_j via

$$\mathcal{L}_4 = -\sum_{j=0}^{N} \frac{1}{4g_j^2} F_{j\mu\nu}^2 - \sum_{j=0}^{N-1} |D_\mu \Phi_j|^2 + \dots , \qquad (5.29)$$

where $D_\mu \Phi_j \equiv \left[\partial_\mu + i\left(A_{j\mu} - q_j A_{j+1\mu}\right)\right] \Phi_j$ and the dots denote, e.g., potentials for

[12] Notice eq.(5.27) has the form of eq.(2.35) in [183], but with the extra necessary condition $q_j = M_j/M_{j+1}$, i.e. non-unit q's are only a consistent choice in the presence of an exponential distribution of Planck scales.

the Φ_j. For simplicity, we will focus on the case of equal charges, couplings, and symmetry breaking scales, but our conclusions hold for any theory in which there are no large hierarchies. If the Φ_j acquire vacuum expectation values $\langle|\Phi_j|^2\rangle = f^2/2$, this results in a clockwork mass matrix for canonically normalized gauge fields of the form

$$-\sum_{j=0}^{N-1} \frac{g^2 f^2}{2} \left(A_{j\mu} - q A_{j+1\mu}\right)^2 \ . \tag{5.30}$$

In order to probe the unbroken clockwork symmetry, we introduce a matter field φ charged under the $U(1)$ gauge group of site k with charge Q_φ. The clockwork gauge symmetry preserved by eq.(5.30) corresponds to $A_{j\mu} \to A_{j\mu} + \partial_\mu \alpha(x)/q^j \ \forall j$. Under such a gauge transformation, $\varphi \to e^{i\alpha Q_\varphi/q^k}\varphi$, which is naturally interpreted as a small and site-dependent charge Q_φ/q^k under the unbroken $U(1)$. This makes clear the sense in which the site-dependent charges found in section 5.2.2 are a direct probe of the asymmetric distribution of the clockwork symmetry among different sites.

Considering clockwork from the perspective of the unbroken symmetry also makes apparent the sense in which theories with the mass matrix eq.(5.30) may *fail* to generate clockwork. In particular, the clockwork theory of eq.(5.29) without any large hierarchies of couplings, charges, and scales ("Theory A") is not the only way of generating the mass matrix in eq.(5.30). An identical mass matrix arises in a theory ("Theory B") of $N+1$ $U(1)$ gauge bosons with N bifundamental scalars Φ_j, likewise described by eq.(5.29), in which the Φ_j carry opposite charges under adjacent groups ($q_j = 1$), the g_j are unequal and satisfy $g_{j+1}/g_j = q$, and the vacuum expectation values v_j of the scalars Φ_j satisfy $g_j^2 v_j^2 = g^2 f^2$. Notably, there is an exponential hierarchy between the couplings and vev's at either end of the Theory B quiver, $g_N/g_0 = v_0/v_N = q^N$. Such a theory likewise preserves a $U(1)$ symmetry, but one that is symmetrically distributed among sites and exhibits no clockwork phenomena. Given a probe field φ of charge Q_φ on the site k, a gauge transformation of the unbroken $U(1)$ symmetry induces a rotation of the probe field by $e^{i\alpha Q_\varphi}$, independent of the position of the site. This universality is born out by diagonalizing the mass matrix and studying the couplings of the massless gauge

field: the zero mode is $\propto \sum_{j=0}^{N} g_j^{-1} A_{j\mu}$, and therefore couples universally to matter fields on different sites. This theory does not clockwork, though it shares the mass matrix of eq.(5.30) with a theory that *does*.

One might object that Theory A and Theory B are actually the same theory, related by rescaling the gauge kinetic terms and the charges of both the link fields Φ_j and the probe fields φ in Theory B to match those of Theory A, so that there is no invariant distinction between the two. This is certainly true if the gauge group at each site is taken to be $\mathbb{R}$ rather than $U(1)$, but in this case there is no notion of natural charge assignments and clockwork is uninteresting to begin with. Rather, an invariant distinction exists when additional criteria restrict the gauge groups to genuine $U(1)$s and fully specify the spectrum of electric and magnetic charges, as is the case in a theory of quantum gravity.

In a theory of quantum gravity (including all known examples in string theory), all continuous gauge groups are compact and satisfy the Completeness Hypothesis [195], namely that every electric and magnetic charge allowed by Dirac quantization is present in the spectrum. In this case, Theory A possesses a spectrum of states at each site carrying all possible electric charges $n \in \mathbb{Z}$ (in units of $g_j = g$) and all possible magnetic charges $2\pi n/g_j$. Theory B possesses a similarly complete spectrum, but with respect to the exponentially varying g_j. Rescaling the charges and couplings of Theory B to match those of Theory A leads to a gap in the spectrum of electric and magnetic charges at each site, in conflict with the Completeness Hypothesis. Equivalently, the spectrum of states charged under the unbroken $U(1)$ differs between the two theories. In Theory A, the number of states of charge $Q \in \mathbb{N}$, in units of the effective coupling of the massless $U(1)$, is the largest $i \leq N+1$ for which q^i divides Q. However, in Theory B, there are simply $N+1$ states of any given charge under the unbroken $U(1)$, which attests to the diagonal nature of the symmetry breaking in this latter case. For instance, in Theory A there is only one state of unit electric charge in units of the effective coupling of the massless $U(1)$, while in Theory B there are $N+1$ such states with unit electric charge under the unbroken $U(1)$. Thus Theory A and Theory B are genuinely distinct theories, with distinct physical observables, and only the former exhibits clockwork phenomena.

The distinction between the two theories is not merely academic, but is essential for generating natural exponential hierarchies in a theory of quantum gravity. For example, Theory A can satisfy the magnetic form of the Weak Gravity Conjecture (WGC) in the UV, but upon higgsing gives rise to an effective theory for the massless $U(1)$ that exponentially violates the magnetic WGC [193]. This is a precise sense in which the clockwork mechanism is a useful generator of natural exponential hierarchies. In contrast, if Theory B satisfies the magnetic WGC in the UV, then the effective theory of the massless $U(1)$ also trivially satisfies the magnetic WGC. Theory B generates no useful exponential hierarchies – rather, it requires them as inputs.

Aside from quantum gravity arguments, discerning whether an abelian gauge theory 'clockworks' or not requires making reference to a localized lattice of charged states. The requirement that states with the same integer charge on different sites have (exponentially) different charges under the unbroken gauge theory singles out models with symmetry-localized zero modes as the only ones that can exhibit clockwork dynamics.

As we will see, the distinction between Theory A and Theory B becomes important when attempting to identify the continuum equivalent of discrete clockwork in an extra dimension. One can always find a metric for which the Kaluza-Klein decomposition of a bulk field gives rise to the mass matrix in eq.(5.30). But as we have argued, this alone is not enough for the continuum theory to generate clockwork. Whether the continuum theory provides a successful realization of clockwork depends on whether its discretization gives Theory A or Theory B. More precisely, continuum clockwork requires a compact 5D $U(1)$ gauge theory to lead, upon compactification, to a 4D effective gauge theory that is non-compact.

While we have focused on abelian vector clockwork, one would expect that identical arguments go through for abelian scalar clockwork whenever there exists a well-defined notion of an asymmetrically-distributed global symmetry (see [196]). For example, in a UV completion of scalar clockwork, the roles of gauge transformations and probe charges in vector clockwork are played by global symmetry transformations and anomaly coefficients. The connection should become partic-

ularly transparent when one considers that all apparent global symmetries should originate as gauge symmetries in a theory of quantum gravity.

Finally, the distinction between Theory A and Theory B makes clear why clockwork is an inherently abelian phenomenon. While one is free to choose the charges and couplings in a quiver theory with abelian symmetry factors to obtain Theory A or Theory B, in a quiver theory with non-abelian symmetry groups the only option consistent with the symmetries is the non-abelian version of Theory B, as we will now see more rigorously.

5.3 No clockwork from geometry

After having rigorously established in section 5.2 that it is only possible to build consistent clockwork models in the spin-0 and abelian spin-1 cases, we now set to answer the question of whether such discrete models could arise from the deconstruction of 5D theories in which the corresponding bosonic fields propagate in a non-trivial background. We find that the answer is negative: geometry alone cannot clockwork bosonic fields. This statement is true in that neither the continuum theory nor its deconstruction exhibits position dependent couplings as a consequence of a symmetry-localization of the scalar or vector massless modes. In particular, we establish how, at best, it is possible to *accommodate* the discrete clockwork models of sections 5.2.1 and 5.2.2 as the deconstruction of 5D theories with conformally flat metrics, but then *ad hoc* exponential hierarchies in the couplings between bulk and brane fields need to be introduced in order for the deconstruction to match clockwork. This is true in particular of 5D theories in linear dilaton backgrounds, as considered in [183], and in section 5.3.3 we make it explicit how couplings involving the dilaton field do not change the above statements. In the language of section 5.2.5, linear dilaton backgrounds always give the unclockworked Theory B. This is particularly clear in the vector case, where continuum clockwork requires a non-compact (therefore $\mathbb{R}$) 4D effective abelian gauge symmetry arising from a compact 5D symmetry (i.e. a genuine $U(1)$). As we emphasize in this section, geometry alone only allows compact higher-dimensional gauge theories to generate compact

4D effective ones, therefore precluding any kind of clockwork dynamics.

We consider an extra dimension compactified on an $S^1/\mathbb{Z}_2$ orbifold, with the fifth dimension parametrized by a coordinate y, and with two end-of-the-world branes present at the orbifold fixed points ($y = 0$ and $y = \pi R$). We will focus on the case in which both the scalar and gauge fields are even under the orbifolding $\mathbb{Z}_2$ symmetry, in order to allow for a massless state to be present in the spectrum of KK-modes. In keeping with the notation introduced in [183], we consider a background metric of the general form

$$ds^2 = g_{MN}dx^M dx^N = X(y)dx_\mu dx^\mu + Y(y)dy^2 \ , \tag{5.31}$$

with $y \in [0, \pi R]$. We consider a bulk scalar field coupled to a brane-localized non-abelian gauge theory in section 5.3.1, and then discuss the case of a bulk $U(1)$ gauge theory in section 5.3.2.

5.3.1 Scalar case

The action of a massless, non-interacting real scalar field propagating in a non-trivial background is given by

$$S_{5,\text{bulk}} = -\frac{1}{2}\int d^4x dy \sqrt{|g|} g^{MN}\partial_M\phi\partial_N\phi \ . \tag{5.32}$$

In a background of the form given in eq.(5.31), and after expanding the 5D scalar field ϕ as a sum over KK-modes as $\phi = \sum_{n=0}^{\infty}\chi_n(y)\phi^{(n)}(x)$, the equations of motion and boundary conditions for the different modes read

$$\partial_y\left(\frac{X^2}{\sqrt{Y}}\partial_y\chi_n\right) + m_n^2\chi_n X\sqrt{Y} = 0 \tag{5.33}$$

$$\partial_y\chi_n = 0 \qquad \text{at} \qquad y = 0, \pi R \ , \tag{5.34}$$

where m_n^2 corresponds to the mass-squared of the n-th KK-mode excitation. In particular, a massless mode is present in the KK-spectrum, whose profile is a constant

$\chi_0(y) = \mathcal{C}_0$.[13]

If we now consider a non-abelian gauge theory localized on a brane at position $y = y_0$ that interacts with the 5D scalar field through an axion-like coupling, the corresponding brane-localized terms in the action have the form

$$S_{5,\text{brane}} = \int d^4x dy \sqrt{|g|} \frac{\delta(y-y_0)}{\sqrt{g_{55}}} \left\{ -\frac{1}{4\overline{g}^2} g^{\mu\rho} g^{\nu\sigma} G_{\mu\nu} G_{\rho\sigma} + \frac{\phi}{16\pi^2 F^{3/2}} \frac{\epsilon^{\mu\nu\rho\sigma}}{\sqrt{|g_{(4)}|}} G_{\mu\nu} G_{\rho\sigma} \right\} , \tag{5.35}$$

where $\sqrt{|g_{(4)}|} = X(y)^2$ in our notation. The effective interaction between the gauge theory and the massless scalar mode is then

$$\mathcal{L}_4 \supset \frac{\mathcal{C}_0 \phi^{(0)}}{16\pi^2 F^{3/2}} G_{\mu\nu} \tilde{G}^{\mu\nu} \equiv \frac{\phi^{(0)}}{16\pi^2 f_0} G_{\mu\nu} \tilde{G}^{\mu\nu} , \tag{5.36}$$

where $G_{\mu\nu}\tilde{G}^{\mu\nu} \equiv \epsilon^{\mu\nu\rho\sigma} G_{\mu\nu} G_{\rho\sigma}$, as usual, and the last expression defines an effective axion coupling f_0, which may be written as

$$f_0 = F^{3/2} \mathcal{C}_0^{-1} = M_{Pl} \left(\frac{F}{M_5} \right)^{3/2} , \tag{5.37}$$

and in the last step we used the relationship between the fundamental scale of the 5D theory, M_5, and the 4D Planck scale M_{Pl}.[14]

Eq.(5.37) illustrates how (*i*) the effective coupling of the massless mode to the brane-localized gauge theory is independent of the position of the brane y_0 for any geometry – a direct consequence of the flat profile of the zero mode – , and (*ii*) a significant hierarchy between f_0 and M_{Pl} only arises if a similar hierarchy between the 5D symmetry breaking scale F and M_5 is introduced *ad hoc* in the fundamental 5D picture.

It is illuminating to consider what happens to this theory when deconstructed. If we latticize the extra dimension in N segments, with lattice spacing a, such that

[13] For a canonically normalized scalar field $\mathcal{C}_0 = \left(\int_0^{\pi R} dy X(y) \sqrt{Y(y)} \right)^{-1/2}$.

[14] In a background of the form specified in eq.(5.31), this is given by $M_{Pl}^2 = M_5^3 \int_0^{\pi R} dy X(y) \sqrt{Y(y)}$.

$Na = \pi R$, the terms in the 4D effective lagrangian corresponding to eq.(5.32) read[15]

$$\mathcal{L}_4 \supset -\frac{1}{2}\sum_{j=0}^{N}(\partial_\mu \phi_j)^2 - \frac{1}{2a^2}\sum_{j=0}^{N-1}\frac{X_j}{Y_j}\left(\phi_j - \frac{X_j^{1/2}Y_j^{1/4}}{X_{j+1}^{1/2}Y_{j+1}^{1/4}}\phi_{j+1}\right)^2 , \tag{5.38}$$

where $f_j \equiv f(aj)$ (for $f = \phi, X, Y$). This corresponds to the effective lagrangian of eq.(5.1), with mass-squared parameters and charges

$$m_j^2 = \frac{1}{a^2}\frac{X_j}{Y_j} , \qquad q_j = \frac{X_j^{1/2}Y_j^{1/4}}{X_{j+1}^{1/2}Y_{j+1}^{1/4}} , \tag{5.39}$$

in agreement with what is found in [183], and the profile of the massless state present in the spectrum is now given by $\phi_{(0)} = \sum_{j=0}^{N} c_j \phi_j$, with

$$c_j = c_0 \frac{X_j^{1/2}Y_j^{1/4}}{X_0^{1/2}Y_0^{1/4}} \qquad \text{and} \qquad c_0 = \left(1 + \sum_{j=1}^{N}\frac{X_j\sqrt{Y_j}}{X_0\sqrt{Y_0}}\right)^{-1/2} . \tag{5.40}$$

In particular, the deconstruction of a real scalar field propagating in a linear dilaton background of the form $X(y) = Y(y) = e^{-4ky}$ corresponds to $m_j^2 = a^{-2}$, and $q_j = e^{3ka}\ \forall\ j$.

However, upon deconstruction, the brane-localized terms of eq.(5.35) read (taking into account the appropriate field redefinitions)

$$\mathcal{L}_4 \supset -\frac{1}{4\overline{g}^2}G_{\mu\nu}G^{\mu\nu} + \frac{\phi_{j_0}}{16\pi^2 F\sqrt{Fa}X_{j_0}^{1/2}Y_{j_0}^{1/4}}G_{\mu\nu}\tilde{G}^{\mu\nu} , \tag{5.41}$$

i.e. the brane-localized interaction of the 5D theory is deconstructed into a coupling of the gauge theory to the scalar field of the j_0 site, where $y_0 = j_0 a$. Written in terms of mass eigenstates, eq.(5.41) includes an effective coupling between the massless scalar and the gauge sector that reads

$$\mathcal{L}_4 \supset \frac{c_0}{X_0^{1/2}Y_0^{1/4}}\frac{\phi_{(0)}}{16\pi^2 F\sqrt{Fa}}G_{\mu\nu}\tilde{G}^{\mu\nu} . \tag{5.42}$$

As expected from our discussion of the continuum 5D theory, the effective axion coupling in the deconstructed theory is independent of the position of the site j_0 –

[15] A field redefinition $\phi_j \to \phi_j (aX_j\sqrt{Y_j})^{-1/2}$ is performed to obtain canonically-normalized scalar fields.

in contrast with the discrete construction of section 5.2.1. At best, conformally flat backgrounds of the linear dilaton type, for which $m_j^2 = a^{-2}$ and $q_j = q$ independent of j (see eq.(5.39)), can *accommodate* discrete clockwork, but only if the hierarchy of effective scales to be obtained in the discrete theory is put in by hand from the 5D perspective.

5.3.2 Vector case

The action of a massless, non-interacting $U(1)$ gauge theory propagating in a non-trivial background is given by

$$S_{5,\text{bulk}} = -\int d^4x dy \sqrt{|g|} \frac{1}{4g_{5D}^2} g^{MR} g^{NS} F_{MN} F_{RS} \ , \tag{5.43}$$

where g_{5D} is the 5D gauge coupling.

Working in the $A_5 = 0$ gauge, and expanding the 5D vector field as a sum over KK-modes $A_\mu = \sum_{n=0}^{\infty} \psi_n(y) A_\mu^{(n)}(x)$, the equations of motion and boundary conditions for the different modes in the background of eq.(5.31) read

$$\partial_y \left(\frac{X}{\sqrt{Y}} \partial_y \psi_n \right) + m_n^2 \psi_n \sqrt{Y} = 0 \tag{5.44}$$

$$\partial_y \psi_n = 0 \qquad \text{at} \qquad y = 0, \pi R \ . \tag{5.45}$$

In particular, a massless mode is present in the KK-spectrum, whose profile is a constant independent of y. Without loss of generality, one may take $\psi_0 = 1$, a choice that defines a 4D gauge coupling, g_{4D}, given by $g_{4D}^{-2} = g_{5D}^{-2} \int_0^{\pi R} dy \sqrt{Y(y)}$.

If we now consider a brane-localized scalar field φ with charge Q_φ under the $U(1)$ gauge group, the corresponding brane-localized terms in the action read

$$S_{5,\text{brane}} = -\int d^4x dy \sqrt{|g|} \frac{\delta(y - y_0)}{\sqrt{g_{55}}} g^{\mu\nu} (D_\mu \varphi)^\dagger D_\nu \varphi \ , \tag{5.46}$$

where $D_\mu \varphi = (\partial_\mu + i Q_\varphi A_\mu)\varphi$. After the appropriate rescaling $\varphi \to \varphi / \sqrt{X(y_0)}$, so that the scalar field features a canonically normalized kinetic term, the terms

involving φ in the 4D effective lagrangian are given by

$$\mathcal{L}_4 \supset -|(\partial_\mu + iQ_\varphi A_\mu(y_0))\varphi|^2 = -|(\partial_\mu + iQ_\varphi A_\mu^{(0)} + ...)\varphi|^2 \ , \tag{5.47}$$

where the dots denote strictly massive vector modes. The effective coupling between $A_\mu^{(0)}$ and the brane-localized scalar field is given by $\sim g_{4D}Q_\varphi$, which is independent of the position of the brane along the extra dimension: two scalar fields with the same fundamental charge under the 5D gauge theory will couple to the massless vector mode with exactly the same strength, regardless of where they are localized – a direct consequence of the lack of symmetry-localization of the vector zero mode.

This is consistent with what one finds upon deconstruction. Now, from eq.(5.43) we obtain a 4D effective lagrangian of the form

$$\mathcal{L}_4 \supset -\sum_{j=0}^{N} \frac{1}{4g_j^2} F_{j\mu\nu}^2 - \frac{1}{2a^2} \sum_{j=0}^{N-1} \frac{X_j}{Y_j} \frac{1}{g_j^2} \left(A_{j\mu} - A_{j+1\mu}\right)^2 \ , \tag{5.48}$$

where $g_j^{-2} = g_{5D}^{-2} a \sqrt{Y_j}$, and eq.(5.48) corresponds to the effective lagrangian of eq.(5.7), with mass-squared parameters and charges

$$g_j^2 v_j^2 = \frac{1}{a^2} \frac{X_j}{Y_j} \ , \qquad q_j = 1 \ . \tag{5.49}$$

In the language of section 5.2.5, we recognize that the linear dilaton background deconstructs into the unclockworked Theory B.

The couplings of the massless vector can be found by the substitution $A_{j\mu} = c_0 A_{(0)\mu} + ...$, where $c_0 = 1$, a choice that defines an effective gauge coupling for the unbroken gauge theory, $g_{(0)}$, given by $g_{(0)}^{-2} = \sum_{j=0}^{N} g_j^{-2}$. Upon deconstruction, the brane-localized terms of eq.(5.46) read

$$\mathcal{L}_4 \supset -|(\partial_\mu + iQ_\varphi A_{j_0\mu})\varphi|^2 = -|(\partial_\mu + iQ_\varphi A_{(0)\mu} + ...)\varphi|^2 \ , \tag{5.50}$$

where the dots denote strictly massive modes. The effective coupling between the massless vector and the brane-localized scalar is $\sim g_{(0)}Q_\varphi$, which is independent of the position where φ is localized – in stark contrast with the discrete theory of 5.2.2.

It becomes clear that an attempt to obtain discrete clockwork from the deconstruction of an abelian gauge theory propagating in a non-trivial background fails, regardless of the choice of geometry. At most, conformally flat metrics, for which $g_j^2 v_j^2 = a^{-2}$ and $q_j = 1$ when deconstructed (see eq.(5.49)), can *accommodate* discrete clockwork, but only if the hierarchy of effective charges between different matter fields to be obtained in the discrete theory is put it by hand from the 5D perspective.

5.3.3 Including dilaton couplings

In theories involving a dilaton, after going from Jordan frame to Einstein frame, a y-dependent factor typically remains present in front of both bulk and brane terms, and corresponds to some power of e^S, where S is the dilaton field that gets a y-dependent vev. One could wonder whether the presence of such terms alters the story told in sections 5.3.1 and 5.3.2, and whether clockwork could arise from the deconstruction of theories with a dilaton. In this section, we show that this is not the case: the presence of dilaton couplings does not qualitatively change our conclusions, so long as no additional breaking of scale invariance is introduced through the coupling of the dilaton to brane-localized states. We emphasize this requirement is a weak restriction. For instance, in the vector case, it ensures that the 5D gauge symmetry is indeed compact. There is no symmetry localization in going from a non-compact 5D gauge symmetry to a non-compact effective 4D construction, and such models do not lead to the emergence of clockwork dynamics.

Let's consider the scalar case of section 5.3.1 first. In the presence of a dilaton, eq.(5.35) will typically include a y-dependent factor $\mathcal{Q}(y)$, of the form[16]

$$S_{5,\text{brane}} = \int d^4x dy \sqrt{|g|}\mathcal{Q}(y)\frac{\delta(y-y_0)}{\sqrt{g_{55}}}\left\{-\frac{1}{4\overline{g}^2}g^{\mu\rho}g^{\nu\sigma}G_{\mu\nu}G_{\rho\sigma} + \frac{\phi}{16\pi^2 F^{3/2}}\frac{\epsilon^{\mu\nu\rho\sigma}}{\sqrt{|g_{(4)}|}}G_{\mu\nu}G_{\rho\sigma}\right\}. \tag{5.51}$$

The presence of a non-trivial function $\mathcal{Q}(y)$ alters the value of the effective gauge

[16]No such factor appears, in Einstein frame, for a bulk scalar field, and so an analogous y-dependent factor does not need to be included in eq.(5.32).

coupling of the brane non-abelian gauge theory, which is now given by $g_*(y_0) = \overline{g}/\sqrt{\mathcal{Q}(y_0)}$. The effective interaction between the gauge theory and the massless scalar mode is modified to

$$\mathcal{L}_4 \supset \left(\frac{\overline{g}}{g_*(y_0)}\right)^2 \frac{\mathcal{C}_0\phi^{(0)}}{16\pi^2 F^{3/2}} G_{\mu\nu}\tilde{G}^{\mu\nu} \ , \tag{5.52}$$

and so the effective axion coupling is now given by

$$f_0 = \left(\frac{g_*(y_0)}{\overline{g}}\right)^2 F^{3/2}\mathcal{C}_0^{-1} = \left(\frac{g_*(y_0)}{\overline{g}}\right)^2 M_{Pl}\left(\frac{F}{M_5}\right)^{3/2} \ . \tag{5.53}$$

From eq.(5.53), we see that if $\mathcal{Q}(y)$ is a non-trivial function of y – a common occurrence in theories with a dilaton – the gauge coupling of the non-abelian theory depends on y_0 and, in turn, the effective axion coupling between the massless scalar and the gauge theory will depend on y_0 through its dependence on g_*. In particular, two non-abelian gauge theories with the same fundamental gauge coupling $\overline{g}$, but localized on different branes, will feature different effective axion couplings only because of the difference in their effective gauge couplings. Crucially, any hierarchy in couplings involving the massless scalar field only arises as a result of the two gauge theories being physically distinct (with different gauge couplings, and therefore different physical properties, like their confinement scales), but not as a consequence of a symmetry-localization of the scalar zero mode.

The same effect persists when deconstructing the brane terms of eq.(5.51). Eq.(5.41) now generalizes to

$$\mathcal{L}_4 \supset -\frac{1}{4g_{*j_0}^2} G_{\mu\nu}G^{\mu\nu} + \left(\frac{\overline{g}}{g_{*j_0}}\right)^2 \frac{\phi_{j_0}}{16\pi^2 F\sqrt{Fa}X_{j_0}^{1/2}Y_{j_0}^{1/4}} G_{\mu\nu}\tilde{G}^{\mu\nu} \ , \tag{5.54}$$

and thus the effective coupling between the massless scalar and the gauge sector reads

$$\mathcal{L}_4 \supset \left(\frac{\overline{g}}{g_{*j_0}}\right)^2 \frac{c_0}{X_0^{1/2}Y_0^{1/4}} \frac{\phi_{(0)}}{16\pi^2 F\sqrt{Fa}} G_{\mu\nu}\tilde{G}^{\mu\nu} \ . \tag{5.55}$$

As expected from our discussion of the continuum 5D theory, the effective axion coupling in the deconstructed theory depends on the position of the site j_0 only through the value of the effective gauge coupling g_{*j_0}. As we move from site to site,

the axion effective coupling will change as a result of the change in the properties of the non-abelian gauge theory. This picture is in stark contrast with the clockwork mechanism described in section 5.2.1, where the effective axion coupling changes as the gauge theory moves from site to site because of the symmetry-localization of the scalar field, whereas the physical properties of the non-abelian gauge theory remain unchanged.

We now turn to the $U(1)$ vector case discussed in section 5.3.2. In the presence of a dilaton, eq.(5.43) will typically include a y-dependent factor in front of the vector kinetic term, of the form

$$S_{5,\text{bulk}} = -\int d^4x dy \sqrt{|g|} \frac{\mathcal{F}(y)}{4g_{5D}^2} g^{MR} g^{NS} F_{MN} F_{RS} \ . \tag{5.56}$$

Although this will in general affect the equations of motion for the KK-modes, which now read

$$\partial_y \left(\mathcal{F} \frac{X}{\sqrt{Y}} \partial_y \psi_n \right) + m_n^2 \psi_n \mathcal{F} \sqrt{Y} = 0 \ , \tag{5.57}$$

a massless mode is present in the spectrum, and its profile remains flat. With the choice $\psi_0 = 1$, the 4D gauge coupling is now defined as $g_{4D}^{-2} = g_{5D}^{-2} \int_0^{\pi R} dy \mathcal{F}(y) \sqrt{Y(y)}$.

Similarly, eq.(5.46) will be generalized to include a y-dependent factor, of the form

$$S_{5,\text{brane}} = -\int d^4x dy \sqrt{|g|} \mathcal{H}(y) \frac{\delta(y - y_0)}{\sqrt{g_{55}}} g^{\mu\nu} (D_\mu \varphi)^\dagger D_\nu \varphi \ , \tag{5.58}$$

where the function $\mathcal{H}(y)$ will in general be different from $\mathcal{F}(y)$.[17] After the appropriate rescaling $\varphi \to \varphi / \sqrt{X(y_0)\mathcal{H}(y_0)}$, so that the scalar field features a canonically normalized kinetic term, the terms involving φ in the 4D effective lagrangian are just given by eq.(5.47). The effective coupling between $A_\mu^{(0)}$ and the brane-localized scalar field is just $\sim g_{4D} Q_\varphi$ – again independent of y_0.

When deconstructed, this more general case features exactly the same properties discussed in section 5.3.2, with the only difference that the gauge couplings on each site are now given by $g_j^{-2} = g_{5D}^{-2} a \sqrt{Y_j} \mathcal{F}_j$, and the presence of dilaton couplings has no effect on our conclusions. The inability of dilaton couplings to reproduce meaningful

[17] In models involving a dilaton, different powers of e^S appear in front of bulk and brane-localized terms when going to Einstein frame, a fact we capture here by considering two different functions $\mathcal{F}(y)$ and $\mathcal{H}(y)$.

clockwork is clear in the language of section 5.2.5: a successful modification of the linear dilaton background to generate clockwork would need to alter the physical spectrum of charged states on probe branes, rather than merely modifying gauge couplings.

5.4 Towards continuum clockwork

In this section, we present a 5D implementation of the clockwork mechanism that, when deconstructed, successfully preserves the appealing features of the discrete set-up described in sections 5.2.1 and 5.2.2. In order to emphasize how geometry plays no role, we consider the case of a flat background, and include bulk and brane mass terms for scalar and abelian vector fields. Both from the 5D perspective, and when deconstructed, the scenario presented here features hierarchical couplings to brane-localized states as a consequence of the symmetry-localization of the corresponding bulk fields. In terms of the discrete clockwork parameters of sections 5.2.1 and 5.2.2, the set-up we consider appears as a small perturbation from the discrete clockwork mechanism in which all parameters are taken to be equal. We discuss the scalar case first in section 5.4.1, albeit only at the level of a toy model; a well-defined notion of a clockworked continuum global symmetry would entail embedding the continuum global symmetry in a continuum gauge symmetry, which lies beyond the scope of the current work (see [196] for work in this direction). In section 5.4.2 we discuss the vector case in full detail, realizing a scenario in which continuum clockwork arises when a compact 5D gauge symmetry leads to a non-compact 4D one. Section 5.4.3 clarifies the connection between our 5D construction and the linear dilaton background implementation of [183].

5.4.1 Continuum scalar clockwork

Apart from the kinetic term of eq.(5.32), the 5D action of a real scalar field may also involve mass terms

$$S_{5,\text{mass}} = -\frac{1}{2}\int d^4x dy \sqrt{|g|}\phi^2 \left(M_\phi^2 + \tilde{m}_\phi \frac{\delta(y) - \delta(y-\pi R)}{\sqrt{g_{55}}} \right) , \tag{5.59}$$

where we fix the brane-localized mass terms to have equal size but opposite sign, in order to allow for a massless state to be present in the KK-mode spectrum. Although the bulk and brane mass terms of eq.(5.59) are certainly consistent from an effective field theory perspective, negative brane masses might pose challenges when trying to embed this framework into a full UV completion – an issue that we do not try to address in this work. In the generic warped background of eq.(5.31), and after expanding the 5D scalar field ϕ as a sum over KK-modes as before, the equations of motion and boundary conditions for the different modes now read

$$\partial_y \left(\frac{X^2}{\sqrt{Y}} \partial_y \chi_n \right) + \chi_n X \sqrt{Y} \left(m_n^2 - X M_\phi^2 \right) = 0 \ , \tag{5.60}$$

$$\left(\partial_y - \frac{\tilde{m}_\phi}{2} \sqrt{Y} \right) \chi_n = 0 \qquad \text{at} \qquad y = 0, \pi R \ . \tag{5.61}$$

As first noted in [197], the presence of non-zero bulk and brane mass terms makes the zero mode's profile non-flat. In particular, if we demand this profile to be of an exponential form $\chi_0(y) \propto e^{\beta y}$, where β is some mass scale, eq.(5.61) requires $Y(y)$ is independent of y, and without loss of generality we may take $Y = 1$, in which case $\beta = \tilde{m}_\phi/2$ and thus $\chi_0(y) \propto e^{\tilde{m}_\phi y/2}$. Moreover, for a given $X(y)$, eq.(5.60) requires bulk and brane mass terms to satisfy

$$\tilde{m}_\phi^2 + 4\tilde{m}_\phi \frac{\partial_y X}{X} - 4M_\phi^2 = 0 \ . \tag{5.62}$$

For instance, in a flat background, where $X(y) = 1$, $\tilde{m}_\phi = \pm 2\sqrt{M_\phi^2}$; whereas in an RS background, where $X(y) = e^{-2ky}$, $\tilde{m}_\phi = 2\left(2k \pm \sqrt{4k^2 + M_\phi^2}\right)$, in agreement with [197]. Although choosing $\tilde{m}_\phi$ such that eq.(5.62) is satisfied may appear like a fine-tuned choice, we emphasize that it is a technically natural one, since only for those values of $\tilde{m}_\phi$ the lowest lying scalar mode recovers a shift symmetry – it is a symmetry enhanced point. Depending on whether $\tilde{m}_\phi$ is positive or negative, the massless mode will be localized towards the $y = \pi R$ or $y = 0$ branes respectively. Here, we consider the case of a flat background ($X = Y = 1$), and, without loss of generality, focus on the choice $\tilde{m}_\phi < 0$, so that the zero mode profile is exponentially localized towards $y = 0$. (The case $\tilde{m}_\phi > 0$ is completely analogous but replaces the

role of the two branes.)

In this case, after setting $\mathcal{Q}(y) = 1$ in eq.(5.35), the effective axion coupling of eq.(5.42) is given by

$$f_0 = F^{3/2}\chi_0(y_0)^{-1} = F^{3/2}\sqrt{\frac{e^{\tilde{m}_\phi \pi R}-1}{\tilde{m}_\phi}}e^{-\tilde{m}_\phi y_0/2} \simeq \frac{F^{3/2}}{\sqrt{|\tilde{m}_\phi|}}e^{|\tilde{m}_\phi| y_0/2} \ , \tag{5.63}$$

where in the last term we have focused on the case $\tilde{m}_\phi < 0$, and assumed $|\tilde{m}_\phi|\pi R = \mathcal{O}(1)$. From eq.(5.63), it is clear that the non-trivial profile of the zero mode translates into an effective axion coupling that depends on the position of the brane where the gauge theory is localized. Two gauge theories with identical properties localized on different branes will feature exponentially different effective axion couplings, as a result of the symmetry-localization of the scalar zero mode along the extra dimension, even for natural choices of the 5D parameters, $m_\phi \pi R = \mathcal{O}(1)$.

We now consider the deconstruction of this theory, and compare it to the discrete clockwork of section 5.2.1. The 4D effective lagrangian of the scalar sector reads

$$\mathcal{L}_4 = -\frac{1}{2}\sum_{j=0}^{N}(\partial_\mu \phi_j)^2 - \frac{1}{2}\sum_{i,j=0}^{N}\mathbb{M}^2_{\phi,ij}\phi_i\phi_j \ , \tag{5.64}$$

with a mass-squared matrix given by

$$\begin{aligned}\mathbb{M}^2_{\phi,ij} =& \delta_{ij}\left(M_\phi^2 + \frac{2}{a^2}\right) - \frac{1}{a^2}(\delta_{ij+1} + \delta_{ij-1}) \\ & -\delta_{iN}\delta_{jN}\left(\frac{\tilde{m}_\phi}{a} + \frac{1}{a^2}\right) + \delta_{i0}\delta_{j0}\left(\frac{\tilde{m}_\phi}{a} - \frac{1}{a^2}\right) \ .\end{aligned} \tag{5.65}$$

As in the continuum case, for a given bulk mass term M_ϕ^2 there are two values of $\tilde{m}_\phi$ that allow for a massless mode to be present in the latticized spectrum, which are of equal size but opposite sign,[18] and, as before, we focus on the case $\tilde{m}_\phi < 0$.

Moreover, upon deconstruction the brane-localized coupling between the 4D gauge theory and the 5D scalar field now reads

$$\mathcal{L}_4 \supset \frac{\phi_{j_0}}{16\pi^2 F\sqrt{Fa}}G_{\mu\nu}\tilde{G}^{\mu\nu} = \frac{c_{j_0}\phi_{(0)}}{16\pi^2 F\sqrt{Fa}}G_{\mu\nu}\tilde{G}^{\mu\nu} + ... \ , \tag{5.66}$$

[18] One can check that $\tilde{m}_\phi = \pm\left(2\sqrt{M_\phi^2} + \mathcal{O}(1/N)\right)$, as expected.

where the dots correspond to strictly massive modes, and the effective axion coupling scale is now given by $f_0 = F\sqrt{Fa}\ c_{j_0}^{-1}$. Unlike the scenarios considered in section 5.3.1, the deconstructed effective coupling now depends on j_0 as a result of the uneven distribution of the massless scalar along the different lattice sites, mirroring the situation found from the 5D perspective.

In particular, it is illuminating to match this deconstructed scenario into the discrete clockwork set-up of section 5.2.1, by finding the corresponding clockwork parameters q_i and m_i^2 $(i = 0, ..., N-1)$, since one may worry that this may now look like an unnaturally hierarchical set of choices, and that the 'naturalness' we recover in the 5D picture by introducing mass terms and considering a flat background, may be lost in the deconstruction. Instead, we find that this is not the case: when deconstructed, the scenario we consider has approximately equal q_j and m_j^2 parameters. To illustrate this fact, in figure 5.1 we show the values of q_i and m_i^2 (normalized to the values on the first site) for $\sqrt{M_\phi^2}\pi R = 15$ (just for illustration). From figure 5.1 one can appreciate that the effective charges and mass-squared parameters are all of similar size, no large hierarchies between them are present, and all of them tend to the same value as one approaches the large N limit. As a result, the profile of the massless mode also very closely resembles an exponential, as we illustrate in figure 5.2.

5.4.2 Continuum vector clockwork

As in the scalar case discussed in the previous section, we may in general include both bulk and brane mass terms for a 5D abelian gauge field,[19]

$$S_{5,\text{mass}} = -\frac{1}{2g_{5D}^2}\int d^4x dy \sqrt{|g|} g^{MN} A_M A_N \left(M_A^2 + \tilde{m}_A \frac{\delta(y) - \delta(y-\pi R)}{\sqrt{g_{55}}} \right) , \quad (5.67)$$

and we note that these may be generated through spontaneous symmetry breaking (due to the non-zero vev of a 5D scalar field featuring both bulk and brane-localized kinetic terms, as pointed out in [198]), and thus do not necessarily require an explicit breaking of the fundamental 5D gauge symmetry. As in section 5.4.1, the presence

[19]The unconventional g_{5D}^{-2} factor in front of eq.(5.67) is in keeping with our notation in previous sections, and in particular with eq.(5.43).

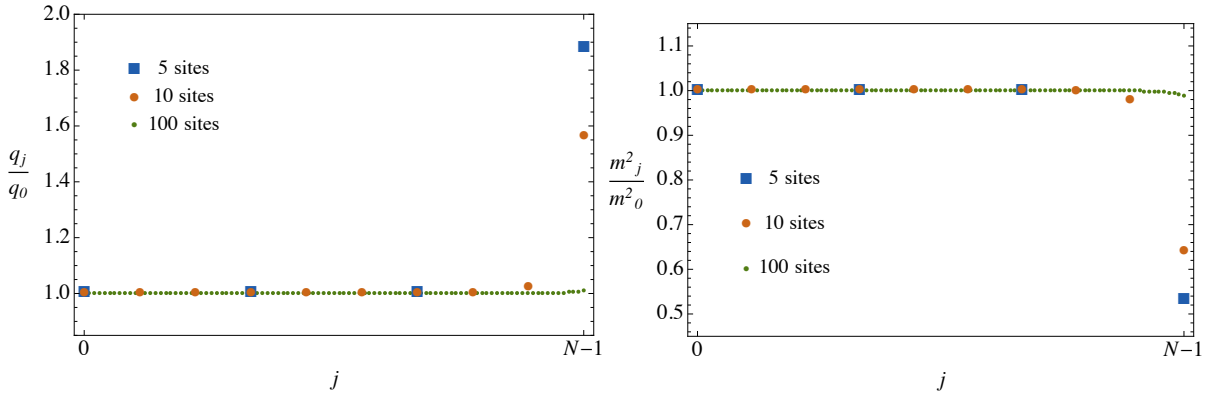

Figure 5.1: **Left:** Values of the charges q_j (normalized to q_0, for $j = 0, ..., N-1$) that correspond to a discrete clockwork mechanism arising from the deconstruction of a massive 5D scalar field in a flat background, as described in section 5.4.1. For illustration, we choose $\sqrt{M_\phi^2}\pi R = 15$, and focus on the case of $N = 5, 10$, and 100 lattice sites. We make the first and last point coincident, so that the hierarchy between the first and last charge parameters, and how it changes as we increase the number of sites, be compared between all three cases. **Right:** Same as in the left figure but for the mass-squared clockwork parameters m_j^2.

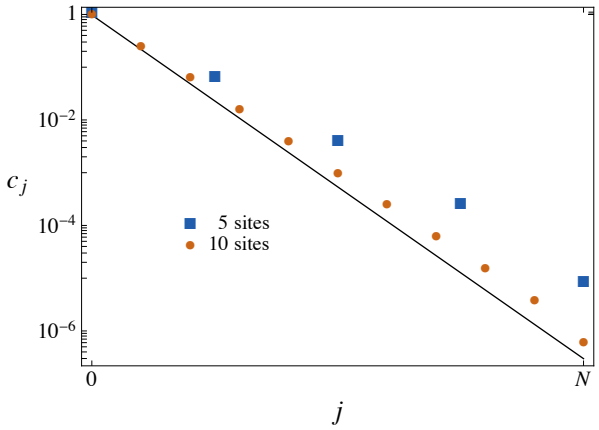

Figure 5.2: Profile of the massless mode obtained from the deconstruction of a massive 5D scalar field in a flat background, as described in section 5.4.1, for the case of $N = 5$ and 10 lattice sites, and for $\sqrt{M_\phi^2}\pi R = 15$ for illustration. The black line corresponds to the case of an exact exponential profile $\propto e^{-\sqrt{M_\phi^2}y}$.

of negative brane-localized mass terms is consistent within an effective description, although such terms may be non-trivial to realize in the context of a full UV completion and potentially pose an obstruction to genuine continuum clockwork.

As was first noted in [198–200], the presence of non-zero bulk and brane mass terms makes the profile of the vector zero mode non-flat. For an exponential profile $\psi_0(y)$, the appropriate boundary conditions require again $Y = 1$, in which case $\psi_0(y) \propto e^{\tilde{m}_A y/2}$. Without loss of generality, one may take $\psi_0(y) = e^{\tilde{m}_A y/2}$, a choice that defines a 4D gauge coupling g_{4D} given by $g_{4D}^{-2} = g_{5D}^{-2}(e^{\tilde{m}_A \pi R} - 1)/\tilde{m}_A$. Moreover, for a given $X(y)$, the equation of motion for the zero mode demands bulk and brane mass terms to satisfy

$$\tilde{m}_A^2 + 2\tilde{m}_A \frac{\partial_y X}{X} - 4M_A^2 = 0 \ . \tag{5.68}$$

For instance, in a flat background, where $X(y) = 1$, $\tilde{m}_A = \pm 2\sqrt{M_A^2}$; whereas in an RS background, where $X(y) = e^{-2ky}$, $\tilde{m}_A = 2\left(k \pm \sqrt{k^2 + M_A^2}\right)$ (in agreement with [200]). As before, the values of $\tilde{m}_A$ that satisfy eq.(5.68) constitute a technically natural choice of parameters, since only for those values the theory recovers 4D gauge invariance of the zero mode – again, a symmetry protected choice.

In the case of a flat background ($X = Y = 1$), the effective interaction term defined through eq.(5.47) is now given by

$$\mathcal{L}_4 \supset -|(\partial_\mu + iQ_\varphi A_\mu(y_0))\varphi|^2 = -|(\partial_\mu + iQ_\varphi e^{\tilde{m}_A y_0/2} A_{(0)\mu} + ...)\varphi|^2 \ . \tag{5.69}$$

The effective coupling between the scalar field and the massless vector is $\sim g_{4D} Q_\varphi e^{\tilde{m}_A y_0/2}$. An exponential hierarchy of effective charges may now be generated by localizing matter on opposite branes, as a result of the physical localization of the vector zero mode.

When deconstructed, the general features of the discrete version are very similar to those of the scalar case described in section 5.4.1. For finite N, the discrete clockwork parameters all have similar size, and asymptote to a common value in the continuum limit, whereas the distribution of the massless mode along the different sites approaches again an exponential profile.

One may try to implement an analogous mechanism for a non-abelian gauge the-

ory. This possibility was considered in [201], where both bulk and brane mass terms (of the right size) are included for a non-abelian gauge theory propagating in a slice of AdS, and the authors of [201] find that an exponentially-localized zero mode is present in the KK-spectrum. As a result of the zero mode's non-trivial profile, its cubic and quartic couplings are found to differ, and brane-localized kinetic terms need to be included to render them equal. This ensures that those terms in the effective lagrangian involving *only* the massless vector mode exhibit 4D gauge invariance. However, gauge invariance of the zero mode also requires interaction terms involving the zero mode and massive KK-modes be gauge invariant independently – a requirement that is not fulfilled in [201]. As a result, although the lowest-lying vector mode appears massless at tree-level, its mass remains unprotected under quantum corrections.

5.4.3 Relation to linear dilaton theories

As we have seen in sections 5.3.1 and 5.4.1, the scalar clockwork parameters corresponding to the deconstruction of a massive scalar field propagating in a flat background are rather similar to those that arise in the deconstruction of a massless field in a linear dilaton geometry. In terms of the discrete clockwork mechanism of section 5.2.1, the latter seem to correspond to identical clockwork parameters across sites, whereas the former appears just as a small perturbation thereof.

The reason for this similarity is a deeper relation between the two theories at the 5D level. The KK-mode spectrum of a massless 5D scalar theory in a background given by functions $X(y)$ and $Y(y)$ is identical to that of a massive theory with an exponentially localized zero mode, $\chi_0(y) \propto e^{\tilde{m}_\phi y/2}$, in a background given by functions $\tilde{X}(y)$ and $\tilde{Y}(y) = 1$, provided

$$Y(y) = e^{2\tilde{m}_\phi y/3} \ , \qquad \text{and} \qquad X(y) = \tilde{X}(y)Y(y) = \tilde{X}(y)e^{2\tilde{m}_\phi y/3} \ . \tag{5.70}$$

(This can be checked from eq.(5.60) and eq.(5.61) by performing a field redefinition $\chi_n \to e^{\tilde{m}_\phi y/2}\chi_n$, and taking into account eq.(5.62).) Whereas the two theories are identical as far as the scalar sector is concerned (the spectrum of KK-mode masses

is the same), the profiles of the different modes in the massive theory correspond to those of the massless theory after a rescaling by a factor of $e^{\tilde{m}_\phi y/2}$. This feature crucially distinguishes the two theories when the 5D scalar couples to brane-localized states: in the flat case, the massless mode is symmetry-localized along the extra dimension, whereas this is not the case in linear dilaton geometries. Only in the flat case, couplings between the scalar zero mode and brane-localized states depend exponentially on the position of the branes as a result of the zero mode's non-trivial profile.

In particular, for a massless scalar field in a linear dilaton geometry $X(y) = Y(y) = e^{-4ky}$, the spectrum of KK-modes is identical to that of a massive theory with $\tilde{m}_\phi = -6k$ (therefore $M_\phi^2 = (3k)^2$), and $\tilde{Y} = \tilde{X} = 1$ – i.e. a massive scalar theory in a flat background, of the kind considered in section 5.4.1. In the continuum limit, the mass spectrum of KK-modes is given by

$$\frac{m_n^2}{(1/R)^2} = (3kR)^2 + n^2 = M_\phi^2 R^2 + n^2 \qquad \text{for } n \geq 1 \ . \tag{5.71}$$

Upon deconstruction, the spectrum of massive states, i.e. the 'clockwork gears', differ between the two theories for a given number of sites N. In particular, in the linear dilaton background with vanishing bulk and brane masses, the mass of the n-th clockwork gear is given by [183]

$$m_n^2\big|_{\text{L.D}} = m^2 \left(q^2 + 1 - 2q \cos \frac{\pi n}{N+1} \right) \ , \tag{5.72}$$

with $q = e^{3ka}$ and $m^2 = a^{-2}$. Taking the large N limit, while keeping $Na = \pi R$ constant,

$$\left.\frac{m_n^2}{(1/R)^2}\right|_{\text{L.D}} = (3kR)^2 + n^2 + \frac{1}{N}\left(\frac{27}{\pi^2}(k\pi R)^3 + n^2(3k\pi R - 2)\right) + \mathcal{O}\left(\frac{1}{N^2}\right) \ , \tag{5.73}$$

and so the mass of the n-th clockwork gear approaches the mass of the n-th KK-mode linearly in $1/N$. Similarly, when deconstructing the theory of section 5.4.1, the mass of the n-th clockwork gear approaches the mass of the n-th KK-mode linearly in $1/N$, although the size of the $\sim 1/N$ corrections in the flat deconstruction is much

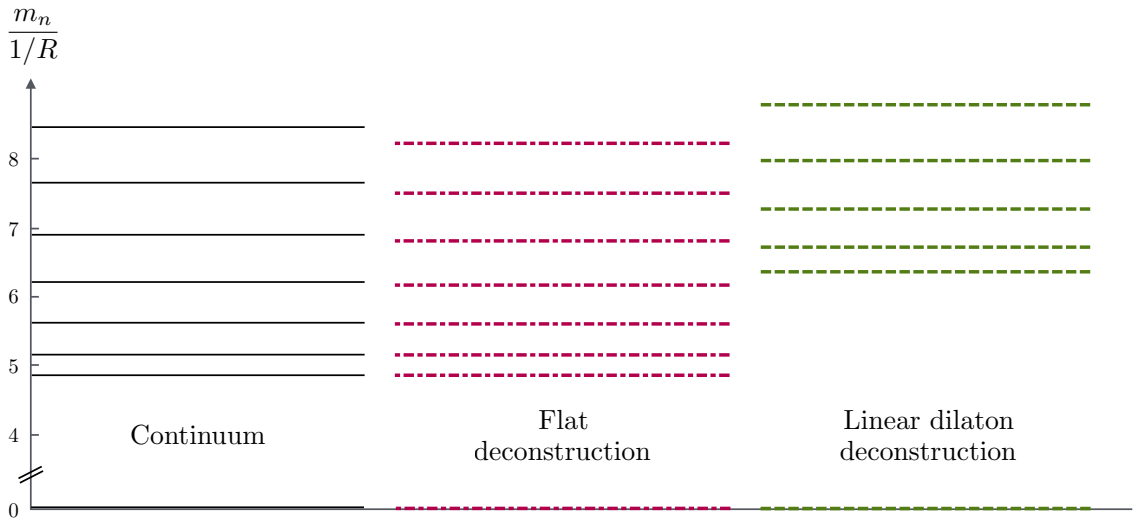

Figure 5.3: **Left:** Spectrum of massive KK-modes for a massless scalar field in a linear dilaton geometry given by $X(y) = Y(y) = e^{-4ky}$, which is identical to that of a scalar field in a flat background with bulk mass $M_\phi^2 = 3k$, and boundary mass parameter $\tilde{m}_\phi = -6k$. **Center:** Spectrum of clockwork gears arising from the deconstruction of a massive scalar field in a flat background. **Right:** Spectrum of clockwork gears arising from the deconstruction of a massless scalar field in a linear dilaton geometry. For illustration, we take $k\pi R = 5$ in all three cases, and the center and right figures correspond to deconstructions featuring $N = 30$ sites.

smaller than in the linear dilaton deconstruction.[20] In any case, both deconstructions reproduce the same mass matrix for the scalar sector up to $1/N$ corrections.

Crucially, however, the symmetry-localization of the zero mode in the theory of section 5.4.1, and the absence of it in linear dilaton theories, leads to similarly different behaviour upon deconstruction: whereas the deconstruction of the theory in flat space with bulk and brane masses leads to a meaningful clockwork mechanism (i.e. it corresponds to Theory A, in the language of section 5.2.5), deconstructing the linear dilaton theory merely leads to a discrete theory with approximately the same spectrum of massive modes, but it does *not* exhibit clockwork dynamics (i.e. it corresponds to Theory B).

The situation for the vector case is completely analogous to the scalar case described above. The KK-mode spectrum of a massless 5D $U(1)$ gauge theory in a background given by $X(y)$ and $Y(y)$ is identical to that of a massive theory with an exponentially localized zero mode, $\psi_0(y) \propto e^{\tilde{m}_A y/2}$, in a background given by $\tilde{X}(y)$

[20] For instance, for $k\pi R = 5$, the mass of the first clockwork gear in the linear dilaton background only comes to within 10% of the first KK-mode for $N \approx 80$. On the other hand, the deconstruction of the flat theory already features the first clockwork gear with a mass less than 2% different from that of the first KK-mode in the most minimal case of three lattice sites ($N = 2$).

and $\tilde{Y}(y) = 1$, provided

$$Y(y) = e^{2\tilde{m}_A y} \ , \qquad \text{and} \qquad X(y) = \tilde{X}(y)Y(y) = \tilde{X}(y)e^{2\tilde{m}_A y} \ . \tag{5.74}$$

As before, although the spectrum of masses is the same in the two theories, the mode profiles differ by an overall factor of $e^{\tilde{m}_A y/2}$, and therefore the two theories exhibit crucially different behavior in their couplings to brane-localized states. In particular, the spectrum of KK-modes of a massless $U(1)$ gauge field in a linear dilaton background is identical to that of a massive theory with $\tilde{m}_A = -2k$, and $\tilde{Y} = \tilde{X} = 1$. Upon deconstruction, the spectrum of massive vector modes will be the same up to $1/N$ corrections, but, just as in the scalar case discussed above, only one of the theories exhibits meaningful clockwork dynamics – that of a massive 5D vector with bulk and brane masses in a flat background.

5.5 Deconstructing gravitational extra dimensions

In this section, we briefly illustrate, following [202], how the deconstruction of a gravitational extra dimension leads to the discrete, unclockworked, scenario of section 5.2.4 – regardless of the choice of metric. We consider perturbations around the geometry defined by eq.(5.31), of the form

$$ds^2 = g_{MN}dx^M dx^N = X(y)\tilde{g}_{\mu\nu}dx^\mu dx^\nu + Y(y)dy^2 \ , \tag{5.75}$$

where $\tilde{g}_{\mu\nu} = \eta_{\mu\nu} + h_{\mu\nu}$. The 5D Einstein-Hilbert action is then given by

$$\begin{aligned} S_{5,\text{EH}} &= \frac{M_5^3}{2}\int d^4x dy \sqrt{|g|} R_5[g] \\ &= \frac{M_5^3}{2}\int d^4x dy \sqrt{|\tilde{g}|}\Bigg(X\sqrt{Y}R_4[\tilde{g}] \\ &\quad + \frac{1}{4}X^{-2}Y^{-1}(\tilde{g}^{\mu\nu}\tilde{g}^{\alpha\beta} - \tilde{g}^{\mu\alpha}\tilde{g}^{\nu\beta})\partial_y(X\tilde{g}_{\mu\nu})\partial_y(X\tilde{g}_{\alpha\beta})\Bigg) \ . \end{aligned} \tag{5.76}$$

Expanding eq.(5.76) to quadratic order in $h_{\mu\nu}$, and writing $h_{\mu\nu}$ as a sum over KK-modes as usual, $h_{\mu\nu} = \sum_{n=0}^{\infty}\varphi_n(y)h_{\mu\nu}^{(n)}(x)$, one can find the corresponding equations of motion and boundary conditions. In particular, a massless mode is present in the

spectrum, whose profile is a constant (to preserve the normalization of the massless mode's self interactions, we take $\varphi_0 = 1$). The first term in eq.(5.76) then defines the effective 4D Planck scale, given by

$$M_{Pl}^2 = M_5^3 \int_{y=0}^{y=\pi R} dy X(y) \sqrt{Y(y)} \ . \tag{5.77}$$

When deconstructed, the first term in the second equality of eq.(5.76) leads to a term of the form

$$\mathcal{L}_4 \supset \sum_{j=0}^{N} \sqrt{|\tilde{g}_j|} \frac{M_5^3}{2} a X_j \sqrt{Y_j} R_4[\tilde{g}_j] \equiv \sum_{j=0}^{N} \sqrt{|\tilde{g}_j|} \frac{M_j^2}{2} R_4[\tilde{g}_j] \ , \tag{5.78}$$

where $\tilde{g}_{j\mu\nu} = \eta_{\mu\nu} + h_{j\mu\nu}$, and M_j corresponds to the effective 4D Planck scale at site j, given by

$$M_j^2 = M_5^3 a X_j \sqrt{Y_j} \ . \tag{5.79}$$

For instance, in a linear dilaton background of the form $X(y) = Y(y) = e^{-4ky}$, $M_j = (M_5^3 a)^{1/2} e^{-3kja}$, whereas in a Randall-Sundrum geometry, $X(y) = e^{-2ky}$, $Y(y)$=1, one finds $M_j = (M_5^3 a)^{1/2} e^{-kja}$, in agreement with [203]. In both cases, the effective Planck scale on a given site depends exponentially on the position of the site.

Moreover, upon deconstruction, the second term in the second equality of eq.(5.76) leads to a mass term of the form (expanding up to $\mathcal{O}(h^2)$)

$$\mathcal{L}_4 \supset \frac{1}{2} \sum_{j=0}^{N-1} \frac{M_j^2}{4a^2} \frac{X_j}{Y_j} \left\{ (h_j - h_{j+1})^2 - (h_{j\mu\nu} - h_{j+1\mu\nu})^2 \right\} \ , \tag{5.80}$$

which corresponds precisely to eq.(5.20), with mass-squared parameters

$$m_j^2 = \frac{1}{a^2} \frac{X_j}{Y_j} \ . \tag{5.81}$$

The deconstructed theory is therefore identical to the discrete 4D scenario described in section 5.2.4, in which no clockwork graviton arises.

5.6 Conclusions

The elusiveness of physics beyond the SM strongly motivates the search for theories in which large hierarchies of effective interactions arise from natural fundamental parameters. The clockwork mechanism beautifully realizes this goal, generating exponentially-suppressed couplings to a symmetry-protected state without significant hierarchies in the UV theory. Such a phenomenon invites both exploration of its full scope and application to extensions of the SM.

In this chapter we have systematically investigated the scope of clockwork phenomena in four dimensions, as well as possible continuum counterparts in five dimensions. We have demonstrated that clockwork is an intrinsically abelian phenomenon, suitable for generating exponentially suppressed couplings to goldstone bosons of spontaneously broken abelian global symmetries, or to gauge bosons of abelian local symmetries. It is manifestly impossible to realize a clockwork mechanism for non-abelian symmetries protecting a light state, precluding the application of clockwork to Yang-Mills theories, non-linear sigma models, or gravity (thereby frustrating any attempts to solve the hierarchy problem by clockworking gravity).

We have also explored the extent to which viable clockwork models in four dimensions have continuum counterparts in five dimensions. We study a general class of five-dimensional theories with a compact fifth dimension, whose metrics preserve four-dimensional Lorentz invariance with warp factors that are a function of the fifth coordinate. Members of the class include flat, Randall-Sundrum, and linear dilaton models. The zero modes of all massless bosonic bulk fields on these metrics are flat in the sense that they couple equally to states localized on codimension-one surfaces anywhere in the fifth dimension. These five-dimensional theories are therefore not continuum counterparts of four-dimensional clockwork. Moreover, their deconstructions cannot be identified with four-dimensional clockwork, as zero modes in the deconstructions couple universally to states localized at specific sites, in contrast with clockwork. In addition, any nontrivial warp factor in the metric of a higher-dimensional theory corresponds to a hierarchy of couplings and scales intrinsic to each site in its deconstruction, again in contrast with clockwork.[21]

[21]For abelian bulk fields the hierarchies of scales and couplings in the deconstruction can be

Among other things, this implies that linear dilaton models (and more generally a broad class of five-dimensional theories whose metrics give nominal hierarchies) are not the continuum counterparts of clockwork. Linear dilaton theories may still be of interest in addressing the hierarchy problem in their own right, but they so in a way that is unrelated to clockwork. In particular, the deconstruction of gravity in linear dilaton backgrounds necessarily involves the same sort of site-by-site scale hierarchies found in the deconstruction of Randall-Sundrum models, rather than the parametrically similar scales found in clockwork.

This leaves the question of what five-dimensional theories, if any, *are* the continuum counterparts of abelian clockwork models. Although physically meaningful coupling hierarchies for the zero modes of bulk bosons cannot be generated by metric factors, they *can* be generated by non-trivial zero mode profiles unrelated to the metric. We have found that candidate continuum counterparts of abelian clockwork involve scalars or vectors with bulk and brane masses tuned to preserve a massless zero mode. This imparts a physically meaningful profile to the zero mode that generates the desired exponential and position-dependent hierarchy in couplings to localized states. Deconstructions of these continuum theories do exhibit clockwork phenomena, and their masses and couplings agree with those of uniform clockwork up to corrections that fall off with the number of sites. These 5D theories may be a fruitful setting for additional clockwork model-building.

absorbed into genuine clockwork-like charges, but the zero mode in these deconstructions still lacks the position-dependent couplings of clockwork unless position-dependent charges are put in by hand at the outset.

Chapter 6

Conclusions

The absence of unambiguous signs of new physics from colliders or DM experiments is calling into question the most traditional solutions to some of the caveats of the SM. In this work, we have considered theories based on the Twin Higgs mechanism, which provide a partial solution to the electroweak hierarchy problem, and have explored their potential for solving the DM mystery. Specifically, we have focused on Fraternal Twin Higgs models, which implement the minimal version of the Twin Higgs idea, and we have seen that these constructions do indeed provide natural DM candidates.

In chapter 3, we have focused on the simplest version of the Fraternal Twin Higgs proposal, in which there is neither a twin hypercharge gauge group nor an asymmetry in the twin sector. In this case, we have seen that twin leptons are in fact the preferred DM candidates, and predictions concerning their scattering cross sections with SM nuclei fall in the region of parameter space of interest for current and future direct dection experiments. So much so that since the work discussed in chapter 3 was originally published in [2], a significant region of parameter space has already been ruled out by the latest results from the LUX detector [110]. These new constraints set the ratio between the twin and SM Higgs vev's to be $f/v \gtrsim 6$, which in turn implies a fine-tuning $\sim 5\%$. This dominates over LHC bounds, which only exclude the regime $f/v \gtrsim 3$. This highlights how exploration of different aspects of theories of Neutral Naturalness is both relevant and timely, with experiments other than colliders likely to be the most interesting probes of these new class of models.

Whereas in chapter 3 the final DM abundance was set purely by freeze-out dynamics, in chapter 4 we considered the case in which an asymmetry was present in the twin sector. In this case, the natural DM candidate happens to be a bound state of three twin quarks, and its relic abundance is purely set by the primordial asymmetry. Naturalness considerations then set the mass of the DM particle to

be in the $1 - 10$ GeV regime, which is the attractive range for models of ADM. A dynamical mechanism to obtain asymmetries of similar size in the SM and twin sector was not considered in chapter 3, and remains an interesting model building challenge.

In chapter 5 we have focused on some structural aspects of the clockwork mechanism for generating hierarchies. We have proved that clockwork can only be consistently implemented in theories with abelian symmetries, and it is precluded in non-abelian theories including Yang-Mills and gravity. The applicability of clockwork is then restricted to models featuring states protected by $U(1)$ symmetries, either global or gauged. In the former case, the prime example is the 'clockwork axion' [9, 10], where a very light axion remains in the spectrum protected by a rather unsual $U(1)$ symmetry that allows the axion decay constant to be parametrically larger than the fundamental scale of spontaneous symmetry breaking, and that might be even larger than m_{Pl}. When gauged, the massless state is a photon, and the clockwork mechanism provides a framework in which matter fields may have exponentially different charges under the unbroken gauge symmetry in a way that is perfectly natural [193]. Although clockwork is intrinsically a 4D discrete construction, we have shown that its continuum limit requires bulk and brane masses to localize the zero modes, and that effects arising from non-trivial extra-dimensional geometries do not lead to clockwork.

Some of the most interesting open questions related to the clockwork mechanism are purely theoretical. For instance, the only non-trivial continuum limit of clockwork requires brane masses with opposite signs to be present on the 4D branes of a compactified 5D orbifold construction. Whereas negative brane masses do not lead to any inconsistency within the effective theory, whether they can be consistently included into a full UV-completion remains unclear. Because of this potential issue, it could well be the case that clockwork is a purely discrete construction. Moreover, reconciling spin-0 clockwork with the statement that unbroken global symmetries do not exist within a theory of quantum gravity would require to either gauge the (originally global) $U(1)$ symmetry, or allow for symmetry-breaking effects suppressed by some power of m_{Pl}. Whether the main features of scalar clockwork survive either

of these attempts requires more thought (see [196] for work in this direction).

Finally, even vector clockwork, in which the $U(1)$ symmetry is gauged, raises interesting theoretical questions regarding the applicability of the WGC as a veto on effective field theories, a discussion originally introduced in [193]. Spin-1 clockwork provides an explicit example in which a theory that violates the WGC in the IR can be consistently UV-completed into a theory that satisfies it. In [193], an extended version of the WGC was introduced, with a milder restriction on the cut-off of the effective theory. Interestingly, clockwork theories appear to saturate this new bound, raising the question of whether other theories exist somewhere in between. Most ambitiously, if a clockwork-like construction could be engineered within a controlled string theory set-up, it would provide the first explicit UV counter-example to the original WGC proposal, a direction that is worth exploring.

References

[1] I. Garcia Garcia, R. Lasenby and J. March-Russell, *Twin Higgs WIMP Dark Matter*, *Phys. Rev.* **D92** (2015) 055034, [1505.07109].

[2] I. Garcia Garcia, R. Lasenby and J. March-Russell, *Twin Higgs Asymmetric Dark Matter*, *Phys. Rev. Lett.* **115** (2015) 121801, [1505.07410].

[3] N. Craig, I. Garcia Garcia and D. Sutherland, *Disassembling the Clockwork Mechanism*, 1704.07831.

[4] I. Garcia Garcia and J. March-Russell, *Rare Flavor Processes in Maximally Natural Supersymmetry*, *JHEP* **01** (2015) 042, [1409.5669].

[5] I. Garcia Garcia, K. Howe and J. March-Russell, *Natural Scherk-Schwarz Theories of the Weak Scale*, *JHEP* **12** (2015) 005, [1510.07045].

[6] I. Garcia Garcia, S. Krippendorf and J. March-Russell, *The String Soundscape at Gravitational Wave Detectors*, 1607.06813.

[7] I. Garcia Garcia, *LHCb anomalies from a natural perspective*, *JHEP* **03** (2017) 040, [1611.03507].

[8] G. 't Hooft, *Naturalness, chiral symmetry, and spontaneous chiral symmetry breaking*, *NATO Sci. Ser. B* **59** (1980) 135–157.

[9] K. Choi and S. H. Im, *Realizing the relaxion from multiple axions and its UV completion with high scale supersymmetry*, *JHEP* **01** (2016) 149, [1511.00132].

[10] D. E. Kaplan and R. Rattazzi, *Large field excursions and approximate discrete symmetries from a clockwork axion*, *Phys. Rev.* **D93** (2016) 085007, [1511.01827].

[11] S. R. Coleman and E. J. Weinberg, *Radiative Corrections as the Origin of Spontaneous Symmetry Breaking*, *Phys. Rev.* **D7** (1973) 1888–1910.

[12] S. Weinberg, *The Cosmological Constant Problem*, *Rev. Mod. Phys.* **61** (1989) 1–23.

[13] S. Dimopoulos and L. Susskind, *Mass Without Scalars*, *Nucl. Phys.* **B155** (1979) 237–252.

[14] L. Randall and R. Sundrum, *A Large mass hierarchy from a small extra dimension*, *Phys. Rev. Lett.* **83** (1999) 3370–3373, [hep-ph/9905221].

[15] N. Arkani-Hamed, S. Dimopoulos and G. R. Dvali, *The Hierarchy problem and new dimensions at a millimeter*, *Phys. Lett.* **B429** (1998) 263–272, [hep-ph/9803315].

[16] S. Weinberg, *Implications of Dynamical Symmetry Breaking*, *Phys. Rev.* **D13** (1976) 974–996.

[17] E. Gildener, *Gauge Symmetry Hierarchies*, *Phys. Rev.* **D14** (1976) 1667.

[18] L. Susskind, *Dynamics of Spontaneous Symmetry Breaking in the Weinberg-Salam Theory*, *Phys. Rev.* **D20** (1979) 2619–2625.

[19] T. Appelquist and J. Carazzone, *Infrared Singularities and Massive Fields*, *Phys. Rev.* **D11** (1975) 2856.

[20] S. R. Coleman and J. Mandula, *All Possible Symmetries of the S Matrix*, *Phys. Rev.* **159** (1967) 1251–1256.

[21] R. Haag, J. T. Lopuszanski and M. Sohnius, *All Possible Generators of Supersymmetries of the s Matrix*, *Nucl. Phys.* **B88** (1975) 257.

[22] J. Polchinski, *String theory. Vol. 1: An introduction to the bosonic string.* Cambridge University Press, 2007.

[23] J. Polchinski, *String theory. Vol. 2: Superstring theory and beyond.* Cambridge University Press, 2007.

[24] S. Dimopoulos, S. Raby and F. Wilczek, *Supersymmetry and the Scale of Unification*, *Phys. Rev.* **D24** (1981) 1681–1683.

[25] S. Dimopoulos and H. Georgi, *Softly Broken Supersymmetry and SU(5)*, *Nucl. Phys.* **B193** (1981) 150–162.

[26] L. E. Ibanez and G. G. Ross, *Low-Energy Predictions in Supersymmetric Grand Unified Theories*, *Phys. Lett.* **105B** (1981) 439–442.

[27] S. P. Martin, *A Supersymmetry primer*, `hep-ph/9709356`.

[28] J. Terning, *Modern supersymmetry: Dynamics and duality.* 2006, 10.1093/acprof:oso/9780198567639.001.0001.

[29] T. Gherghetta, B. von Harling, A. D. Medina and M. A. Schmidt, *The Scale-Invariant NMSSM and the 126 GeV Higgs Boson*, *JHEP* **02** (2013) 032, [1212.5243].

[30] A. Arvanitaki, M. Baryakhtar, X. Huang, K. van Tilburg and G. Villadoro, *The Last Vestiges of Naturalness*, *JHEP* **03** (2014) 022, [1309.3568].

[31] E. Hardy, *Is Natural SUSY Natural?*, *JHEP* **10** (2013) 133, [1306.1534].

[32] J. L. Feng, *Naturalness and the Status of Supersymmetry*, *Ann. Rev. Nucl. Part. Sci.* **63** (2013) 351–382, [1302.6587].

[33] T. Gherghetta, B. von Harling, A. D. Medina and M. A. Schmidt, *The price of being SM-like in SUSY*, *JHEP* **04** (2014) 180, [1401.8291].

[34] J. Fan and M. Reece, *A New Look at Higgs Constraints on Stops*, *JHEP* **06** (2014) 031, [1401.7671].

[35] G. G. Ross, K. Schmidt-Hoberg and F. Staub, *Revisiting fine-tuning in the MSSM*, *JHEP* **03** (2017) 021, [1701.03480].

[36] J. E. Kim and H. P. Nilles, *The mu Problem and the Strong CP Problem*, *Phys. Lett.* **B138** (1984) 150–154.

[37] G. F. Giudice and A. Masiero, *A Natural Solution to the mu Problem in Supergravity Theories*, *Phys. Lett.* **B206** (1988) 480–484.

[38] G. R. Dvali, G. F. Giudice and A. Pomarol, *The Mu problem in theories with gauge mediated supersymmetry breaking*, *Nucl. Phys.* **B478** (1996) 31–45, [hep-ph/9603238].

[39] G. F. Giudice and A. Strumia, *Probing High-Scale and Split Supersymmetry with Higgs Mass Measurements*, *Nucl. Phys.* **B858** (2012) 63–83, [1108.6077].

[40] A. Arvanitaki, N. Craig, S. Dimopoulos and G. Villadoro, *Mini-Split*, *JHEP* **02** (2013) 126, [1210.0555].

[41] J. Pardo Vega and G. Villadoro, *SusyHD: Higgs mass Determination in Supersymmetry*, *JHEP* **07** (2015) 159, [1504.05200].

[42] ATLAS Collaboration collaboration, *Search for supersymmetry in final states with two same-sign or three leptons and jets using* 36 fb^{-1} *of* $\sqrt{s} = 13$ *TeV pp collision data with the ATLAS detector*, Tech. Rep. ATLAS-CONF-2017-030, CERN, Geneva, May, 2017.

[43] Z. Chacko, H.-S. Goh and R. Harnik, *The Twin Higgs: Natural electroweak breaking from mirror symmetry*, *Phys.Rev.Lett.* **96** (2006) 231802, [hep-ph/0506256].

[44] Z. Chacko, H.-S. Goh and R. Harnik, *A Twin Higgs model from left-right symmetry*, *JHEP* **0601** (2006) 108, [hep-ph/0512088].

[45] Z. Chacko, Y. Nomura, M. Papucci and G. Perez, *Natural little hierarchy from a partially goldstone twin Higgs*, *JHEP* **0601** (2006) 126, [hep-ph/0510273].

[46] N. Craig, A. Katz, M. Strassler and R. Sundrum, *Naturalness in the Dark at the LHC*, 1501.05310.

[47] G. Burdman, Z. Chacko, R. Harnik, L. de Lima and C. B. Verhaaren, *Colorless Top Partners, a 125 GeV Higgs, and the Limits on Naturalness*, *Phys. Rev.* **D91** (2015) 055007, [1411.3310].

[48] A. Falkowski, S. Pokorski and M. Schmaltz, *Twin SUSY*, *Phys. Rev.* **D74** (2006) 035003, [hep-ph/0604066].

[49] S. Chang, L. J. Hall and N. Weiner, *A Supersymmetric twin Higgs*, *Phys. Rev.* **D75** (2007) 035009, [hep-ph/0604076].

[50] N. Craig and K. Howe, *Doubling down on naturalness with a supersymmetric twin Higgs*, *JHEP* **03** (2014) 140, [1312.1341].

[51] P. Batra and Z. Chacko, *A Composite Twin Higgs Model*, *Phys. Rev.* **D79** (2009) 095012, [0811.0394].

[52] M. Geller and O. Telem, *Holographic Twin Higgs Model*, *Phys. Rev. Lett.* **114** (2015) 191801, [1411.2974].

[53] R. Barbieri, D. Greco, R. Rattazzi and A. Wulzer, *The Composite Twin Higgs scenario*, *JHEP* **08** (2015) 161, [1501.07803].

[54] M. Low, A. Tesi and L.-T. Wang, *Twin Higgs mechanism and a composite Higgs boson*, *Phys. Rev.* **D91** (2015) 095012, [1501.07890].

[55] N. Craig, S. Knapen and P. Longhi, *Neutral Naturalness from Orbifold Higgs Models*, *Phys. Rev. Lett.* **114** (2015) 061803, [1410.6808].

[56] N. Craig, S. Knapen and P. Longhi, *The Orbifold Higgs*, *JHEP* **03** (2015) 106, [1411.7393].

[57] D. Curtin and C. B. Verhaaren, *Discovering Uncolored Naturalness in Exotic Higgs Decays*, *JHEP* **12** (2015) 072, [1506.06141].

[58] C. J. Morningstar and M. J. Peardon, *The Glueball spectrum from an anisotropic lattice study*, *Phys.Rev.* **D60** (1999) 034509, [hep-lat/9901004].

[59] Y. Chen, A. Alexandru, S. Dong, T. Draper, I. Horvath et al., *Glueball spectrum and matrix elements on anisotropic lattices*, *Phys.Rev.* **D73** (2006) 014516, [hep-lat/0510074].

[60] B. Lucini, M. Teper and U. Wenger, *Glueballs and k-strings in SU(N) gauge theories: Calculations with improved operators*, *JHEP* **06** (2004) 012, [hep-lat/0404008].

[61] F. Zwicky, *Die Rotverschiebung von extragalaktischen Nebeln*, *Helv. Phys. Acta* **6** (1933) 110–127.

[62] F. Zwicky, *On the Masses of Nebulae and of Clusters of Nebulae*, *Astrophys. J.* **86** (1937) 217–246.

[63] V. C. Rubin and W. K. Ford, Jr., *Rotation of the Andromeda Nebula from a Spectroscopic Survey of Emission Regions*, *Astrophys. J.* **159** (1970) 379–403.

[64] V. C. Rubin, D. Burstein, W. K. Ford, Jr. and N. Thonnard, *Rotation velocities of 16 SA galaxies and a comparison of Sa, Sb, and SC rotation properties*, *Astrophys. J.* **289** (1985) 81.

[65] K. G. Begeman, A. H. Broeils and R. H. Sanders, *Extended rotation curves of spiral galaxies: Dark haloes and modified dynamics*, *Mon. Not. Roy. Astron. Soc.* **249** (1991) 523.

[66] Y. Sofue and V. Rubin, *Rotation curves of spiral galaxies*, *Ann. Rev. Astron. Astrophys.* **39** (2001) 137–174, [astro-ph/0010594].

[67] M. Milgrom, *A Modification of the Newtonian dynamics: Implications for galaxies*, *Astrophys. J.* **270** (1983) 371–383.

[68] M. Milgrom, *A modification of the Newtonian dynamics: implications for galaxy systems*, *Astrophys. J.* **270** (1983) 384–389.

[69] M. Milgrom, *A Modification of the Newtonian dynamics as a possible alternative to the hidden mass hypothesis*, *Astrophys. J.* **270** (1983) 365–370.

[70] R. H. Sanders, *Resolving the virial discrepancy in clusters of galaxies with modified newtonian dynamics*, *Astrophys. J.* **512** (1999) L23, [astro-ph/9807023].

[71] R. H. Sanders, *Clusters of galaxies with modified Newtonian dynamics (MOND)*, *Mon. Not. Roy. Astron. Soc.* **342** (2003) 901, [astro-ph/0212293].

[72] R. Massey, T. Kitching and J. Richard, *The dark matter of gravitational lensing*, *Rept. Prog. Phys.* **73** (2010) 086901, [1001.1739].

[73] D. Clowe, M. Bradac, A. H. Gonzalez, M. Markevitch, S. W. Randall, C. Jones et al., *A direct empirical proof of the existence of dark matter*, *Astrophys. J.* **648** (2006) L109–L113, [astro-ph/0608407].

[74] V. Springel et al., *Simulating the joint evolution of quasars, galaxies and their large-scale distribution*, *Nature* **435** (2005) 629–636, [astro-ph/0504097].

[75] M. Vogelsberger, S. Genel, V. Springel, P. Torrey, D. Sijacki, D. Xu et al., *Properties of galaxies reproduced by a hydrodynamic simulation*, *Nature* **509** (2014) 177–182, [1405.1418].

[76] Planck collaboration, R. Adam et al., *Planck 2015 results. I. Overview of products and scientific results*, 1502.01582.

[77] G. Steigman, *Primordial Nucleosynthesis: A Cosmological Probe*, *IAU Symp.* **268** (2010) 19–26, [0912.1114].

[78] L. Dugger, T. E. Jeltema and S. Profumo, *Constraints on Decaying Dark Matter from Fermi Observations of Nearby Galaxies and Clusters*, *JCAP* **1012** (2010) 015, [1009.5988].

[79] M. G. Baring, T. Ghosh, F. S. Queiroz and K. Sinha, *New Limits on the Dark Matter Lifetime from Dwarf Spheroidal Galaxies using Fermi-LAT*, *Phys. Rev.* **D93** (2016) 103009, [1510.00389].

[80] J. M. Overduin and P. S. Wesson, *Dark matter and background light*, *Phys. Rept.* **402** (2004) 267–406, [astro-ph/0407207].

[81] E. W. Kolb and M. S. Turner, *The Early Universe*, *Front. Phys.* **69** (1990) 1–547.

[82] J. Fan, A. Katz, L. Randall and M. Reece, *Double-Disk Dark Matter*, *Phys. Dark Univ.* **2** (2013) 139–156, [1303.1521].

[83] D. Harvey, R. Massey, T. Kitching, A. Taylor and E. Tittley, *The non-gravitational interactions of dark matter in colliding galaxy clusters*, *Science* **347** (2015) 1462–1465, [1503.07675].

[84] D. N. Spergel and P. J. Steinhardt, *Observational evidence for selfinteracting cold dark matter*, *Phys. Rev. Lett.* **84** (2000) 3760–3763, [astro-ph/9909386].

[85] R. Dave, D. N. Spergel, P. J. Steinhardt and B. D. Wandelt, *Halo properties in cosmological simulations of selfinteracting cold dark matter*, *Astrophys. J.* **547** (2001) 574–589, [astro-ph/0006218].

[86] B. W. Lee and S. Weinberg, *Cosmological Lower Bound on Heavy Neutrino Masses*, *Phys. Rev. Lett.* **39** (1977) 165–168.

[87] S. Nussinov, *TECHNOCOSMOLOGY: COULD A TECHNIBARYON EXCESS PROVIDE A 'NATURAL' MISSING MASS CANDIDATE?*, *Phys.Lett.* **B165** (1985) 55.

[88] G. Gelmini, L. J. Hall and M. Lin, *What Is the Cosmion?*, *Nucl.Phys.* **B281** (1987) 726.

[89] R. S. Chivukula and T. P. Walker, *TECHNICOLOR COSMOLOGY*, *Nucl.Phys.* **B329** (1990) 445.

[90] S. M. Barr, R. S. Chivukula and E. Farhi, *Electroweak Fermion Number Violation and the Production of Stable Particles in the Early Universe*, *Phys.Lett.* **B241** (1990) 387–391.

[91] D. B. Kaplan, *A Single explanation for both the baryon and dark matter densities*, *Phys.Rev.Lett.* **68** (1992) 741–743.

[92] D. Hooper, J. March-Russell and S. M. West, *Asymmetric sneutrino dark matter and the Omega(b) / Omega(DM) puzzle*, *Phys.Lett.* **B605** (2005) 228–236, [hep-ph/0410114].

[93] R. Kitano and I. Low, *Dark matter from baryon asymmetry*, *Phys.Rev.* **D71** (2005) 023510, [hep-ph/0411133].

[94] N. Cosme, L. Lopez Honorez and M. H. Tytgat, *Leptogenesis and dark matter related?*, *Phys.Rev.* **D72** (2005) 043505, [hep-ph/0506320].

[95] G. R. Farrar and G. Zaharijas, *Dark matter and the baryon asymmetry*, *Phys.Rev.Lett.* **96** (2006) 041302, [hep-ph/0510079].

[96] D. Suematsu, *Nonthermal production of baryon and dark matter*, *Astropart.Phys.* **24** (2006) 511–519, [hep-ph/0510251].

[97] M. H. Tytgat, *Relating leptogenesis and dark matter*, hep-ph/0606140.

[98] H. An, S.-L. Chen, R. N. Mohapatra and Y. Zhang, *Leptogenesis as a Common Origin for Matter and Dark Matter*, *JHEP* **1003** (2010) 124, [0911.4463].

[99] D. E. Kaplan, M. A. Luty and K. M. Zurek, *Asymmetric Dark Matter*, *Phys.Rev.* **D79** (2009) 115016, [0901.4117].

[100] P. Fox, A. Pierce and S. D. Thomas, *Probing a QCD string axion with precision cosmological measurements*, hep-th/0409059.

[101] P. Sikivie, *Axion Cosmology*, *Lect. Notes Phys.* **741** (2008) 19–50, [astro-ph/0610440].

[102] B. Carr, F. Kuhnel and M. Sandstad, *Primordial Black Holes as Dark Matter*, 1607.06077.

[103] B. J. Carr, K. Kohri, Y. Sendouda and J. Yokoyama, *New cosmological constraints on primordial black holes*, *Phys. Rev.* **D81** (2010) 104019, [0912.5297].

[104] F. Kahlhoefer, *Review of LHC Dark Matter Searches*, *Int. J. Mod. Phys.* **A32** (2017) 1730006, [1702.02430].

[105] D. G. Cerdeno and A. M. Green, *Direct detection of WIMPs*, 1002.1912.

[106] A. K. Drukier, K. Freese and D. N. Spergel, *Detecting Cold Dark Matter Candidates*, *Phys. Rev.* **D33** (1986) 3495–3508.

[107] J. I. Read, *The Local Dark Matter Density*, *J. Phys.* **G41** (2014) 063101, [1404.1938].

[108] DAMA, LIBRA collaboration, R. Bernabei et al., *New results from DAMA/LIBRA*, *Eur. Phys. J.* **C67** (2010) 39–49, [1002.1028].

[109] PandaX-II collaboration, A. Tan et al., *Dark Matter Results from First 98.7-day Data of PandaX-II Experiment*, 1607.07400.

[110] D. S. Akerib et al., *Results from a search for dark matter in LUX with 332 live days of exposure*, 1608.07648.

[111] D. Malling, D. Akerib, H. Araujo, X. Bai, S. Bedikian et al., *After LUX: The LZ Program*, 1110.0103.

[112] L. Bergstrom and G. Bertone, *Gamma-rays*, in *In *Bertone, G. (ed.): Particle dark matter* 491-506*, 2010.

[113] Fermi-LAT collaboration, M. Ackermann et al., *Searching for Dark Matter Annihilation from Milky Way Dwarf Spheroidal Galaxies with Six Years of Fermi-LAT Data*, 1503.02641.

[114] Fermi-LAT collaboration, M. Ajello et al., *Fermi-LAT Observations of High-Energy γ-Ray Emission Toward the Galactic Center*, *Astrophys. J.* **819** (2016) 44, [1511.02938].

[115] IceCube collaboration, M. G. Aartsen et al., *Search for annihilating dark matter in the Sun with 3 years of IceCube data*, *Eur. Phys. J.* **C77** (2017) 146, [1612.05949].

[116] A. W. Strong, I. V. Moskalenko and V. S. Ptuskin, *Cosmic-ray propagation and interactions in the Galaxy*, *Ann. Rev. Nucl. Part. Sci.* **57** (2007) 285–327, [astro-ph/0701517].

[117] P. Mertsch and S. Sarkar, *AMS-02 data confront acceleration of cosmic ray secondaries in nearby sources*, *Phys. Rev.* **D90** (2014) 061301, [1402.0855].

[118] PAMELA collaboration, O. Adriani et al., *An anomalous positron abundance in cosmic rays with energies 1.5-100 GeV*, *Nature* **458** (2009) 607–609, [0810.4995].

[119] Fermi-LAT collaboration, M. Ackermann et al., *Measurement of separate cosmic-ray electron and positron spectra with the Fermi Large Area Telescope*, *Phys. Rev. Lett.* **108** (2012) 011103, [1109.0521].

[120] AMS collaboration, M. Aguilar et al., *First Result from the Alpha Magnetic Spectrometer on the International Space Station: Precision Measurement of the Positron Fraction in Primary Cosmic Rays of 0.5-350 GeV*, *Phys. Rev. Lett.* **110** (2013) 141102.

[121] R. Kappl and A. Reinert, *Secondary Cosmic Positrons in an Anisotropic Diffusion Model*, 1609.01300.

[122] AMS-02 Collaboration, "Talks at the 'AMS Days at CERN'."

[123] G. Giesen, M. Boudaud, Y. Genolini, V. Poulin, M. Cirelli et al., *AMS-02 antiprotons, at last! Secondary astrophysical component and immediate implications for Dark Matter*, 1504.04276.

[124] R. D. Pisarski and F. Wilczek, *Remarks on the Chiral Phase Transition in Chromodynamics*, *Phys.Rev.* **D29** (1984) 338–341.

[125] C. Alexandrou, A. Borici, A. Feo, P. de Forcrand, A. Galli et al., *The Deconfinement phase transition in one flavor QCD*, *Phys.Rev.* **D60** (1999) 034504, [hep-lat/9811028].

[126] M. Fromm, J. Langelage, S. Lottini and O. Philipsen, *The QCD deconfinement transition for heavy quarks and all baryon chemical potentials*, *JHEP* **1201** (2012) 042, [1111.4953].

[127] L. Yaffe and B. Svetitsky, *First Order Phase Transition in the SU(3) Gauge Theory at Finite Temperature*, *Phys.Rev.* **D26** (1982) 963.

[128] M. Panero, *Thermodynamics of the QCD plasma and the large-N limit*, *Phys.Rev.Lett.* **103** (2009) 232001, [0907.3719].

[129] L. P. Csernai and J. I. Kapusta, *Nucleation of relativistic first order phase transitions*, *Phys.Rev.* **D46** (1992) 1379–1390.

[130] B. Beinlich, F. Karsch and A. Peikert, *SU(3) latent heat and surface tension from tree level and tadpole improved actions*, *Phys.Lett.* **B390** (1997) 268–274, [hep-lat/9608141].

[131] S. Borsanyi, G. Endrodi, Z. Fodor, S. Katz and K. Szabo, *Precision SU(3) lattice thermodynamics for a large temperature range*, *JHEP* **1207** (2012) 056, [1204.6184].

[132] G. Belanger, F. Boudjema, A. Pukhov and A. Semenov, micrOMEGAs$_3$*: A program for calculating dark matter observables*, *Comput.Phys.Commun.* **185** (2014) 960–985, [1305.0237].

[133] LUX collaboration, D. Akerib et al., *First results from the LUX dark matter experiment at the Sanford Underground Research Facility*, *Phys.Rev.Lett.* **112** (2014) 091303, [1310.8214].

[134] D. B. Kaplan and A. Manohar, *Strange Matrix Elements in the Proton from Neutral Current Experiments*, *Nucl.Phys.* **B310** (1988) 527.

[135] J. E. Juknevich, *Pure-glue hidden valleys through the Higgs portal*, *JHEP* **1008** (2010) 121, [0911.5616].

[136] K. Jedamzik, *Big bang nucleosynthesis constraints on hadronically and electromagnetically decaying relic neutral particles*, *Phys.Rev.* **D74** (2006) 103509, [hep-ph/0604251].

[137] W. Hu and J. Silk, *Thermalization constraints and spectral distortions for massive unstable relic particles*, *Phys.Rev.Lett.* **70** (1993) 2661–2664.

[138] T. R. Slatyer, *Energy Injection And Absorption In The Cosmic Dark Ages*, *Phys.Rev.* **D87** (2013) 123513, [1211.0283].

[139] Fermi-LAT collaboration, M. Ackermann et al., *Constraints on the Galactic Halo Dark Matter from Fermi-LAT Diffuse Measurements*, *Astrophys.J.* **761** (2012) 91, [1205.6474].

[140] D. Hooper and T. R. Slatyer, *Two Emission Mechanisms in the Fermi Bubbles: A Possible Signal of Annihilating Dark Matter*, *Phys.Dark Univ.* **2** (2013) 118–138, [1302.6589].

[141] K. N. Abazajian, N. Canac, S. Horiuchi and M. Kaplinghat, *Astrophysical and Dark Matter Interpretations of Extended Gamma-Ray Emission from the Galactic Center*, *Phys.Rev.* **D90** (2014) 023526, [1402.4090].

[142] Planck collaboration, P. Ade et al., *Planck 2015 results. XIII. Cosmological parameters*, 1502.01589.

[143] N. Craig and A. Katz, *The Fraternal WIMP Miracle*, 1505.07113.

[144] M. Farina, *Asymmetric Twin Dark Matter*, 1506.03520.

[145] F. Farchioni, I. Montvay, G. Munster, E. Scholz, T. Sudmann et al., *Hadron masses in QCD with one quark flavour*, *Eur.Phys.J.* **C52** (2007) 305–314, [0706.1131].

[146] S. Hannestad, J. Hamann and Y. Y. Wong, *Current and future constraints on neutrino physics from cosmology*, *J.Phys.Conf.Ser.* **485** (2014) 012008.

[147] S. Bashinsky and U. Seljak, *Neutrino perturbations in CMB anisotropy and matter clustering*, *Phys.Rev.* **D69** (2004) 083002, [astro-ph/0310198].

[148] I. Garcia Garcia, R. Lasenby and J. March-Russell, *Twin Higgs WIMP Dark Matter*, 1505.07109.

[149] E. Hardy, R. Lasenby, J. March-Russell and S. M. West, *Big Bang Synthesis of Nuclear Dark Matter*, *JHEP* **1506** (2015) 011, [1411.3739].

[150] G. Krnjaic and K. Sigurdson, *Big Bang Darkleosynthesis*, 1406.1171.

[151] D. Harvey, R. Massey, T. Kitching, A. Taylor and E. Tittley, *The non-gravitational interactions of dark matter in colliding galaxy clusters*, *Science* **347** (2015) 1462–1465, [1503.07675].

[152] I. Low, P. Schwaller, G. Shaughnessy and C. E. Wagner, *The dark side of the Higgs boson*, *Phys.Rev.* **D85** (2012) 015009, [1110.4405].

[153] J. Giedt, A. W. Thomas and R. D. Young, *Dark matter, the CMSSM and lattice QCD*, *Phys.Rev.Lett.* **103** (2009) 201802, [0907.4177].

[154] A. Crivellin, M. Hoferichter and M. Procura, *Accurate evaluation of hadronic uncertainties in spin-independent WIMP-nucleon scattering: Disentangling two- and three-flavor effects*, *Phys.Rev.* **D89** (2014) 054021, [1312.4951].

[155] M. A. Shifman, A. Vainshtein and V. I. Zakharov, *Remarks on Higgs Boson Interactions with Nucleons*, *Phys.Lett.* **B78** (1978) 443.

[156] P. Cushman, C. Galbiati, D. McKinsey, H. Robertson, T. Tait et al., *Working Group Report: WIMP Dark Matter Direct Detection*, 1310.8327.

[157] M. Heikinheimo, M. Raidal, C. Spethmann and H. Veermäe, *Evidence for Dark Matter Self-Interactions via Collisionless Shocks in Cluster Mergers*, 1504.04371.

[158] E. Gabrielli, L. Marzola, M. Raidal and H. Veermäe, *Dark matter and spin-1 milli-charged particles*, 1507.00571.

[159] F.-Y. Cyr-Racine and K. Sigurdson, *Cosmology of atomic dark matter*, *Phys.Rev.* **D87** (2013) 103515, [1209.5752].

[160] J. M. Cline, Z. Liu, G. Moore and W. Xue, *Scattering properties of dark atoms and molecules*, *Phys.Rev.* **D89** (2014) 043514, [1311.6468].

[161] C. M. Hirata and N. Padmanabhan, *Cosmological production of H(2) before the formation of the first galaxies*, *Mon.Not.Roy.Astron.Soc.* **372** (2006) 1175–1186, [astro-ph/0606437].

[162] H. Goldberg and L. J. Hall, *A New Candidate for Dark Matter*, *Phys.Lett.* **B174** (1986) 151.

[163] J. L. Feng, M. Kaplinghat, H. Tu and H.-B. Yu, *Hidden Charged Dark Matter*, *JCAP* **0907** (2009) 004, [0905.3039].

[164] D. E. Kaplan, G. Z. Krnjaic, K. R. Rehermann and C. M. Wells, *Atomic Dark Matter*, *JCAP* **1005** (2010) 021, [0909.0753].

[165] J. M. Cline, Z. Liu and W. Xue, *Millicharged Atomic Dark Matter*, *Phys.Rev.* **D85** (2012) 101302, [1201.4858].

[166] L. Okun, *Mirror particles and mirror matter: 50 years of speculations and search*, *Phys.Usp.* **50** (2007) 380–389, [hep-ph/0606202].

[167] R. Foot, *Mirror dark matter: Cosmology, galaxy structure and direct detection*, *Int.J.Mod.Phys.* **A29** (2014) 1430013, [1401.3965].

[168] P. J. Fox, G. D. Kribs and T. M. Tait, *Interpreting Dark Matter Direct Detection Independently of the Local Velocity and Density Distribution*, *Phys.Rev.* **D83** (2011) 034007, [1011.1910].

[169] J. F. Cherry, M. T. Frandsen and I. M. Shoemaker, *Halo Independent Direct Detection of Momentum-Dependent Dark Matter*, *JCAP* **1410** (2014) 022, [1405.1420].

[170] H. Vogel and J. Redondo, *Dark Radiation constraints on minicharged particles in models with a hidden photon*, *JCAP* **1402** (2014) 029, [1311.2600].

[171] J. M. Cline, Z. Liu, G. Moore and W. Xue, *Composite strongly interacting dark matter*, *Phys.Rev.* **D90** (2014) 015023, [1312.3325].

[172] J. Kopp, L. Michaels and J. Smirnov, *Loopy Constraints on Leptophilic Dark Matter and Internal Bremsstrahlung*, *JCAP* **1404** (2014) 022, [1401.6457].

[173] S. Davidson, S. Hannestad and G. Raffelt, *Updated bounds on millicharged particles*, *JHEP* **0005** (2000) 003, [hep-ph/0001179].

[174] A. Prinz, R. Baggs, J. Ballam, S. Ecklund, C. Fertig et al., *Search for millicharged particles at SLAC*, *Phys.Rev.Lett.* **81** (1998) 1175–1178, [hep-ex/9804008].

[175] P. W. Graham, D. E. Kaplan and S. Rajendran, *Cosmological Relaxation of the Electroweak Scale*, *Phys. Rev. Lett.* **115** (2015) 221801, [1504.07551].

[176] N. Arkani-Hamed, L. Motl, A. Nicolis and C. Vafa, *The String landscape, black holes and gravity as the weakest force*, *JHEP* **06** (2007) 060, [hep-th/0601001].

[177] J. E. Kim, H. P. Nilles and M. Peloso, *Completing natural inflation*, *JCAP* **0501** (2005) 005, [hep-ph/0409138].

[178] K. Choi, H. Kim and S. Yun, *Natural inflation with multiple sub-Planckian axions*, *Phys. Rev.* **D90** (2014) 023545, [1404.6209].

[179] A. de la Fuente, P. Saraswat and R. Sundrum, *Natural Inflation and Quantum Gravity*, *Phys. Rev. Lett.* **114** (2015) 151303, [1412.3457].

[180] M. Farina, D. Pappadopulo, F. Rompineve and A. Tesi, *The photo-philic QCD axion*, *JHEP* **01** (2017) 095, [1611.09855].

[181] T. Hambye, D. Teresi and M. H. G. Tytgat, *A Clockwork WIMP*, 1612.06411.

[182] R. Coy, M. Frigerio and M. Ibe, *Dynamical Clockwork Axions*, 1706.04529.

[183] G. F. Giudice and M. McCullough, *A Clockwork Theory*, *JHEP* **02** (2017) 036, [1610.07962].

[184] O. Aharony, M. Berkooz, D. Kutasov and N. Seiberg, *Linear dilatons, NS five-branes and holography*, *JHEP* **10** (1998) 004, [hep-th/9808149].

[185] A. Kehagias and A. Riotto, *Clockwork Inflation*, *Phys. Lett.* **B767** (2017) 73–80, [1611.03316].

[186] A. Ahmed and B. M. Dillon, *Clockwork Composite Higgses*, 1612.04011.

[187] N. Arkani-Hamed, A. G. Cohen and H. Georgi, *(De)constructing dimensions*, *Phys. Rev. Lett.* **86** (2001) 4757–4761, [hep-th/0104005].

[188] C. T. Hill, S. Pokorski and J. Wang, *Gauge invariant effective Lagrangian for Kaluza-Klein modes*, *Phys. Rev.* **D64** (2001) 105005, [hep-th/0104035].

[189] L. Randall, Y. Shadmi and N. Weiner, *Deconstruction and gauge theories in AdS(5)*, *JHEP* **01** (2003) 055, [hep-th/0208120].

[190] I. Antoniadis, A. Arvanitaki, S. Dimopoulos and A. Giveon, *Phenomenology of TeV Little String Theory from Holography*, *Phys. Rev. Lett.* **108** (2012) 081602, [1102.4043].

[191] I. Antoniadis, S. Dimopoulos and A. Giveon, *Little string theory at a TeV*, *JHEP* **05** (2001) 055, [hep-th/0103033].

[192] N. Fonseca, L. de Lima, C. S. Machado and R. D. Matheus, *Large field excursions from a few site relaxion model*, *Phys. Rev.* **D94** (2016) 015010, [1601.07183].

[193] P. Saraswat, *Weak gravity conjecture and effective field theory*, *Phys. Rev.* **D95** (2017) 025013, [1608.06951].

[194] N. Arkani-Hamed, H. Georgi and M. D. Schwartz, *Effective field theory for massive gravitons and gravity in theory space*, *Annals Phys.* **305** (2003) 96–118, [hep-th/0210184].

[195] T. Banks and N. Seiberg, *Symmetries and Strings in Field Theory and Gravity*, *Phys. Rev.* **D83** (2011) 084019, [1011.5120].

[196] K. Choi, S. H. Im and C. S. Shin, *Coupling or scale hierarchies with generalized continuum clockwork*, *To appear* (2017) .

[197] T. Gherghetta and A. Pomarol, *Bulk fields and supersymmetry in a slice of AdS*, *Nucl. Phys.* **B586** (2000) 141–162, [hep-ph/0003129].

[198] I. I. Kogan, S. Mouslopoulos, A. Papazoglou and G. G. Ross, *Multilocalization in multibrane worlds*, *Nucl. Phys.* **B615** (2001) 191–218, [hep-ph/0107307].

[199] K. Ghoroku and A. Nakamura, *Massive vector trapping as a gauge boson on a brane*, *Phys. Rev.* **D65** (2002) 084017, [hep-th/0106145].

[200] B. Batell and T. Gherghetta, *Localized U(1) gauge fields, millicharged particles, and holography*, *Phys. Rev.* **D73** (2006) 045016, [hep-ph/0512356].

[201] B. Batell and T. Gherghetta, *Yang-Mills Localization in Warped Space*, *Phys. Rev.* **D75** (2007) 025022, [hep-th/0611305].

[202] N. Arkani-Hamed and M. D. Schwartz, *Discrete gravitational dimensions*, *Phys. Rev.* **D69** (2004) 104001, [hep-th/0302110].

[203] L. Randall, M. D. Schwartz and S. Thambyahpillai, *Discretizing gravity in warped spacetime*, *JHEP* **10** (2005) 110, [hep-th/0507102].